University of Sheffield

SAFE DYNAMIC DESIGN OF STRUCTURES

Mojtaba Moatamedi

Doctor of Philosophy

(PhD)

Department of Mechanical Engineering

August 2000

SUMMARY

The Design of structures under dynamic loading is a demanding subject in safety of engineering design since conventional static failure criteria are unable to deal with structures under transient loading. This work is a contribution to this significant phenomenon to investigate the response and failure of structures to pulse loading. An experimental rig has therefore been designed to achieve the target. A series of experiments has then been carried out to investigate the structural failure under pulse loading using a shock tunnel. A non-linear transient analysis of plates and cylindrical structures under pulse loading has also been performed using ANSYS finite element code in order to introduce a failure criterion for these specific conditions. A large-scale heat exchanger under pressure pulse loading was also analysed experimentally and numerically. The impulsive load has been chosen to be above the static design pressure to investigate the effects of impulsive load and its duration on the plate failure. A critical curve is presented to determine the critical pulse loading and its duration for structures. The relations between the transient pressure loading, its duration and the natural frequency of the structure are also explored. It is indicated that the value of the impulsive load on structures may exceed the static design pressure without structural failure. Both experimental work and numerical analyses suggest that the design criteria for structures under dynamic loading are more flexible than those under static loading in which no freedoms in deviation of any simple yield criterion exist. It is concluded that using a proper failure criterion for any specific problem can increase safe working region of the structures which leads to economical and safe dynamic design of structures.

TO MY DEAREST PARENTS

Awards

Who's Who in Science and Engineering
Marquis Who's Who, NJ, USA, 1998-1999

HVIS Student Award
1998 Hypervelocity Impact Symposium, Huntsville, Alabama, USA, 1998

PVP Student Competition Award
1997 Pressure Vessels & Piping Conference, Orlando, Florida, USA, 1997

IChemE Second Best Poster Award
The 1997 Jubilee Research Event, IChemE, Nottingham, UK, 1997

Poster Competition Award
Research Poster Conference, The University of Sheffield, Sheffield, UK, 1997

Publications

Design Considerations to prevent Heat Exchanger Failure
Journal of Hydrocarbon Processing, Volume 79, No. 11, 66-69
November 2000

Design aspects of Chemical Plant Exposed to Transient Pressure Loads
Journal of chemical engineering research and design, Transaction of Institution of Chemical Engineers, Volume 76, Number A6, 866-870
September 2000

Experimental and Numerical Investigation of Circular Plates Failure Due to Shock Loading
18th International Modal Analysis Conference, San Antonio, Texas, USA
Feb. 2000

Safety Aspects of Dynamic Overpressure in Process Plant Structures
The 1998 IChemE Research Event, Institution of Chemical Engineers, Newcastle, UK
April 1998

Damage and Response of Cylindrical Structures from Asymmetric External and Internal Impulsive Loading
1997 ASME Pressure Vessels and Piping Conference, Orlando, Florida, USA
July 1997

Failure Assessment of Cylindrical Structures Subjected to Internal Impulsive Spot Loading
12th Biennial Conference on Reliability, Stress Analysis, & Failure Prevention, Virginia Beach, USA
April 1997

Safe Design of Process Plant Structures Against Explosions
The 1997 Jubilee Research Event, Institution of Chemical Engineers, Nottingham, UK
April 1997

Acknowledgements

I would like to express my deep and extreme appreciation and respect to my supervisor and advisor, Dr. Bruce C. R. Ewan for his pleasant sense of humour and for his helpful and constructive criticism and suggestions pointed out and for his great guidance through this research and also his valuable and precious time.

I also would like to thank Dr. John L. Wearing for his professional comments and useful advice on this work.

Most importantly, my special and greatest debt of gratitude remains, as ever, to my family who kindly and deeply support me throughout my entire life and whose careful attention and everlasting love build up hopes in my heart and make me successful through the life.

The financial support EPSRC (Engineering and Physical Sciences Research Council - UK) is also gratefully acknowledged.

I am also greatly indebted to all my friends whose moral supports have always been around me.

At last, not least, my many thanks to the technicians who provided me with their technical supports and thanks also due to all academic, secretarial and technical staff of the department for their assistance.

Nomenclature

θ	angle
ρ	density
ω	frequency
ν	Poisson's ratio
ε	strain
σ	stress
σ_y	yield stress
a	mid-surface radius
C	damping matrix
d	diameter
E	elastic modulus
E_t	tangent modulus
f	natural frequency
h	thickness
I	impulse
K	stiffness matrix
l	length
m	mass
M	mass matrix
P	pressure
Q	Shear force
T	fundamental period
t	time
u	velocity

w	displacement
x	Coordinate in X direction
y	Coordinate in Y direction
z	Coordinate in Z direction

List of figures

List of tables

Contents

1. Introduction

1.1 Introduction

Dynamic loading such as accidental explosions can occur in a variety of different circumstances which may lead to the failure of structures such as pressure vessels. Generally, such loading can cause catastrophic damage and failure to engineering structures. Therefore, the study of shell dynamics and its response to transient loading may enhance the structural safety of vessels and pressure vessels.

The use of shells and pressure vessels is widespread in industry. In many cases the vessels are gas filled and are operated at high pressure. However, external explosions may occur which will subsequently cause the shell structure to be under dynamic loading. There are also some liquid filled shells, such as heat exchangers, which experience lower pressure than the gas filled tubes which are fixed inside the shell. Failure of one or more tubes for any reason, such as corrosion or fretting, will overpressurise the shell to failure due to internal impulsive loading.

In the above cases, the question arises as to whether the shell can withstand overpressure for the short duration of transient loading when the shell structures are designed for the static pressure which is less than that dynamic load. In this event it becomes necessary to investigate the shell behaviour more accurately by considering a fuller analysis of the spatial and temporal variation of pressure and its link with shell dynamics.

As will be seen in the literature review, analytical studies of the dynamics of shells have been carried out for many years, and due to the complex kinematics of the response, these have often focused on small displacements and a high degree of symmetry in the geometry and applied loads, which enable a priori judgement of the form of solution.

Numerical methods however offer freedom to examine more realistic geometries incorporating elements which break the symmetry and permit material non-linearities, which are important in the true representation of the strain behaviour and application of failure criteria.

This work is concerned with extending the understanding of the way in which failure criteria for metal vessels can be related to the transient pressure loadings and the vessel design pressure.

In other words, the main objective of the research is to investigate the way in which the maximum allowable pressures of structures vary with the time duration of the loads in a transient state in order to introduce the dynamic failure criteria for structures.

1.2 Objectives and methodology

The main objective of the current research is to investigate the response and behaviour of the structures to impulsive pressure loading and to predict the structural response using the finite element method and compare the results to the experimental ones in order to validate the results. It has also been the aim of the work to explore the limits which must be applied to pressure transients, in terms of pulse width and amplitude, in order to remain within a safe working envelop. In other words, it is attempted to find out or introduce the best possible failure criteria for the structures under such loading.

In this work, the elastic, plastic and elasto-plastic response of the structure due to pressure pulse loading will be discussed.

The ANSYS finite element code is used to predict the response of the structure under pressure loading and also numerically investigate the structural failure. In order to show the capability of ANSYS code to handle the structures under pressure pulse loading a case study whose experimental results are available is carried out and the results are compared with the experimental ones.

ANSYS 5.5 has been used for all analysis using Pentium II 450 MHz with 128 RAM. The typical running time for each analysis was approximately 24 hours. Shell 82 element was used in all cases. ANSYS was the tool to perform pre-processing, solution and also post-processing parts of analyses.

Two sources of experimental data have been used in the current research. A set of experimental data has been collected at the laboratory scale using a shock tube to

generate the pressure pulses with different pulse width and amplitudes and using as test-pieces a range of plates and small cylindrical vessels. In order to build up a data base to interpret the structural behaviour and failure due to pressure pulse loading, the following approach has been taken. First, simple circular plates made of aluminium were used as test pieces in the shock tube to investigate the plate behaviour under the shock load and the results were compared with the calculated stresses and strains using ANSYS finite element code. A small cylindrical vessel was then constructed and used with the shock tube as a test piece to measure the stresses and strains and to demonstrate the failure limits of the system. The finite element model of the cylindrical vessel was also studied in ANSYS and the results were compared with the experimental work.

The study has also made use of the second source of experimental results from a Joint Industry Project (The Institute of Petroleum, 2000), EPSRC under the management of the Institute of Petroleum involving internal tube rupture tests on a large scale heat exchanger shell made of steel as a real large scale industrial case.

A parallel numerical study using ANSYS code has also modelled some large scale case studies to confirm the capability of the code to analyse the large scale industrial cases. The numerical results for the these cases were compared with the available experimental results which will be discussed in details. The numerical analysis of the above heat exchanger was also carried out and the results were compared with the experimental ones.

From these experimental and numerical results at both the laboratory and large scale, a methodology is proposed to define the safe working envelope for the structures under pressure pulse loading.

1.3 Conclusions

The overall objective of the present research is to understand and interpret the structural response due to pressure pulse loading. Therefore, the work reports results at the laboratory and full scale, of the response of structures to transient pressure loads.

The overall strategy of the work is based on developing a good understanding of the structural behaviour to pressure pulse loading by a step by step investigation of response of structures from simple plates to a complicated heat exchanger shell to the pulse load.

A properly selected failure criterion for structures under pressure pulse loading will increase the safe working region and economical benefits in structural design.

2. Literature review

2.1 Introduction

The study of safe dynamic design of structures is vital because a thorough understanding of structural responses to dynamic loading assists the design process and also leads to improved structural safety. It also helps to predict structural behaviour under dynamic loading and also to introduce appropriate failure criteria for process plant structures such as shells and plates subjected to impulse loading.

Maximum allowable stresses of structures are usually determined when the structures are under static loading. However, dynamic loading plays a very important role in practice, since according to existing failure criteria (ASME, 1983), the structures should be designed for the maximum applied dynamic pressure even when the static pressure is less than the dynamic value.

The importance of the research is revealed by the study carried out by Gaylord and Mainstone (1980) who showed that the most common accidental loads are explosion blast loads by the investigation of data on tall buildings. Dynamic loads imposed by impulsive loads on structures, such as vessels, can be internal or external ones. External explosion loads drastically affect the structure of pressure vessels, as evidenced by the study of Tinawi et al. (1993) on the damage to the base of a tank from blast loading. The evidence is that in July 1990, a series of five blasts took place about 200 m from two liquified natural gas (LNG) tanks belonging to Gaz Metropolitain in Montreal which caused the damage because of the external pressure pulse. Internal transient loads may also lead to the failure of the heat exchangers shells as the analysis of potential overpressure of a heat exchanger shell due to a ruptured tube was also studied. (Fowler et al., 1969)

The next section focuses on the review of the literature on the structural response to dynamic transient loading of plates and shells to impulsive loading, of solid-liquid interactions, such as the dynamic response of submerged shells to pulse loading, and also their associated failure criteria. This review is important as it builds up the background study of the plates and shells to pressure pulse loading.

2.2 Impulsive loading

First the impulsive loading and structures are discussed in general and then the responses of structures to impulsive loading will be presented.

2.2.1 Impulsive loads and structures

The detonation of high explosives is independent of atmospheric oxygen and occurs very rapidly within a very small space. Within this small space large quantities of very high temperature gas are produced and consequently is accompanied by a very high pressure rise. A shock wave is thus generated which spreads from the source of the explosion at a speed well in excess of the speed of sound. Bulson (1986) and Horoschun (1992) stated that the pressure which is associated with the shock, varies with time exponentially. The general form of this pressure-time profile is illustrated in Fig. 2.1.

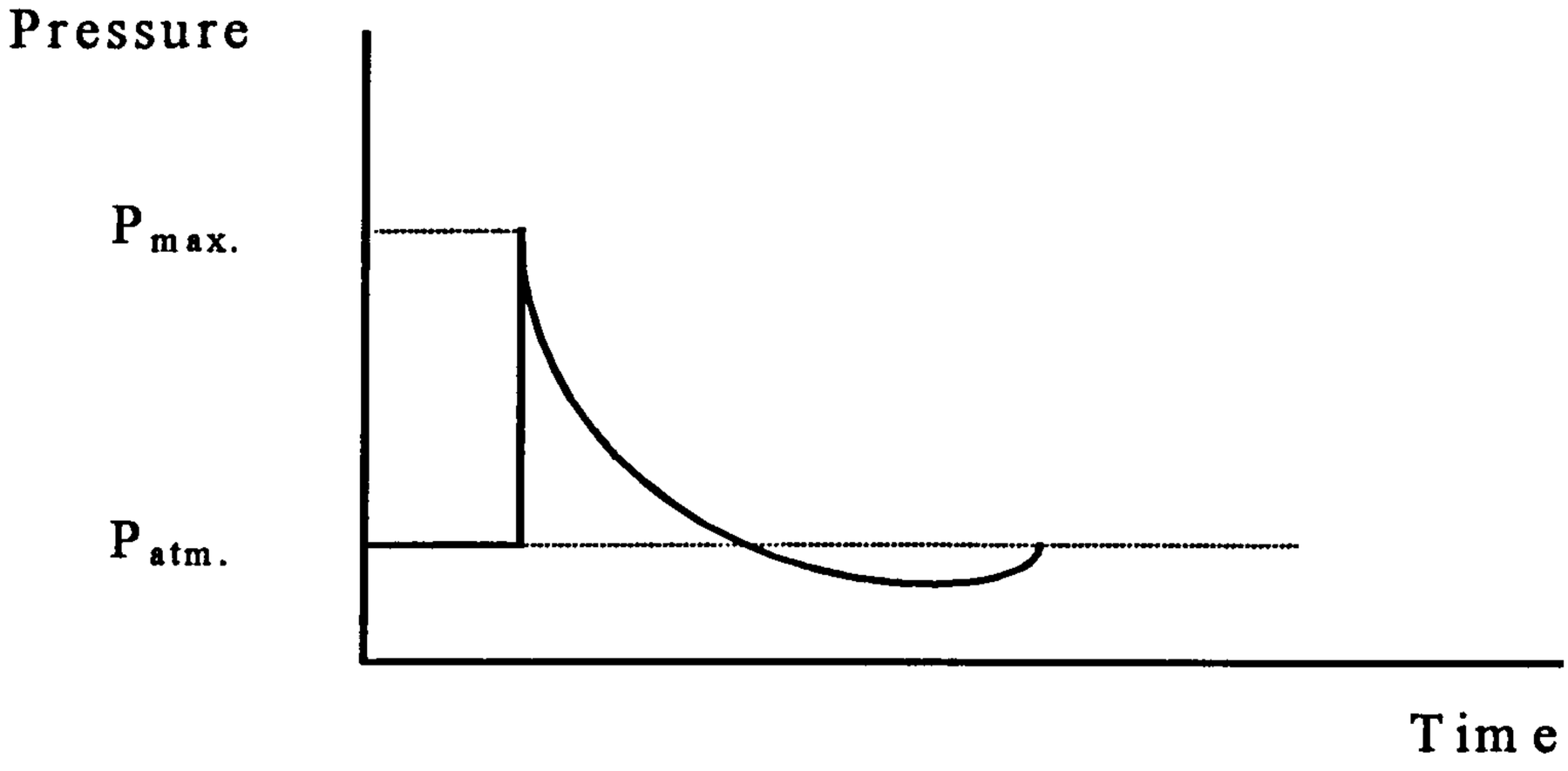

Fig. 2.1. Pressure-time profile of explosions for high explosives

Gas explosions represent an accelerative source where combustion of a premixed gas cloud, i.e. fuel-air or fuel/oxidiser causes rapid increase of pressure. Gas explosions can occur inside process equipment or pipes, in buildings or off-shore modules, in open process areas or in unconfined areas.

2.2.1 Impulsive loads and structures

The detonation of high explosives is independent of atmospheric oxygen and occurs very rapidly within a very small space. Within this small space large quantities of very high temperature gas are produced and consequently is accompanied by a very high pressure rise. A shock wave is thus generated which spreads from the source of the explosion at a speed well in excess of the speed of sound. Bulson (1986) and Horoschun (1992) stated that the pressure which is associated with the shock, varies with time exponentially. The general form of this pressure-time profile is illustrated in Fig. 2.1.

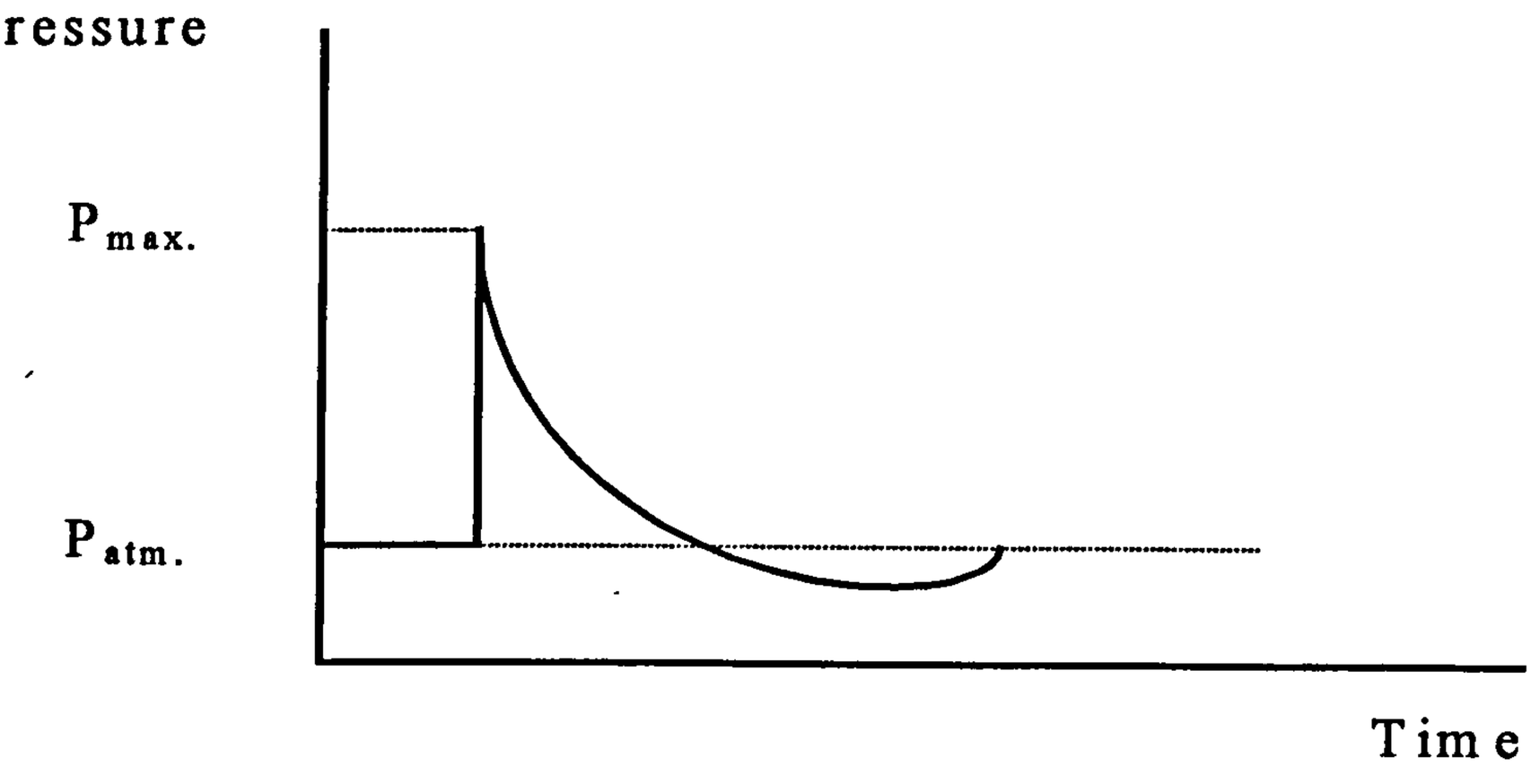

Fig. 2.1. Pressure-time profile of explosions for high explosives

Gas explosions represent an accelerative source where combustion of a premixed gas cloud, i.e. fuel-air or fuel/oxidiser causes rapid increase of pressure. Gas explosions can occur inside process equipment or pipes, in buildings or off-shore modules, in open process areas or in unconfined areas.

Bulson (1986) presented an exponential equation which satisfies the above curve. He also stated that the maximum pressure ($P_{max.}$), which is also called peak over pressure, is dependent on the distance of the reference point (the point which the maximum pressure is measured) from the centre of the explosion. This distance is an important factor for blast-resistant design which was studied by Dharaneepathy et al. (1995). In other words the design of structures subjected to over pressure caused by an explosion depends on the distance of the structure to the centre of the explosion which is called critical distance. These investigators concluded that the critical distance should be used as the design distance, particularly for tall structures. They also advised that the blast wave can have a spherical or a cylindrical shock front depending on the distance between the explosion source and the location of the structures.

When the structural responses due to impulsive loads are investigated, the time duration of the above curve is probably the most important consideration in the study. Galambos (1988) indicates that if the time duration is sufficiently long, the stress can be considered constant throughout the structure so that a stress wave does not exist through the structure. However, if the duration is short and also, the strain rate of the structure is sufficiently high, elasto-plastic wave propagation may be present in the structure. For relatively slow loading rates and long durations, the fundamental mode, similar to the static configuration, dominates the shape. However for higher loading rates and shorter durations, the higher modes are excited. For instance in the impulsively loaded column, if the duration of the load is sufficiently long, the axial load can be considered constant along the length, being a function of time only. If the duration is sufficiently short, the longitudinal wave must be

considered in the analysis and if in addition to the duration being short, the strain rate is sufficiently high as well the stress wave may be present as well, and the consideration of material strain rate sensitivity may be required.

Abrahamson and Lindberg (1971) studied the critical pulse load characterisation in terms of peak load and impulse which is basically a consideration of the time duration of pulse loading. They came to the conclusion that pulse load can be considered as an 'impulsive load', where the time duration of the load is very short. In this case, the load may be regarded as producing an instantaneous initial velocity in the structure under the load. The studies of Pegg (1991) and Schwer et al. (1988) are two examples of considering instantaneous initial velocity for impulse loading, whereas Jiang and Oslon (1991) and Ruiz et al. (1989) applied the impulsive load. On the other hand, if the time duration of pulse load is sufficiently long, it is treated as a 'quasi-static' case. In other words, if the time duration is short compared to structural response time, the pulse load is 'impulse', and if the time duration is long, the load is 'quasi-static'. The same conclusions were also obtained by the very recent study of Pegg (1994). In this work, dynamic pulse buckling of cylindrical structures with different radius to thickness ratios was numerically investigated. It was concluded that dynamic pulse buckling occurs in higher-order modes and therefore the details of modelling such as the chosen elements can affect the results. If the pulse duration is very long, the lower modes of the structure are excited and the response is quasi-static.

In the above mentioned study, Pegg (1991) investigated the dynamic pulse buckling of cylinders of various radius to thickness ratios and found out that if the ratio is less than about 30 the plastic deformation is observed however if the ratio is more than

about 240 the response will be elastic buckling. Schwer et al. (1988) also modelled the impulsive load as the initial velocity in the study of a metal tank under external impulsive spot load and found a good agreement between experimental results and numerical results produced by the finite element code DYNA3D to predict the behaviour of the tank.

As mentioned above, Jiang and Oslon (1991) and Ruiz et al. (1989) applied step loading on their studies. The former developed a nonlinear analysis procedure based on finite strip analysis for cylindrical shell structures under blast loading and compared the results with the finite difference method. The latter was on the elastic response of thin-wall cylindrical vessels to blast loading to compare the difference between axisymmetric buckling and lateral buckling and showed the predicted deformation for the second case using the numerical finite element code ABAQUS.

As stated above, different researchers (Pegg, 1991; Holmes and Kirkpatrick, 1988; Jiang and Oslon, 1991; Ruiz et al., 1989) have used various models (velocity or pressure) of pulse loading in their works. In order to investigate the differences among the pulse load shapes and their effects on structures, Abrahamson and Lindberg (1971) carried out a study using rectangular, triangular and exponential pulses. They indicated that rectangular (step load), triangular, and exponential modelling of pulse loading give similar responses from structures for impulsive (short duration) and quasi-static (long duration) loads. However discrepancies are observed when the duration of the load is somewhere between the above mentioned cases where elasto-plastic response of structures is present.

General attempts, such as the work of Xu and Kirkvik (1991), which discusses a design philosophy to consider dynamic loading and material ductility in design, have been performed to investigate problems involving explosions and structures.

Although some general attempts have been made, detailed analyses considering all non-linearities of the materials and loading shapes are required to predict the true behaviour of plates and shells to impulsive loading. It is because too many factors such as the structural and loading shape of the application affect the structural response and behaviour to dynamic loading in the transient analysis. Therefore their associated failure criteria, which is the concern of this study, will be different from the static cases because of the present of non-linearities.

2.2.2 Structural responses to impulsive loading

In order to carry out the complex investigation of shell behaviour to dynamic loading, the study of the simpler cases such as plate responses to impulsive loading can build up useful background of the subject.

The failure of circular plates subjected to impulsive velocities was investigated by Teeling-Smith and Nurick (1991). These investigators conducted a series of experiments on fully clamped circular mild steel plates subjected to a uniformly distributed impulse. They identified three modes of failures i.e. mode I (large ductile deformation), mode II (tensile-tearing and deformation) and mode III (transverse shear). An energy analysis was used on their test results which enables an energy balance equation relating input, deformation, tearing and disc energy to be calculated.

Their analysis of the experimental data produced equations to determine the deflection-thickness ratio as a function of impulse. Liang et al. (1991) also studied the dynamic analysis of plates to shock loadings. They used the finite element method with inclusion of the large deflection effects in transient analysis. If the rotations are large in elements but mechanical strains are small, then the large deflection effects must be considered in analysis. It was concluded that the response may remain in the elastic range and the plates may have an elastic oscillation behaviour which depends on the plate thickness and the shock load. The elastic behaviour of the structure means the final displacement of the plate is zero and no final deflection will remain when there is no continuation of loading.

The dynamic large deflection analysis of plates subjected to transient shock loading was also studied analytically by Manoach (1994). In this study two kinds of nonlinearities, i.e. geometry and material nonlinearities, were investigated. It was found that the geometry nonlinearity leads to reinforcement of plate stiffness and decreases the vibration period and amplitude, while the material nonlinearity tends to soften and increase the period and amplitude of vibration. A numerical method was introduced to study non-linear plate problems. The behaviour and failure of plates to impulse loading was also investigated recently by Wierzbicki and Nurick (1996). In this study, a theoretical approach was applied to investigate the effect of localised impulse loads on the plate behaviour. They introduced a profile to show the final deflection and obtained a good correlation between the predicted and measured normalised deflection profile. A rigid-plastic membrane was assumed in their analysis. Using an elastic-perfectly plastic (rigid-plastic) stress/strain model was confirmed by Jones (1989) to be an acceptable approximation for the case when the pulse duration

is short relative to the natural period. An elastic-perfectly plastic model of the material means that the material behaves in the elastic region up to a certain point and after that it will have a permanent deflection during and after applying the load and this deflection will be the same in both conditions. Although the above attempts were carried out on the plate responses to the pressure impulsive loading, no specific dynamic failure criteria have been introduced, which is the concern of this present study.

As was mentioned above the shell behaviour, which is the concern of this study, is more complex than the plate response to shock loading. The design of vessels under dynamic loading is governed by the determination of maximum resulting stresses of the shell due to the dynamic transient pressure.

If a vessel is subjected to an internal explosion pressure, the maximum allowable stress can be obtained by applying the formula given by Nicholas (1971). It is dependent on the maximum allowable stress of the structure under static loading. In this very early work, the effect of time duration of internal explosion load is also observed. It was also considered that the internal pressure is uniform. However the external explosion or spot loading will be discussed in the present work. The works of Mal'tsev et al. (1984) and of Duffy et al. (1993) also concern pressure vessels under internal explosive loading. In the first study the authors gave data from an experimental study of the process of deformation of an air-filled thin-walled spherical shell under the action of a blast wave from centrally positioned concentrated charges; they also carried out a frequency analysis of the vibrational modes excited in the shell and estimate the level of the flexural and membrane stresses acting in it. It was concluded that flexural vibration modes, the maximum stresses from which are

comparable in absolute value with the maximum membrane stresses, provide a significant contribution to the stress-strain state of a thin spherical shell. In the second study Duffy et al. (1993) presented a correlation of the experimentally recorded dynamic response of a spherical containment vessel with theoretical finite element calculations. Pressure-time loading on the inner wall of the vessel was recorded for each test using pressure transducers. Resulting dynamic response of the vessel was recorded for each test using strain gages mounted at selected locations on the outer surface of the vessel. The response of the vessel was primarily elastic. A finite element model of the vessel was run using DYNA3D, and comparison between experiments and analysis were generally good for frequency and strain magnitude at most locations. Comparisons of experimental and calculated pressure-time histories were less satisfactory.

It should be mentioned that maximum allowable stress of the pressure vessels under internal static loading can be found in textbooks such as Spence and Tooth (1994). All above works deal with the vessels under internal uniform pressure loading, however the investigation to introduce a proper failure criterion for shell structures subjected to non-uniform transient pressure loading is often required and this is also considered in the present work.

The design of externally pressurised vessels and also non-uniform internally pressurised vessels involves quite different problems from those arising in the design of internally uniform pressurised vessels. The difference arises in part from the greater importance of elastic and plastic buckling in the externally pressurised case and also non-linearity in both externally pressurised and non-uniform internally pressurised (such as internal spot loading) cases. According to the pressure vessels

ASME standard (1983), the maximum allowable stress of the pressure vessels under external pressures can be determined for the vessels under static uniform pressure. In other words, safe static design of the pressure vessels under external pressures is presented, however there is no standard to determine the maximum allowable stress of the pressure vessels under non-uniform transient loading. Although some general investigations such as the study of Brown and Nolan (1985) have been carried out on the subject, detailed studies are required to standardise the safe dynamic design of pressure vessels under non-uniform transient pressure loading. In the above study, the resistance of common chemical plant items to blast loadings was investigated by subjecting scale models of cylindrical plant items to simulated vapour cloud explosions. The effects of the magnitude of the peak pressure and the total impulse of the wave were examined and the stiffening of vessels was suggested.

As previously mentioned, the time duration of the applied load is an important factor in determining the structural response due to impulsive loading. Anderson and Lindberg (1968) proposed a theory of dynamic pulse buckling which was developed for cylindrical shells subjected to uniform lateral pressure pulses. They considered a wide range of the time duration of pulse loading from a very short, ideal impulse, to a duration so long that the pulse is quasi-static. They also presented a profile called the critical curve for cylindrical shells to specify the shell's response to pulse loading. A general critical curve which shows the relation between the applied dynamic pressure with impulse (P.dt) is plotted in Fig. 2.2.

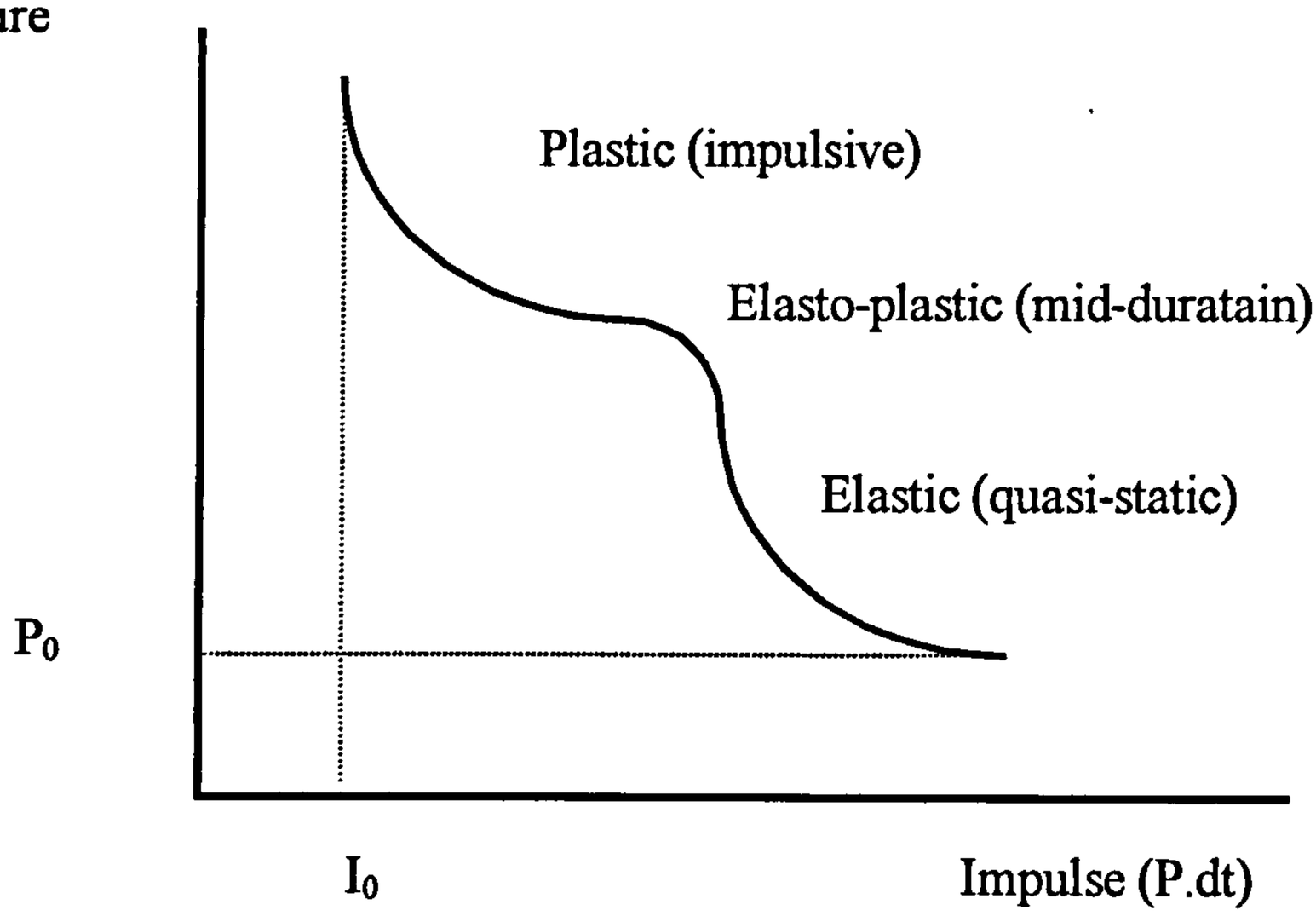

Fig. 2.2. Critical curve of cylindrical structures

The above curve is the generalised for dynamic buckling of cylindrical shells under uniform lateral pulse loads. In this condition, a cylindrical shell, acted upon by a uniform external pressure pulse, develops compressive hoop stresses that resist inward motion. The compressive hoop stresses cause elements of the shell that have an initial departure from circularity to be thrust ahead of the average motion and elements that have an initial outward departure to be thrust behind. It turns out that certain mode numbers of the initial departure from circularity grow faster than others and this determines the buckling pattern. The lower branch (elastic) of the curve indicates that the P-I combinations for which the initial non-uniformities grow by a factor of large value for 'I ' during the inward elastic motion. The upper branch (plastic) indicates the combinations for which the non-uniformities grow by factor of large value for 'P', during inward motion beyond the elastic range. In other words, in

a physical sense, the mode numbers are much greater for the plastic branch of the curve than for the elastic one as the high modes of the structure is excited.

They also studied the effect of shell parameters on the above curve. The variations of the value of the length to diameter ratio (l/d) of the cylindrical shells affect only the elastic branch of the curve, so that increasing l/d causes the elastic buckling with a lower impulse. The reason is that in the plastic range the modes are so high that the ends of the cylinder have little effect. However, their experimental works showed that the behaviour of the cylindrical shell structures under pulse loading strongly depends on the value of the radius to thickness ratio (a/h). The elastic behaviour moves to plastic, as the value of a/h decreases. They found that (a/h)=24 and (a/h)=270 gives the plastic and elastic responses, respectively. Pegg (1991) also obtained similar results. He found that if (a/h)<60, the response of the cylindrical shell due to pulse loading is plastic, and, if (a/h)>260, the response is perfectly elastic. He also observed that if 60<(a/h)<260, the behaviour of the shell is elasto-plastic.

Some attempts have focused on the elastic behaviour of shell structures under pulse loading. Lindberg (1964) produced a theory of elastic pulse buckling for long shells subjected to non-uniform loading. He finally introduced the critical instantaneous velocity, under impulsive loading, which causes elastic pulse buckling. In this very early work, a theory was introduced which predicted that the wrinkles around the cylinder under the pulse load occur at a wave length which depends on the magnitude of the pressure pulse as well as on the cylinder parameters. To and Wang (1993) analysed the response of non-uniform shell structures to pulse loading. They carried out finite element analysis for the shell with the dimensions (large a/h) which gave perfectly elastic behaviour. Ruiz et al. (1989) also studied the behaviour of a thin wall

cylindrical vessel with (a/h)=2000 which is perfectly elastic. They applied two types of loading namely rotationally non-uniform and sideways pulse loads. The results of both cases were obtained experimentally. The former was compared to the analytical approach proposed by themselves, simulating the load as a rectangular pressure pulse and good agreement was observed. The latter was analysed by the ABAQUS finite element code because of the non-linearity of the case and a comparison with the experimental results was also made. Both above cases proved the elastic behaviour for very thin-walled cylindrical shells. It should be mentioned that in the above work, the lateral pulse was modelled as a cosine distribution model which is the most common approach. In this model the pressure is applied to the cylinder as a factor of the cosine of the angle of the cylinder which means the pressure is the maximum in the face to the load and minimum in the sides and back of the cylinder as the pressure is laterally applied. Wierzbicki and Hoo Fatt (1993), Prantil et al. (1986) and Kirkpatrick and Holmes (1989) also used the cosine model in their works.

Some other studies have also been carried out to investigate the behaviour of shell structures under pulse loading into the plastic region . Abrahamson and Goodier (1962) presented the plastic flow pulse buckling theory for cylindrical shells which covers low radius to thickness ratios. They predicted the final shape of the cylinders with low radios to thickness ratio under pulse loading. Wierzbicki and Hoo Fatt (1993) also proposed a model for the analysis of cylindrical shells with low radius to thickness ratios under dynamic loading. They in fact determined the deflections of the shells under lateral impulsive loading analytically so that the response was perfectly plastic. In another study, Hoo Fatt and Wierzbicki (1992) worked on the dynamic plastic response of a ring-stiffened cylindrical shell subjected to high intensity

pressure loading and introduced an approximate analytical solution for the plastic response of shells. The analytical solution was developed based on a simple computational model and some experimental observations of the final damaged structure. Their analytical model showed good agreement with a limited amount of experimental data. The work of Kormi and Duddell (1991) is another study which was performed to find the critical pressure value for a 10 μs step load in the plastic region of a cylindrical shell on using numerical method to demonstrate the power of the finite element method in modelling the response of structures to abnormal loads.

All the above mentioned investigations are about the elastic and plastic response behaviour of shell structures subjected to impulsive loading, whereas most practical cases have the elasto-plastic response to dynamic loading which introduce the complications. Therefore this creates the need for the present investigations in order to introduce the dynamic failure criteria for shell structures subjected to impulsive loading.

Elasto-plastic behaviour of structures presents complexities throughout the analyses of such problems. The response of midrange radius to thickness ratio shells to pulse loading, when the radius to thickness ratio is between 60 and 260 [60<(a/h)<260] which covers many practical cases, is not particularly well predicted by either elastic pulse or plastic flow buckling theory. It is thus required to apply a numerical approach such as a non-linear finite element solution to investigate these cases. Oslon (1991) proposed the finite strip method for dynamic blast loading on shell structures. He analysed a cylindrical shell under lateral blast loading, as an example, compared his results with the results obtained by both finite element and finite difference methods. It should be mentioned that the finite difference method for the inelastic

shell response to an impulsive load was applied by Underwood (1972). Jiang and Oslon (1991) used the above method and applied it to some problems using both step and exponential loading. They also compared their own results with the available experimental data and good agreement between the two was obtained. The above method was further developed recently by Jiang and Oslon (1993) so that the formulation of new super element for non-linear dynamic analysis of shell structures was proposed. In the conventional finite element modelling, the complex structures usually require a large number of elements and very expensive computer runs. However in the their new super element, the structure was first divided into some sub-structures and then elements were defined and analysed. The results obtained by the above new formulation showed satisfactory performance of the new super element method when the final deflection results were compared to the results obtained by finite strip and finite difference methods.

The elasto-plastic response of shells under external pulse loading has been also investigated experimentally. Schwer et al. (1988) studied failure analysis of an impulsively spot loaded tank with different impulses and 200 μs duration of impulse. The study was also carried out numerically using DYNA3D finite element computer code for pressurised and unpressurised tanks. The pressurised shell indicated that fracture occurred after a complex sequence of loading in the shell consisting of axial tension followed by compression. Prantil et al. (1986) also did an experiment to obtain the response of a cylindrical shell with the radius to thickness ratio (a/h) equal to 257 under lateral impulse load with 50 μs duration. They compared the results with a numerical method and found that initial imperfections in both shell geometry and loading should be considered in numerical methods in order to obtain realistic

results. Initial imperfections in a cylindrical shell with radius to thickness ratio (a/h) of 240 subjected to impulsive external load were considered in a finite element analysis by Kirkpatrick and Holmes (1988). Both idealised and measured shape imperfections were considered in the above study. The load imperfections were also included in the analysis. Shape imperfections and load imperfections were simulated mathematically. The above investigators found that measured shape imperfections with mathematically modelled load imperfections gave the best results compared to their experiments. Kirkpatrick and Holmes (1989) also performed an experiment to determine the effects of initial imperfections on the cylindrical shell subjected to an impulsive half-cosine external load applied with explosives. The experiment was carried out for the cylinder with (a/h)=240 and consequently an elasto-plastic response was observed, as expected. They also used the DYNA3D computer code to analyse the problem numerically with and without considering imperfections. The results obtained by considering initial imperfections in thickness of the shell, showed good agreement with experiment. Some mathematical models, such as the model presented by Ben-Haim (1993), have been proposed to simulate the imperfections. Making an imperfection such as a discontinuity in the shell thickness can also be useful in some design. The investigation of Stanley and Ganesan (1995) showed that the maximum stress and displacement can be reduced by introducing a certain discontinuity on the shell thickness.

Although the above discussed investigations are on the elasto-plastic response of shell structures to pressure impulsive loading, no appropriate failure criteria have been used to predict the failure of the structures to enhance and assure the pressure vessels safety. This work aims to investigate the response and also explore a proper

methodology for failure criteria and design strategies for the vessels under non-uniform pressure transient loading, since most reported works carry a high symmetry in both geometry and loading.

2.3 Fluid-structure interaction

Submerged shell structures subjected to transient pressure loading may deform to an unacceptably large amplitude. Such situations may arise in submarine structures subjected to under water explosions. Other examples are piping systems and pressure vessels in the nuclear and chemical industries, which may undergo local damage or failure due to an accidental internal release of energy.

Molyneaux et al. (1993) carried out an investigation to observe the impact responses of circular cylindrical shells to pressure pulse loading resulting from an under water explosion in the interior of the shell. Their model was analysed using DYNA3D, incorporating both hydrodynamic and large structural deformation treatments. From the numerical study, it was concluded that the maximum transient stress obtained from the strain-rate-dependent model is higher than that obtained from the strain-rate-independent model as the dynamic yield stress is increased when the strain rate effect is included. The response of the cylindrical shells to external impulsive hydrostatic pressure was also studied by Pegg (1994). The weakness of his study was that the hydrostatic pressure and impulsive loading were considered separately but applied simultaneously. However, the propagation of the shock wave through the fluid environment is very significant and requires to be taken into account. The work

of Mustafa et al. (1993) is another study of dynamic buckling of submerged circular cylindrical structures subjected to an external pressure impulse. They also applied numerical analysis, using the ABAQUS finite element code, and discovered that the predominant harmonic of the buckling response increases both with the cylinder length and with the radius to thickness ratio of the cylinder. Lewis et al. (1994) introduced a new calculation with coupled finite element and finite volume methods to predict the response of a submerged circular cylindrical vessel to pressure loading. They also compared the predicted response with the experiment with good agreement.

Non-linear dynamic fluid-structure interaction for shell structures have also been studied analytically. The very recent work of Brevart and Fuller (1996) is an example which focused on elastic cylindrical shells. In this investigation the time domain response of an infinite fluid-filled pipe to an impulsive line force was derived, based on the shell equations fully coupled to the interior acoustic field and computing a double Fourier integration in the wave number and frequency domain. The transient radial velocity of the shell was used to compute the coupled pressure field in the fluid and investigate the instantaneous intensity vectors in the fluid field. These vectors, evaluated in the near field of the shell wall at several distances from the input force for increasing time, which gave insight into the exchange of energy between the structure and the fluid as the various waves propagate through the system.

The study of O'Regan and DiMaggio (1990) is another attempt which uses a high degree of symmetry in the transient loading. To determine the dynamic response of submerged structures with complex internal geometry to shock loading, it is often necessary to uncouple the equations of motion of the infinite surrounding fluid from

those of the structure by means of acoustic approximations. In this work a method was developed that can be used to compute the motion of the structure.

Some investigations have also been performed on the dynamic response of stiffened cylindrical shells to the transient pressure shock wave considering fluid-structure interaction. Xu and Huang (1991) applied the finite difference method to study the effect of stiffening the cylinder on the submerged shell response to external transient pressure loading. However experimental data is required to validate their results. Pedron and Combescuse (1995) also carried out an analytical approach to the response of elastic stiffened cylindrical shells to the transient lateral pressure produced by an under water explosion which forms a non-uniform loading. They came to the conclusion that the theory developed by Anderson and Lindberg (1968) is well adapted for the shell structures and pressure pulse in the fluid environment for an infinite elastic stiffened shell submitted to quasi-static or quasi impulsive lateral loads. The issue of imperfection is another key subject and which was studied by Shin and Hooker (1994) for ring-stiffened long circular cylinders submerged in the fluid. The parametric studies on the effect of the initial geometric imperfections to the damage response patterns of submerged structures were investigated in their research. The type of the submerged structure investigated was the ring-stiffened long circular cylinders submerged in the fluid. The numerical analyses were performed to look into the details of damage response patterns of ring-stiffened cylindrical shells.

As can be observed, most investigations apply a high degree of symmetry and also elastic or plastic response. More investigation is inevitably needed to predict the

behaviour and failure of submerged shell structures to non-uniform transient pressure loading with elasto-plastic response which is discussed in the present research.

2.4 Failure criteria

Existing failure criteria deal with the static loads and pressures and use Von Mises and Tresca failure criteria. However some attempts have been made to introduce new failure criteria and design strategies for structures under dynamic impulsive loading.

Before looking at the literature available on this subject, it seems to be useful to briefly explain Von Mises and Tresca failure criteria.

The following equations respectively express Von Mises and Tresca failure criteria for the structure under loading:

Von Mises: $$\text{Max}\{|\sigma_1-\sigma_2|,|\sigma_2-\sigma_3|,|\sigma_3-\sigma_1|\}=\sigma_0 \qquad (2.1)$$

Tresca: $$\{(\sigma_1-\sigma_2)^2-\sigma_0^2\}\{(\sigma_2-\sigma_3)^2-\sigma_0^2\}\{(\sigma_3-\sigma_1)^2-\sigma_0^2\}=0 \qquad (2.1)$$

σ_0 : yield stress of the material

σ_1 & σ_2 & σ_3 : principal stresses

In two dimensional cases the above equations become:

Von Mises: $$\sigma_1^2-\sigma_1\sigma_2+\sigma_2^2=\sigma_0^2 \qquad (2.3)$$

Tresca: $$\{(\sigma_1-\sigma_2)^2-\sigma_0^2\}\{\sigma_2^2-\sigma_0^2\}\{\sigma_1^2-\sigma_0^2\}=0 \qquad (2.4)$$

The first equation (Von Mises) is that of an ellipse, and is the trace of the intersection of the circular cylinder with the (σ_1,σ_2) plane. Similarly, the Tresca hexagon of the second equation lies within the Von Mises ellipse. It is therefore obvious that both criteria predict the same limit $\sigma_1=\sigma_2=\sigma_0$ in equal biaxial tension and that of course both give the same breakdown limit σ_0 in simple tension.

Geefken et al. (1988) performed some experiments on unpressurised and pressurised cylindrical vessels to identify the structural response to external radial impulsive loads. It was observed that for unpressurised shells the response modes consisted of dynamic pulse buckling followed by large inward deflections of the loaded surface. In shells with high internal pressure, the dynamics are the same but the final deflection is outward. They developed the shell load-damage relationships to predict the failure by formulating the energy balance equations. Their failure criterion, which is based on the experiments and formulations, suggests that the failure occurs when the sum of the two principal strains reaches 14%. This failure criterion is specific to the tensile tests carried out in their experiments. Although a good agreement was obtained in their experiment and analyses, a more general failure criterion, that can be expressed for thin shells, may be obtained by carrying on their analysis further. Holmes and Kirkpatrick (1988) also investigated the failure of metal tanks to external impulsive spot loading. They also suggested that a sum of axial and hoop strain of 14% is sufficient to fail the geometry which they studied. The same results are also reported by Holmes et al. (1988) in another publication on the ductile failure of shells under transient pressure histories. Baltov et al. (1993) also investigated the failure of thin cylindrical shells under high intensity external impulsive loading in which the volume damage can occur. The failure and damage of thin metal shells in their study was

based on the following three criteria: (I) strength criterion - if the damage limit to fracture of the material is reached, (II) deformation criterion - if the limit of the shell admissible deflection is reached, (III) stability criterion - if an unbounded increase of the deflection velocity occurs for a relatively small increase of the external loading. They used the finite element method to analyse the response of the thin shell and subsequently introduced curves regarding the above failure criteria.

The failure by plastic response of cylindrical shells to impulsive loading has also been investigated. Li and Jones (1995) conducted a theoretical approach to predict the critical conditions for transverse shear failure of a short cylindrical shell, which is made from rigid, perfectly plastic material. They combined their theoretical results with an elementary failure criterion, a yield criterion, to predict the failure of the shell. The results from their theoretical work for the maximum permanent displacements of impulsively loaded fully clamped cylindrical shells were compared with the experimental data. Zhao et al. (1995) also studied the response and failure of rigid, perfectly plastic structures to transient pressure loading with finite-deflections in the structures. They also used the approximate yield surface criterion to predict the damage and failure of the structures. The rectangular shape for the pulse load was used in this work and it was concluded that the other shapes may be used applying the approximate yield surface criterion.

In the very recent work of Wierzbicki and Nurick (1996), from MIT, on plate behaviour under localised impulsive loading, it was reported that a long-range goal of their research is to predict the magnitude of the critical impulse to failure of the plate. This report obviously reveals the need of the research on the failure criteria for structures under impulse loading which is carried out on the present study.

2.5 Conclusions

The review of the research subject undertaken has particularly focused on cylindrical shells and their associated failure criteria. The review has shown that there is no standard for the safe design of pressure vessels under impulsive loading. In other words, the concern of all existing failure criteria is the static pressure and therefore the dynamic cases are considered under the static failure criteria. As reviewed above, some attempts have been carried out to investigate the behaviour and responses of vessels subjected to impulsive loading, but none of them has proposed the maximum allowable stresses for safe design. Another point is that the time variation of the dynamic loading has not been fully considered to determine a suitable failure criterion for safe dynamic design. However time duration of the dynamic loading on structures is a significant factor in determining the failure criterion of structures.

Therefore, the overall goal of the research is to provide a methodology for design of process plant structures, particularly plates and shells, under impulsive loading by investigating the effect of time duration and the maximum applied pressure of impulse loads on the maximum allowable stresses of the structures.

In other words, the plastic and elastic response and behaviour of cylindrical shell structures under highly uniform impulsive loading have been covered in the literature, whereas the elasto-plastic behaviour subjected to non-uniform impulse loading requires more investigation. Therefore, the objective of this research is to introduce a suitable design strategy for elasto-plastic response of plates and shell structures under impulsive loading.

First the elastic and plastic theories for cylindrical shell structures under impulsive loading will be explained, then a series of numerical analyses will be carried out and the results will be compared with the existing experimental results. The experimental procedure will then be presented and consequently the results and discussion for the failure criteria will be covered. Finally the conclusions will be drawn.

3. Theory

3.1 Introduction

Dynamic behaviour of structures is a very broad subject that includes not only the different types of loading such as vibratory and pulse loads, but also interaction of structures with other media, such as in heat exchangers shells and submerged structures subjected to impulsive loading in the water.

The structural response to pulse loading is obviously different from that to vibratory loading. The main distinction between structural response to transient and to oscillatory load is that the pulse load is characterised by its amplitude, shape, and duration. In vibration buckling of structures, the amplitudes of vibration caused by an oscillating load become unacceptably large at critical combinations of load amplitude, load frequency, and structure damping, whereas in pulse buckling, the structure

deforms to an unacceptably large amplitude as the result of the transient response to the applied load.

Since this work concentrates on the structural response and behaviour to impulsive loading, the elastic and plastic pulse buckling theories of shells first explained in this chapter.

3.2 Shells pulse buckling

Dynamic buckling of shells under external radial pulse loads was experimentally investigated by Lindberg (1964). A very thin shell (a/h=480) was loaded by an impulsive radial pressure over one side of the shell. The final shape of the shell showed a very high mode number of buckling (in terms of number of buckles) since the number of buckles around the circumference was between 50 to 100. The same experiment was carried out on a much thicker cylinder (a/h=19) and it was found that the radial velocity required to produce buckling was much higher than the previous case. The hoop strain was several percent, well into the plastic range, which resulted in another form of pulse buckling, which is called dynamic plastic flow buckling. The permanent wrinkles in the first case (a/h=480), elastic buckling, were found by late-time plastic hinges following the elastic buckling. Whereas in plastic flow buckling, the buckles form while the material throughout the entire wall thickness is flowing plastically from hoop compression. Resistance to buckling therefore comes from the plastic tangent modulus rather than from the elastic modulus. The tangent modulus in metals is typically about 100 times smaller than the elastic modulus. Therefore the

buckle wavelengths, which are proportional to the square root of the modulus (Lindberg and Florence, 1987), are about 10 times shorter than the elastic buckling.

As mentioned earlier, in the preceding chapter, there are two theories, namely plastic flow pulse buckling theory (Abrahamson and Goodier, 1962) and plastic pulse buckling theory (Lindberg, 1964), which present the analytical solution for plastic and elastic response of shells under impulsive loading.

3.2.1 Plastic theory

The wavelengths of buckles for impulsive loading are short compared with the shell length, therefore buckling from impulsive load is assumed to be independent of the axial coordinate. This gives an adequate description of buckling in the main span of the shell, where the buckle amplitudes are greatest and nearly constant along the length. With this simplification, the complexities of plastic flow buckling can be analysed with a reasonably simple theory.

For mathematical simplicity, the strain-hardening (tangent modulus) is taken to be constant. Dynamic plastic flow buckling with a strain-hardening modulus that decreases continuously with increasing compression strain will be discussed later in this chapter.

Cylindrical shells subjected to uniform impulsive external pressures of sufficient intensity exhibit a characteristic behaviour as indicated in Fig.3.1. The circle represents the original size (outer surface), and the thick black somewhat crumpled circle inside is the deformed shape at the end of the shell. It shows a general radius

reduction with wrinkles in a manner sufficiently regular to permit a count of the number of crests and troughs.

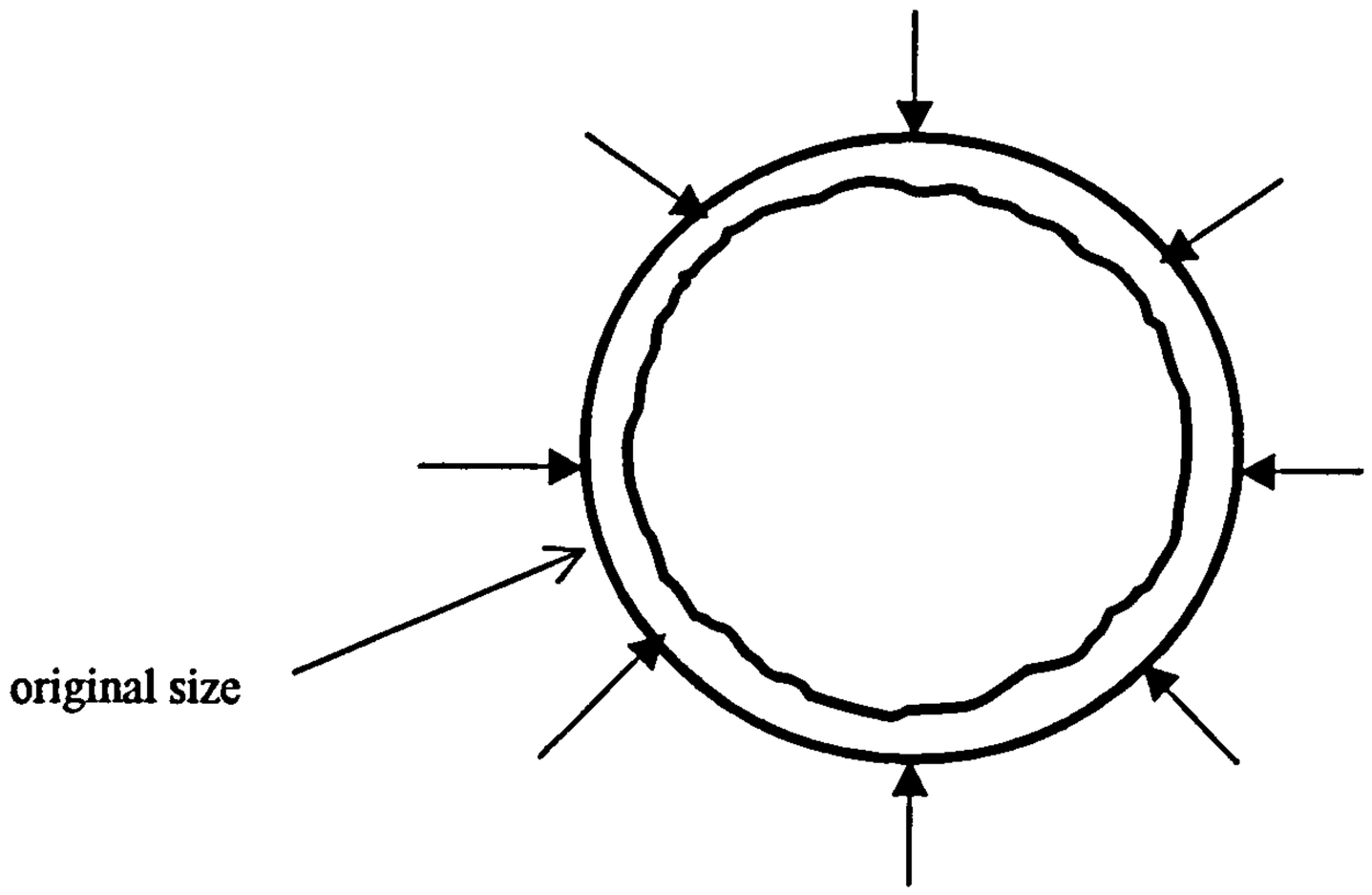

Fig. 3.1. Original and deformed shapes of idealised cylinder under uniform external impulsive loading

This section presents a theory of the formation of wrinkled shape, developed by Abrahamson and Goodier (1962), based on the dynamics of a metal shell that deforms plastically with a constant strain-hardening. It is considered that for a cylindrical shell loaded in such a manner, that all elements receive a large initial radial velocity simultaneously. In the absence of imperfections, the material flows into a uniform cylindrical shell of smaller radius (and thicker wall) until the initial kinetic energy has been absorbed in the work of plastic deformation. But with the inevitable small imperfections in the uniformity of initial velocity around the shell and the imperfections in the material properties and the shape (geometrical imperfections), there will be perturbations from this uniform converging motion. It would complicate matters to include all sorts of imperfections together. Instead, the basic problem is

taken as that of a geometrically and materially perfect cylindrical shell, with a slight imperfection in the uniformity of the initial velocity. There is consequently a departure from the circular form throughout the motion, but this is regarded as always small.

Neglecting rotary inertia, it can be shown from the element of shell (unit axial length of shell) in Fig.3.2. that

$$Q = \frac{\partial M}{\partial \lambda} \tag{3.1}$$

Q being the shear force and $d\lambda$, the arc element corresponding to $d\theta$.

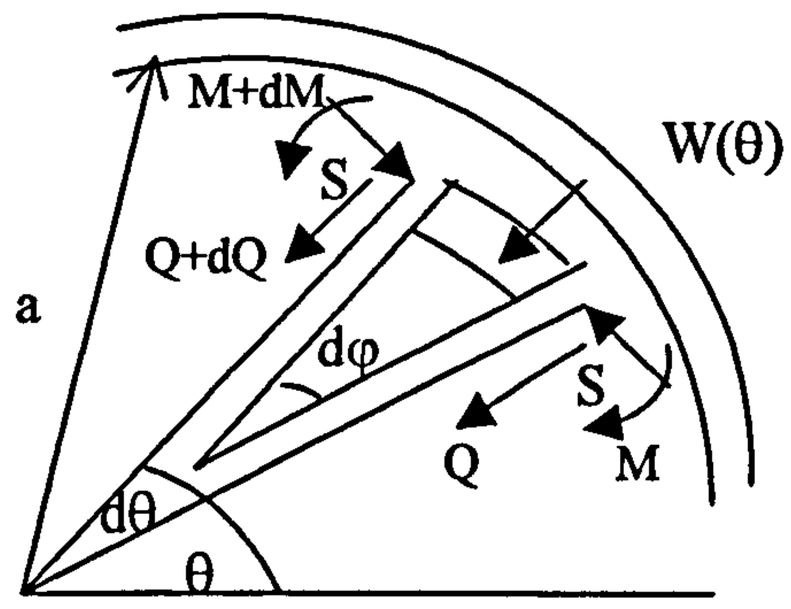

Fig.3.2. Element of shell in motion

where M is defined by:

$$M = E_t I \tag{3.2}$$

where $$I = \frac{1}{12} h^3$$

and E_t is tangent modulus and h is the shell thickness.

The dynamic equation for the radial motion is

$$\frac{\partial Q}{\partial \lambda} + S\frac{\partial \varphi}{\partial \lambda} = -m\frac{\partial^2 w}{\partial t^2} \qquad (3.3)$$

where w is the radial inward displacement, m is the mass per unit run of circumference and t is time.

For the curvature

$$\frac{\partial \varphi}{\partial \lambda} = \frac{1}{a} + \kappa \qquad (3.4)$$

where κ is the curvature which is defined by

$$\kappa = \frac{1}{a^2}\left[\frac{d^2 w}{d\theta^2} + w\right] \qquad (3.5)$$

Putting equation (3.4) in equation (3.3), eliminating Q by means of equation (3.1) and M by means of (3.2), one finds that w satisfies the equation

$$\frac{E_t I}{a^4}\left[\frac{\partial^4 w}{\partial \theta^4} + \frac{\partial^2 w}{\partial \theta^2}\right] + S\left[\frac{1}{a} + \frac{1}{a^2}\left(\frac{\partial^2 w}{\partial \theta^2} + w\right)\right] = -m\frac{\partial^2 w}{\partial t^2} \qquad (3.6)$$

It is convenient to change to dimensionless inward radial displacement and time

$$u = \frac{w}{a},\ \tau = \sqrt{\frac{E_t I}{ma^4}}t = \frac{1}{\sqrt{12}}\sqrt{\frac{E_t}{\rho}}.\frac{h}{a}.\frac{t}{a} \qquad (3.7)$$

where ρ is density, and to introduce the dimensionless constant

$$s^2 = \frac{Sa^2}{E_t I} = 12\frac{Sa^2}{E_t h} = 12\frac{\sigma a^2}{E_t h^2} \qquad (3.8)$$

where

$$\sigma = \frac{S}{h} \tag{3.9}$$

which is approximately the yield stress in simple compression. Then the equation (3.6) can be written in the form of

$$\frac{\partial^4 u}{\partial \theta^4} + (1+s^2)\frac{\partial^2 u}{\partial \theta^4} + s^2 u + \frac{\partial^2 u}{\partial \tau^2} = -s^2 \tag{3.10}$$

This is for a cylindrical shell that initially is perfectly circular. If instead it departs from the circular form by an initial displacement $w_i(\theta)$ in the unstressed state, and if one uses $w(\theta,t)$ for the additional inward radial displacement during the motion, equations (3.1), (3.2) and (3.3) remain unchanged, but equation (3.4) becomes

$$\frac{\partial \varphi}{\partial \lambda} = \frac{1}{a} + \frac{1}{a^2}\left[\frac{\partial^2}{\partial \theta^2} + 1\right](w_i + w) \tag{3.11}$$

and using the remaining equations (3.7) and (3.8) with the new meaning of w and u, equation (3.10) changes to

$$\frac{\partial^4 u}{\partial \theta^4} + (1+s^2)\frac{\partial^2 u}{\partial \theta^2} + s^2 u + \frac{\partial^2 u}{\partial \tau^2} = -s^2\left[1 + u_i + \frac{d^2 u_i}{d\theta^2}\right] \tag{3.12}$$

The above equation concerns the effect of velocity perturbations from impulsive loading discontinuities which allows one to calculate and determine the final shape of a cylindrical shell under impulsive loading with the plastic response where the strain-hardening is assumed to be constant. An example of using this equation and comparison with the experimental results are given by Lindberg and Florence (1987). In this example a buckled cylinder was produced with the experimental set-up using the explosive. A precise comparison of the experiment with the theory is not possible

because the nonuniformities in the experimental velocity distributions, which are required for the theory, are unknown. Instead, the number of buckles observed around the cylinder, which is independent of the nonuniformities, was compared with the theoretical results and qualitative comparisons were made of experimental and theoretical amplitudes and permanent strains showing good agreement.

3.2.1.1 Strain hardening

In order to study the actual behaviour of shells to impulse loads, it is necessary to use a more accurate description of strain hardening than the constant hardening modulus E_t used above. Tests on several alloys (Payton, 1961) show that an accurate description for strain hardening is given by

$$\frac{\sigma}{E_t} = \begin{cases} \sigma/E = \varepsilon & 0 \le \varepsilon \le \varepsilon_y \\ \varepsilon_y + K(\varepsilon - \varepsilon_y) & \varepsilon \ge \varepsilon_y \end{cases} \qquad (3.13)$$

Where E_t is the tangent modulus, E is Young's modulus, ε_y is the yield strain, and K is a parameter that describes the post-yield shape of the stress-strain curve. Large values of K describes stress-strain curves in which tangent modulus drops quickly after yield. Examples of stress-strain curves from the above formula are given in Fig. 3.3. Large values of K describe curves with abrupt yield, for which the tangent modulus drops quickly after yield. Small values describe more rounded curves with substantial strain hardening.

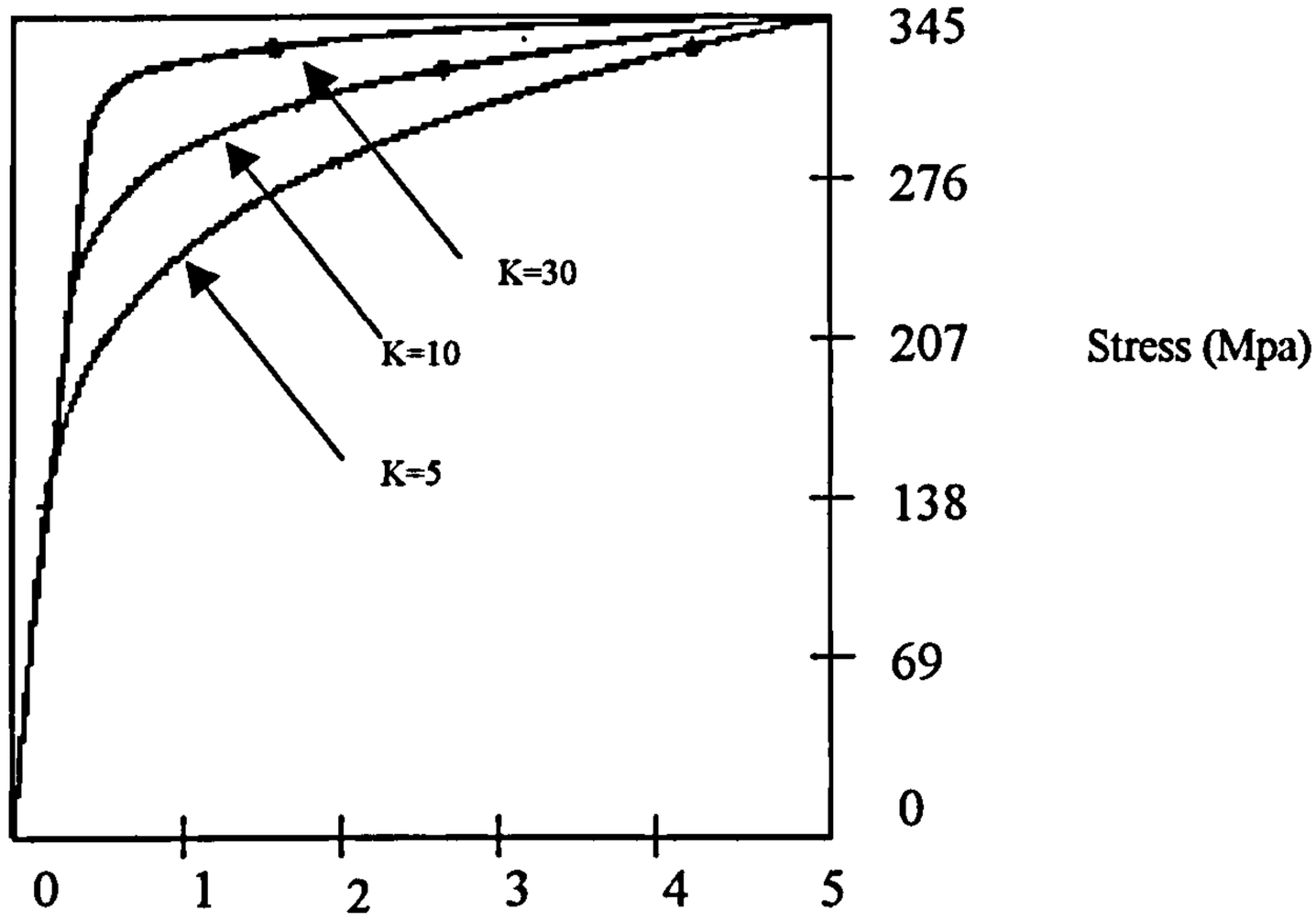

Fig. 3.3. Examples of stress-strain curves

3.2.1.2 Pressure impulse

Applying the short duration pressure *(P*)* rather than ideal impulse (initial velocity) and also considering stress-strain relationship described in equation (3.13), the plastic equation of motion, equation 3.12, (Anderson and Lindberg, 1968) becomes

$$\frac{\partial^4 u}{\partial \theta^4} + (1+s^2)\frac{\partial^2 u}{\partial \theta^2} + s^2 u + \left(\frac{1}{\alpha^2 \beta^2}\right)\frac{\partial^2 u}{\partial \tau^2} =$$

$$= -s^2\left[1 + u_i + \frac{d^2 u_i}{d\theta^2}\right] + \left(\frac{a}{\alpha^2 \beta^2 Eh}\right)P \qquad (3.14)$$

In order to treat a continuously changing tangent modulus, which varies from the elastic modulus at small strains to much smaller values given by equation (3.13) for plastic strains, the dimensionless time τ is that used above, for an ideal impulse, and additional dimensionless parameters, in equation (3.14), are introduced as follows:

$$\tau = \frac{ct}{a} \tag{3.15}$$

where

$$c^2 = \frac{E}{\rho}$$

and

$$\alpha^2 = \frac{h^2}{12a^2}\ ,\ \beta^2 = \frac{E_t}{E}\ ,\ s^2 = \frac{\sigma_\theta}{\alpha^2 E_t} \tag{3.16}$$

where σ_θ is the circumferential membrane stress.

And a dimensionless form of the external pressure P^*, including small non-uniform perturbations, is given by (Anderson and Lindberg, 1968),

$$P(\theta,\tau) = \left(\frac{a}{Eh}\right) P^*(\theta,\tau) \tag{3.17}$$

3.2.2 Elastic theory

The experimental results from Lindberg and Florence (1987) showed that when cylindrical shells are projected inward by an impulsive pressure, a characteristic form of dynamic wrinkling occurs at wavelengths determined by material tangent modulus

in plastic radial flow. In experiments on a very thin cylindrical shell (a/h=480), carried out by Lindberg (1964), it was observed that buckle wavelengths were six times those predicted by the plastic flow buckling theory. In these shells it was found that the duration of elastic motion was long enough that elastic buckles formed with amplitudes much larger than any initial imperfections at the plastic wavelengths. The elastic buckling also quickly reduced the average hoop stress so that radial plastic flow, which would have occurred in the absence of any velocity or displacement perturbations, never occurred. As a result, buckling was restricted to the elastic modes. Radial impulse above that for elastic unperturbed hoop motion served only to provide energy eventually absorbed by plastic hinges at the elastic buckle wavelengths.

A theoretical analysis of dynamic elastic pulse buckling, developed by Lindberg (1964) is presented in this section. Because the motion is elastic, another form of dynamic buckling can also occur which is called autoparametric vibration buckling. This is a special form of vibration buckling in which elastic vibrations in the hoop mode become unstable. At radial impulse well below that required to produce pulse buckling wrinkles as just described, the shell vibrates in and out in the hoop mode. Because of inevitable imperfections, flexural modes with natural frequencies near half that of the hoop mode begin to grow in amplitude by extracting energy from the hoop mode. Eventually, nearly all the energy can be transferred to a flexural mode. This vibration buckling is not discussed here and the elastic pulse buckling theory is only presented in this section.

The notation adopted is shown in Fig.3.4. The governing equation of motion for the elastic model are obtained using shallow-shell Donnel equations (Batdorf, 1947 and Lindberg, 1964) with the addition of inertia terms.

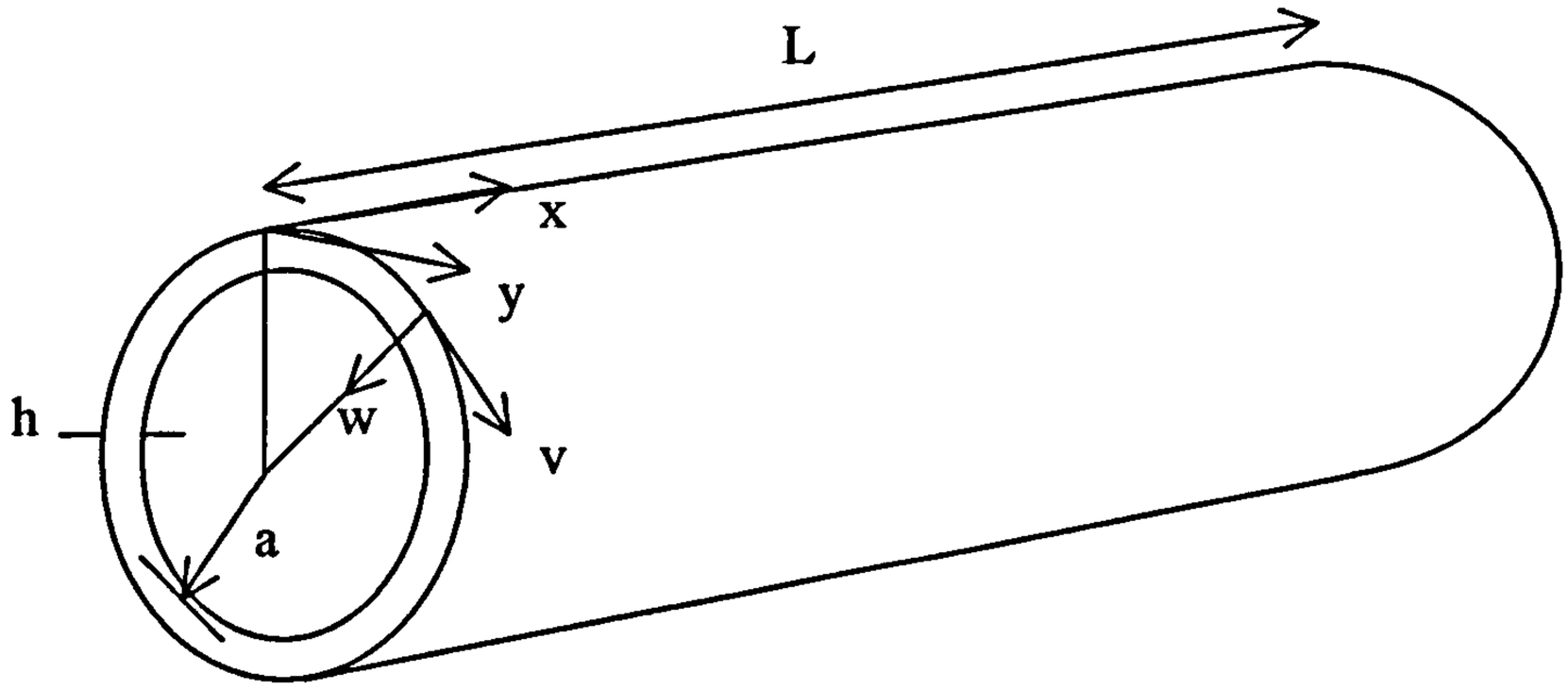

Fig.3.4. Coordinates and shell nomenclature

As in the static buckling analysis of cylindrical shells, the uniform radial deformation is assumed to be independent of the length and end conditions, but it is required that the superimposed flexural deformations satisfy the end constraints. This assumption allows the equation of motion to be separated into individual uncoupled equations for each mode.

The equation of equilibrium in the radial direction is

$$D\nabla^4 w + N_x \frac{\partial^2}{\partial x^2}(w + w_i) + \frac{2N_{x\theta}}{a}\frac{\partial^2}{\partial x \partial \theta}(w + w_i) + \\ + \frac{N_\theta}{a^2}\frac{\partial^2}{\partial \theta^2}(w + w_i) + \frac{N_\theta}{a} + ph\frac{\partial^2 w}{\partial t^2} - P^* = 0 \qquad (3.18)$$

where,

$$\nabla^4 = \nabla^2\nabla^2 = \left[\frac{\partial^2}{\partial x^2} + \frac{\partial^2}{\partial y^2}\right]^2$$

and N_x, $N_{x\theta}$, N_θ are the membrane forces with the sign convention chosen so that compression is considered positive, D is the flexural rigidity of the shell wall, and ∇^2 the Laplacian operator:

$$D = \frac{Eh^3}{12(1-\nu^2)} \tag{3.19}$$

$$\nabla^2 = \frac{\partial^2}{\partial x^2} + \frac{\partial^2}{a^2\partial\theta^2} \tag{3.20}$$

The force N_θ is taken as the sum of two parts, one caused by the uniform radial deformation and the other caused by flexural deformation; thus

$$N_\theta = \frac{Eh}{1-\nu^2}\frac{w_0}{a} + \frac{\partial^2 F}{\partial x^2} \tag{3.21}$$

where F is the stress function for the membrane forces produced by flexural deformations and w_0 is the uniform radial deformation. The membrane forces N_x and $N_{x\theta}$ are assumed to be independent of the uniform radial motion, and for the flexural motion are given in the usual manner in terms of F:

$$N_x = \frac{\partial^2 F}{a^2\partial\theta^2} \tag{3.22}$$

$$N_{x\theta} = -\left(\frac{\partial^2 F}{a\partial\theta\partial x}\right) \tag{3.23}$$

and F is obtained by the compatibility condition between the mid-surface strains as follows:

$$\nabla^4 F = \left(\frac{Eh}{a}\right)\left(\frac{\partial^2 w}{\partial x^2}\right) \tag{3.24}$$

A series of experiments has been performed by Lindberg and Florence (1987) to demonstrate the essentials of the theory are correct. They used the explosive to apply the pressure to a cylindrical vessel for a number of loading durations. They found that the results from long duration loading compare well with the theory. However if the duration is very short the plastic theory should be used.

3.3 Conclusions

Analytical solutions of cylindrical shell structures to uniform pressure pulse loading were explained in this chapter. Abrahamson and Goodier (1962) plastic theory and Lindberg (1964) elastic theory were presented with a number of assumptions in order to simplify the theories. However to predict and determine the actual response and behaviour of shell structures to pulse loads, it is necessary to consider all imperfections i.e. loading, geometry and material defects. Therefore analytical solutions of the dynamics of shells are not complete and accurate enough due to the complex kinematics of the response which leads to the requirement of a high degree of symmetry in the geometry and applied loads. However these developed theories enable a priori judgement of the form of solution. The elasto-plastic response of shell is too complex to allow a proper analytical solution.

Numerical methods such as finite element analysis provide a powerful and fast method of analysing non-linear problems when the structures are subjected to large deformations. It also enables the analysis of shell structures with imperfections and non-uniformity in the shell shape and pressure impulsive loading. Therefore the finite element method provides the freedom to solve very complex structural problems due to its division into thousands of elements.

A series of non-linear transient finite element analyses, using the ANSYS finite element code, on various geometries subjected to pressure impulsive loading will be presented in the next chapter.

4. NUMERICAL ANALYSES

4.1 Introduction

The review of the studies of transient dynamic response of cylindrical shell structures for different radius to thickness ratios and also the plastic and elastic theories for cylindrical structures under transient pressure loading have been carried out in the preceding chapters. In order to investigate the effects of dynamic pressure loading on shell structures, a plastic, elastic and elasto-plastic analysis, using the ANSYS finite element code, are performed in this chapter. The effects of the various pulse models and also pulse duration on the response of the structure to transient loading are also investigated.

As explained in earlier in the literature review and referred to in Anderson and Lindberg (1968), the response of the shell structure can be plastic, elastic or elasto-plastic depending on the radius to thickness ratio. For the elastic and plastic cases, an

external pressure transient load is applied whereas the internal spot (localised) pressure transient load is considered for the elasto-plastic case. The results are compared with experimental available results from the literature.

4.1.1 ANSYS finite element code

ANSYS is a general purpose finite element programme. Many different types of problems may be analysed using the code. Some examples would include: structural, thermal, magnetic field, electric field, and fluids analyses. ANSYS is also a self contained programme in that the Pre-processor (model definition), Processor (solver), and Post-processor (output) are all integrated into a single code.

All models including 3D finite element models in this chapter are solved using ANSYS which has a wide range of capabilities including the transient dynamic analysis.

4.1.2 Transient dynamic analysis

Transient dynamic analysis, also called time-history analysis, is a technique used to determine the dynamic response of a structure under the action of any general time-dependent loads. This type of analysis may be used to determine the time-varying displacements, strains, stresses, and forces in a structure as it responds to any combination of static, transient, and harmonic loads. The time scale of the loading is such that the inertia or damping effects are considered to be important. In this

chapter, this type of analysis is used to determine the response of shell structures to pressure transient loading.

The basic equation of motion solved by a transient dynamic analysis is

$$[M]\{\ddot{u}\}+[C]\{\dot{u}\}+[K]\{u\}=\{F(t)\} \tag{4.1}$$

where

$[M]$: mass matrix

$[C]$: damping matrix

$[K]$: stiffness matrix

$\{\ddot{u}\}$: nodal acceleration vector

$\{\dot{u}\}$: nodal velocity vector

$\{u\}$: nodal displacement vector

$\{F(t)\}$: load vector

At any time t, these equations can be thought of as a set of "static" equilibrium equations that also take into account inertia forces, $[M]\{\ddot{u}\}$, and damping forces, $[C]\{\dot{u}\}$.

4.2 Plastic response

In order to observe the plastic response of the cylindrical vessels to blast loading, a case study, for which experimental results as well as finite difference and finite strip analyses results have been reported, is analysed here by the ANSYS code. As will be seen, the response of the above mentioned pressure vessel is perfectly plastic.

The main objective of this section is firstly to observe the plastic response of the shell structure and more importantly is to show that the results obtained by the present analysis are in a good agreement with the other available results, which assist the further investigations.

4.2.1 Descriptions

The transient analysis of a cylindrical vessel structure under external explosive loading using the finite element method is investigated here. The experimental results of the case, which is analysed here, have been obtained from Lindberg and Sliter (1969) and a finite difference analysis has been carried out by Underwood (1972). The finite strip analysis of the case has been also reported by Jiang and Oslon (1991).

The parameters and the loading conditions of the case are as follows:

4.2.1.1 Parameters

Material: Aluminium

Length: $l = 15.24$ cm

Radius: $a = 7.62$ cm

Thickness: $h = 0.3175$ cm

Modulus of elasticity: $E = 6.8 \times 10^4$ MPa

Tangent modulus: $E_t = 0$ MPa

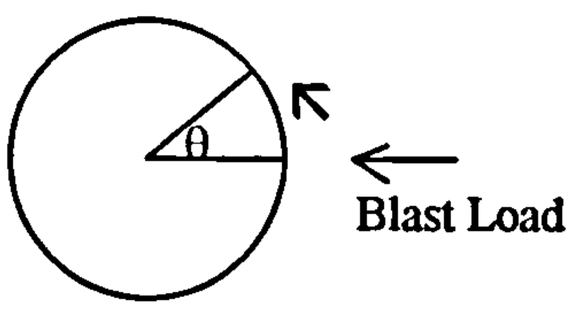

Yield stress: $\sigma_y = 2.8 \times 10^2$ MPa

Density: $\rho = 30479$ kg/m^3

Poisson's ratio: $\nu = 0.3$

4.2.1.2 Loading

The ends of cylinder were taken as clamped. The shell was loaded by a spherical explosive charge off to one side of the shell in the experiment (Lindberg and Sliter, 1969). The following experimental formula was fitted to the experimentally measured peak pressures on a rigid cylinder which is used in the present finite element analysis:

$$P(\theta,t) = [(P_R - P_I)\cos^2\theta + P_I]P_0(t) \qquad -90 \le \theta \le 90 \qquad (4.2)$$

$$P(\theta,t) = P_I P_0(t) \qquad |\theta| > 90 \qquad (4.3)$$

where

$$P_0(t) = exp.\ [-t/t_0] \qquad (4.4)$$

and $t_0 = I / P_R$. Here I is the unit impulse measured at $\theta = 0$ and P_R and P_I are the reflected and incident pressure, respectively.

The analysis has been carried out for $P_R = 56.53\ MPa$, $P_I = 8.27\ MPa$ and $t_0 = 31$ μsec. These data were suggested by Lindberg and Sliter (1969) to satisfy the above equation for the experimentally applied pressure in their experiments.

Fig. 4.1 and Fig. 4.2, respectively, show the pressure-time profile for the above case when $\theta = 0$ and also pressure around the cylinder for t = 31 μsec.

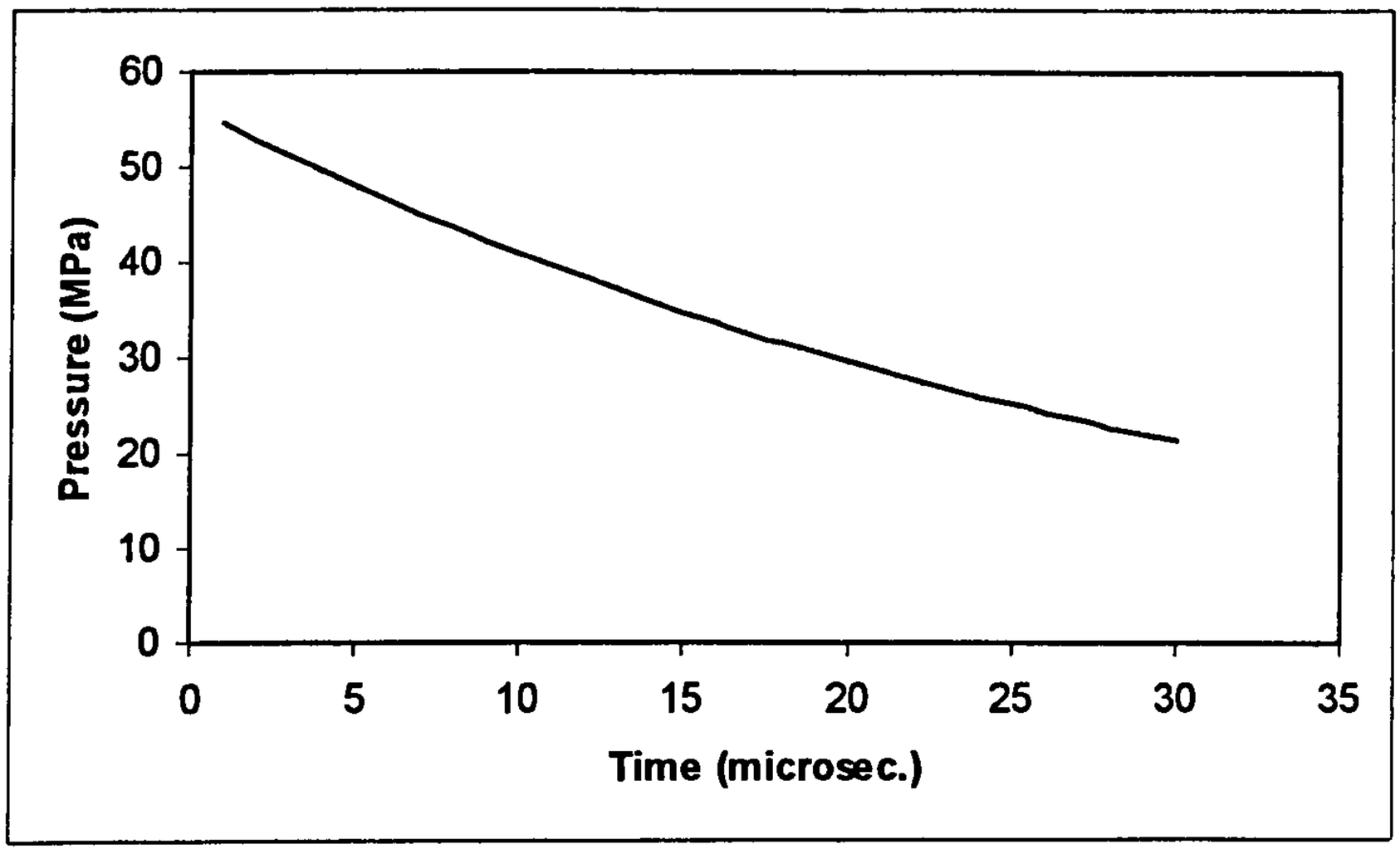

Fig 4.1. Pressure-time profile for $\theta = 0$

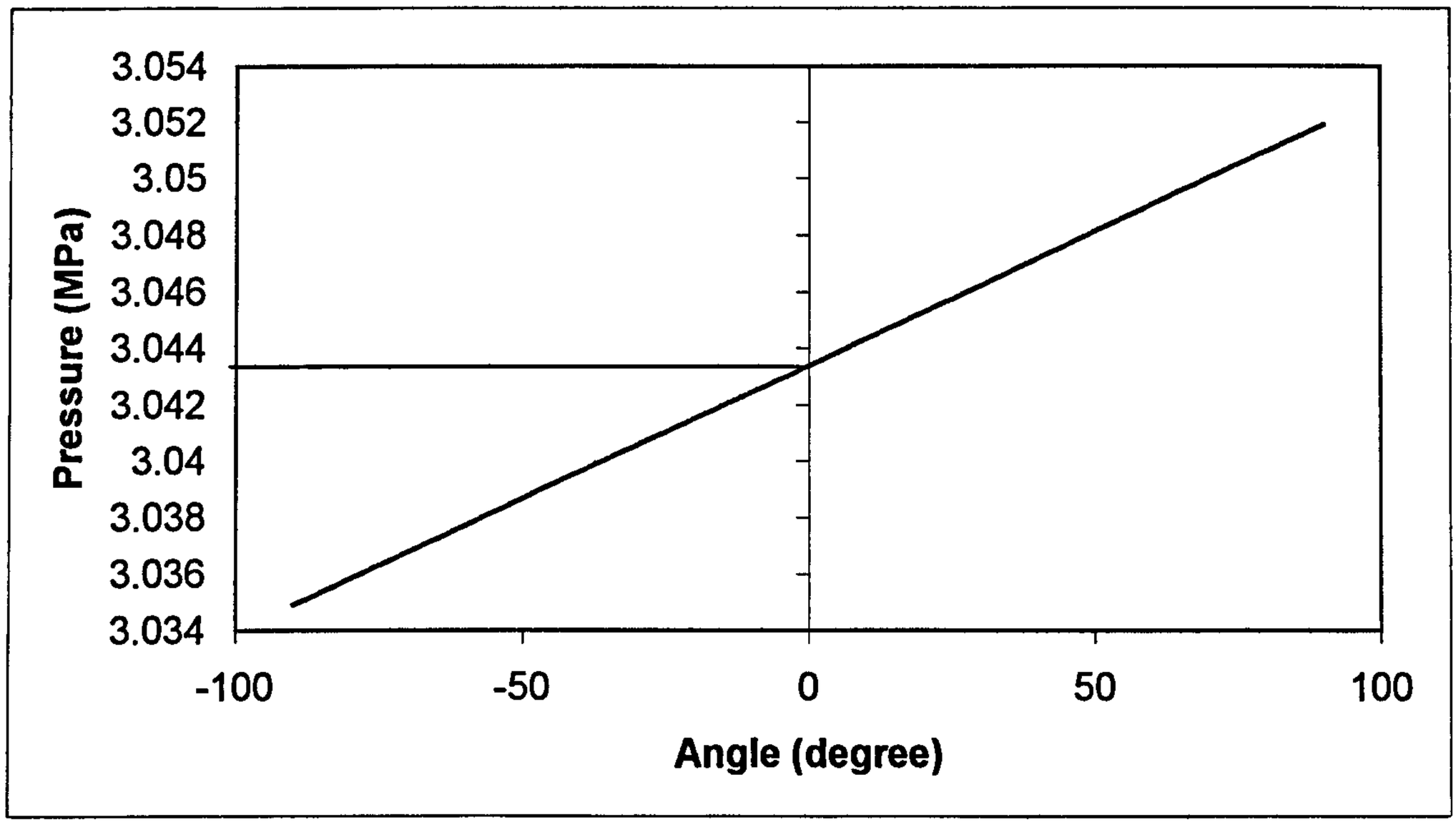

Fig.4.2. Pressure profile around the cylinder when t = 31 microseconds

4.2.1.3 Nonlinearity

The radius to thickness ratio of the cylinder is: $a/h = 3/0.125 = 24$. Therefore, according to chapter 1, the response of this cylindrical vessel to blast loading is perfectly plastic.

The stress-strain relationship of the material has been assumed to be elastic-perfectly plastic as shown in Fig.4.3. This assumption was used by Lindberg and Sliter (1969), Underwood (1972) and Jiang and Oslon (1991) for the analysis.

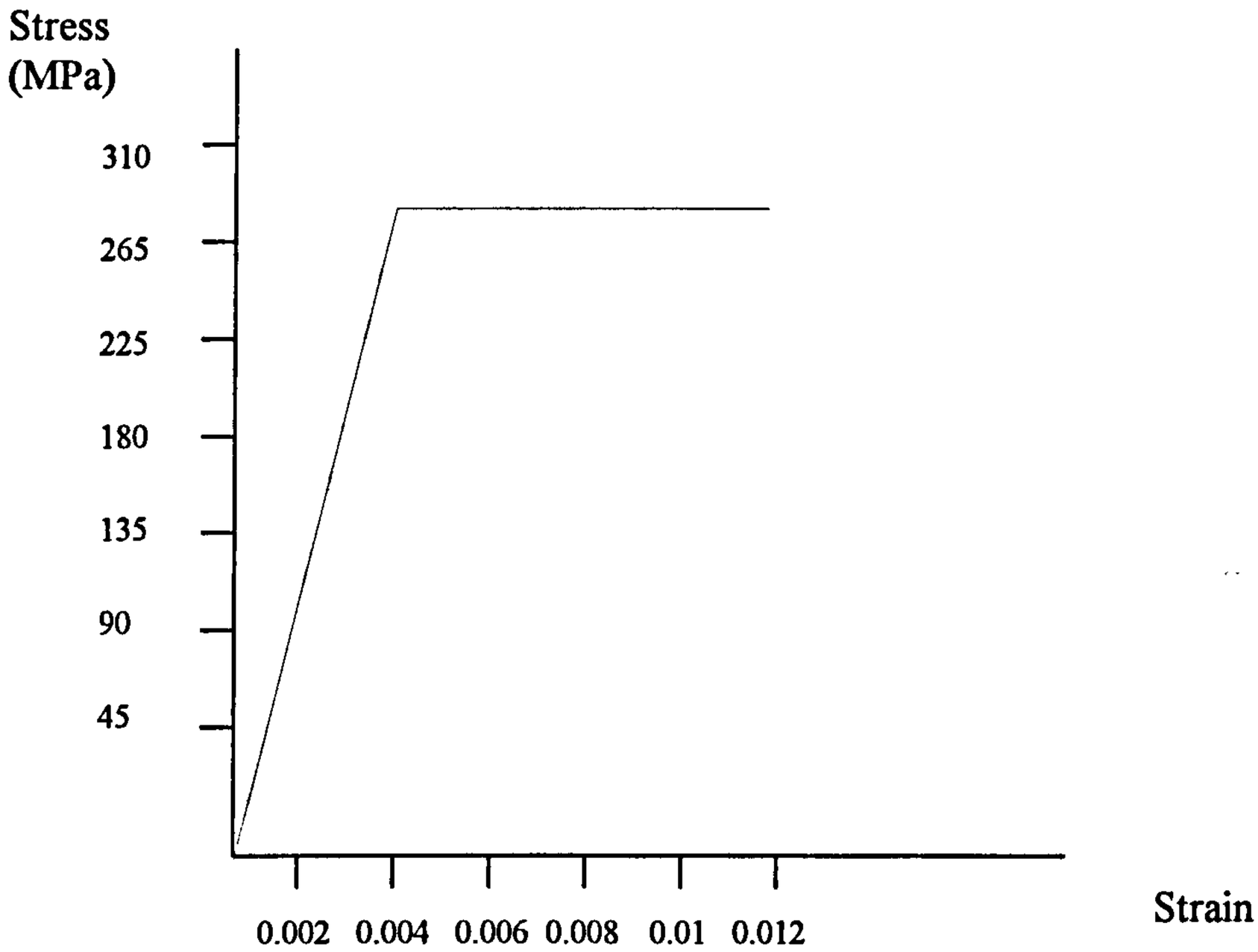

Fig.4.3. Stress-strain relationship for the material

4.2.2 Results and comparisons

A non-linear transient finite element analysis on the cylindrical vessel under explosive loading is now presented. 192 eight-noded shell elements (Shell 82) were used to model the structure and exponential modelling was used for the loading.

The modal analysis of the pressure vessel was first undertaken to determine its natural frequencies as there is no analytical solution to calculate the fundamental frequency for this case. This enables the calculation of the proper integration time step for the transient analysis of the case. Integration time step (*ITS*) was then calculated by the ANSYS (finite element code) recommended *1/(20f)* formula where *"f"* is the fundamental frequency of the structure. The fundamental frequency of the case was determined by Jiang and Oslon (1991) to be *3270 Hz*. The above named

frequency was obtained equal to *3265.6* Hz by the present analysis which is very close to the reported value.

Fundamental frequency (Hz)	
Finite strip (Jiang and Oslon, 1991)	Finite element (present study)
3270	**3265.6** (192 shell elements) 2943.7 (160 shell elements) 2379.3 (128 shell elements)

Table 4.1. The comparison of the calculated fundamental frequencies

The transient analysis of the case was then carried out by the ANSYS code. The undeformed and permanently deformed shapes of the cylinder are shown in Fig.4.4.

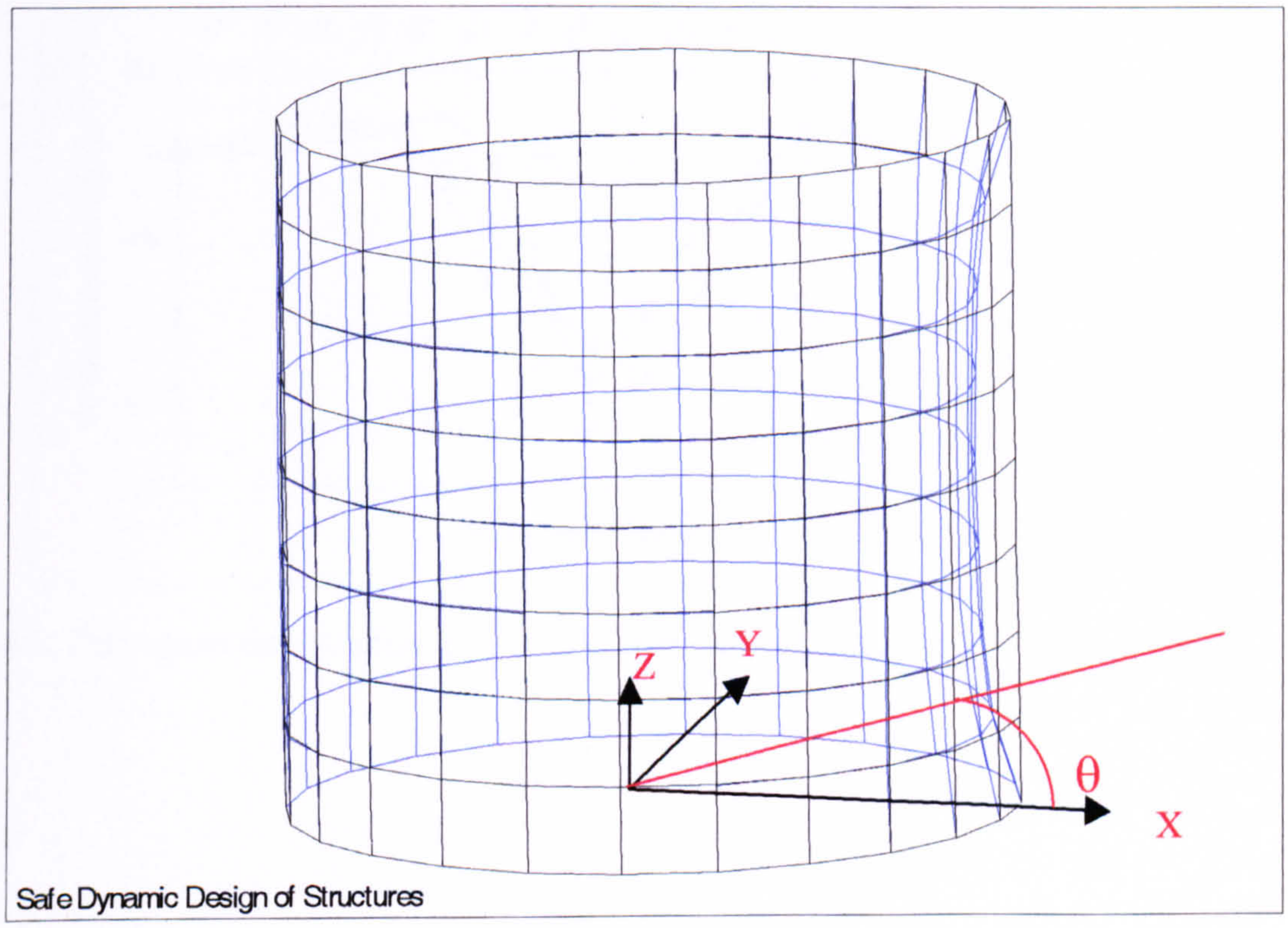

Fig.4.4. Undeformed and permanently deformed (after removing the load) shapes - for load defined by equations 4.2 – 4.4

Fig.4.5 and Fig.4.6 show the circumferential and longitudinal distributions of the permanent radial displacements from the present analysis as well as the other reported ones. Permanent deformation means the final shape of the structure after removing the load from structure. It can be seen that the results of finite strip analysis are not in good agreement with the experimental results near the ends of the cylinder, and, the finite difference analysis does not give good results near the middle of the shell compared to the experimental results. Although the finite strip method and finite difference method have been acceptable methods compared to experiments (Jiang and Oslon, 1993) as the above comparisons were made, the present finite element method performs better results compared to the experimental one which means the results from the current analysis represent good results both in the corners and the middle of the graph.

Fig.4.6. Permanent deformation at $z=L/2$ vs. circumferential location

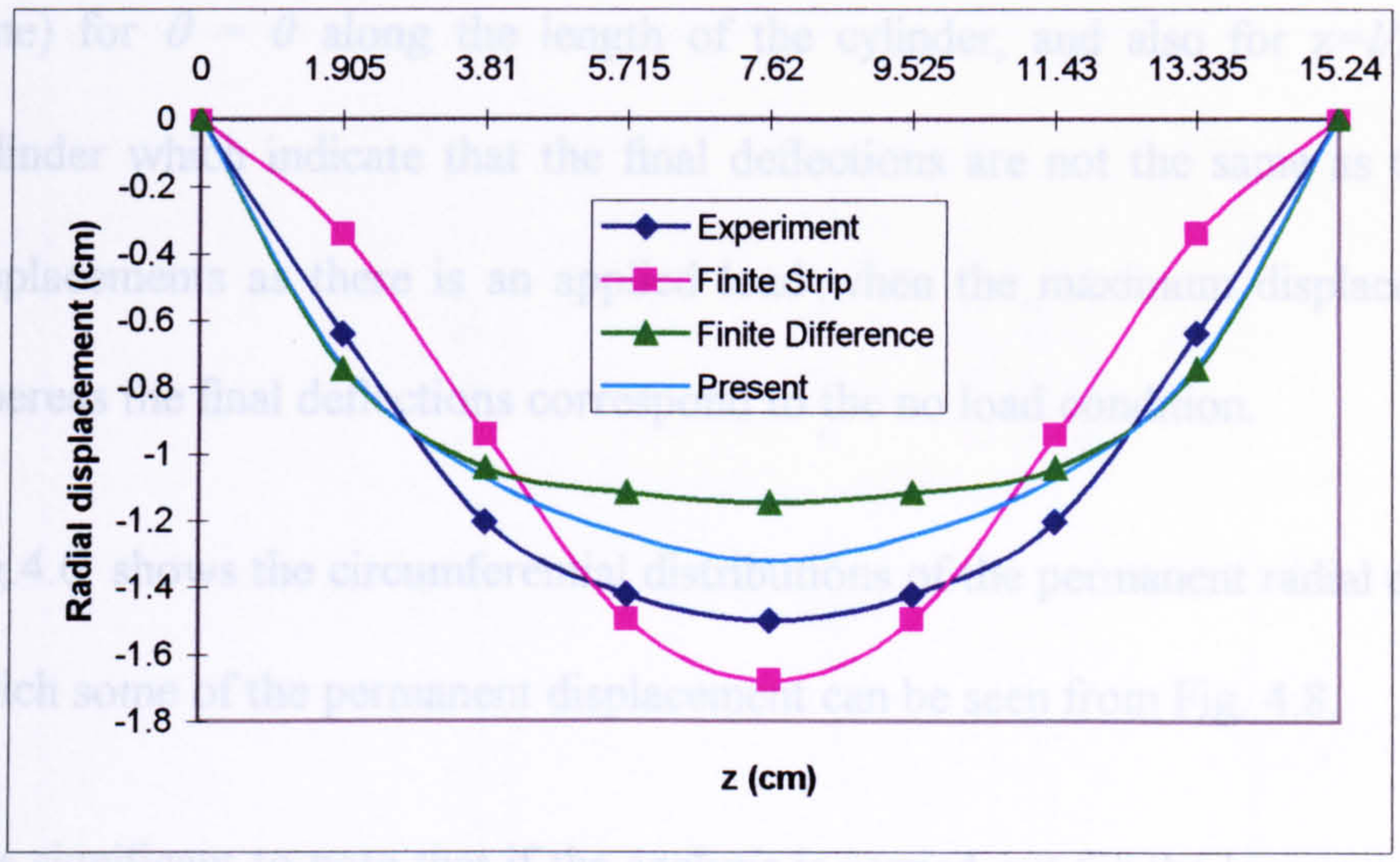

Fig.4.5. Permanent deformation at $\theta = 0$ vs. meridional location

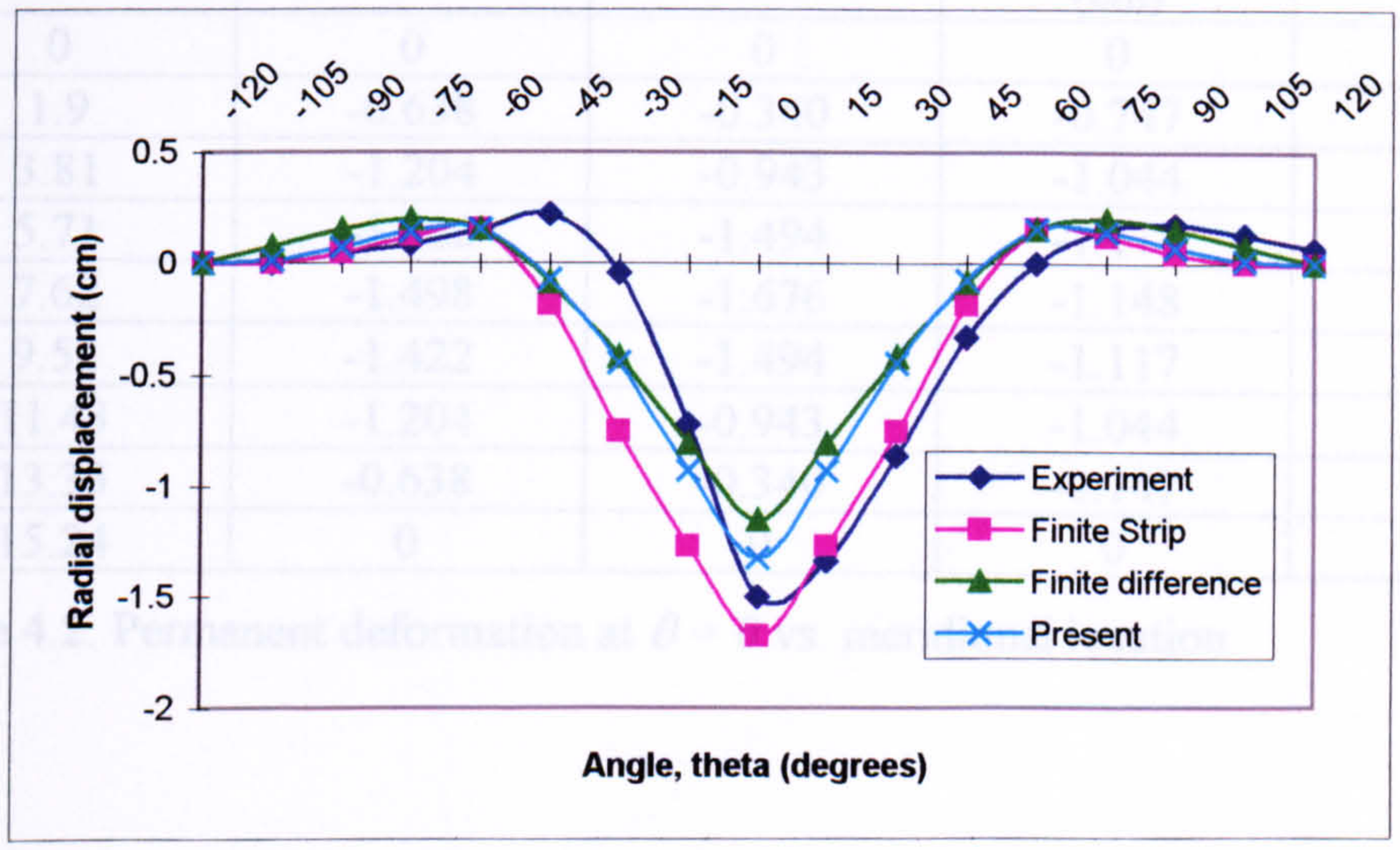

Fig.4.6. Permanent deformation at z=*l/2* vs. circumferential location

Finally, Fig.4.7 and Fig.4.8 show the transient responses (radial displacements versus time) for $\theta = 0$ along the length of the cylinder, and also for $z=l/2$ around the cylinder which indicate that the final deflections are not the same as the maximum displacements as there is an applied load when the maximum displacement occurs whereas the final deflections correspond to the no load condition.

Fig.4.6. shows the circumferential distributions of the permanent radial displacements which some of the permanent displacement can be seen from Fig. 4.8.

It is significant to note that if the analysis is carried out for the longer period of time, the final deflection of the points in Fig. 4.7. and Fig.4.8. will not be altered.

x (cm)	Experiment (cm)	Finite Strip (cm)	Finite Difference (cm)	Present (Finite Element) (cm)
0	0	0	0	0
1.9	-0.638	-0.340	-0.747	-0.736
3.81	-1.204	-0.943	-1.044	-1.074
5.71	-1.422	-1.494	-1.117	-1.244
7.62	-1.498	-1.676	-1.148	-1.320
9.52	-1.422	-1.494	-1.117	-1.244
11.43	-1.204	-0.943	-1.044	-1.074
13.33	-0.638	-0.340	-0.747	-0.736
15.24	0	0	0	0

Table 4.2. Permanent deformation at $\theta = 0$ vs. meridional location

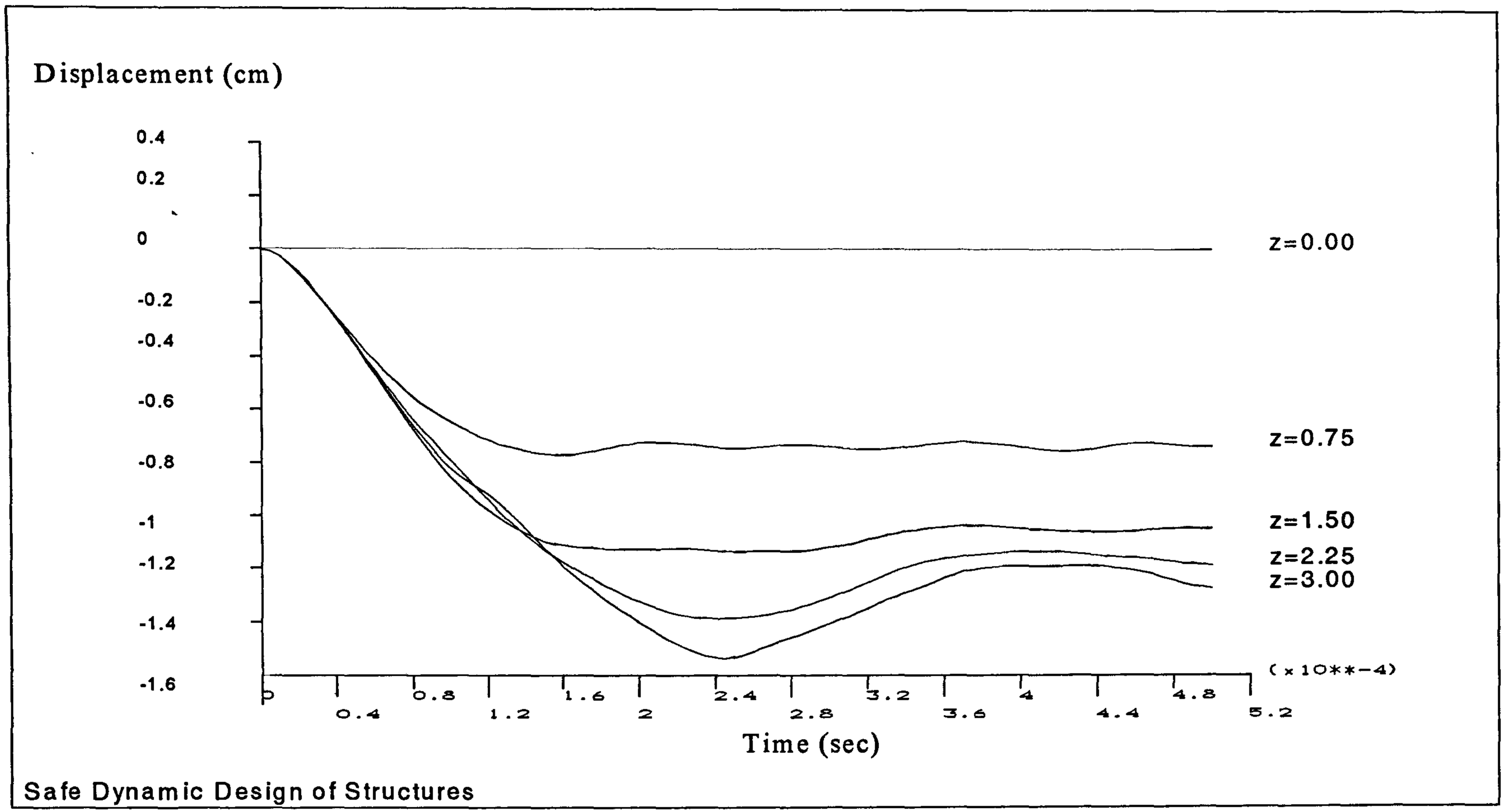

Fig.4.7. Transient responses for $\theta = 0$ with different z

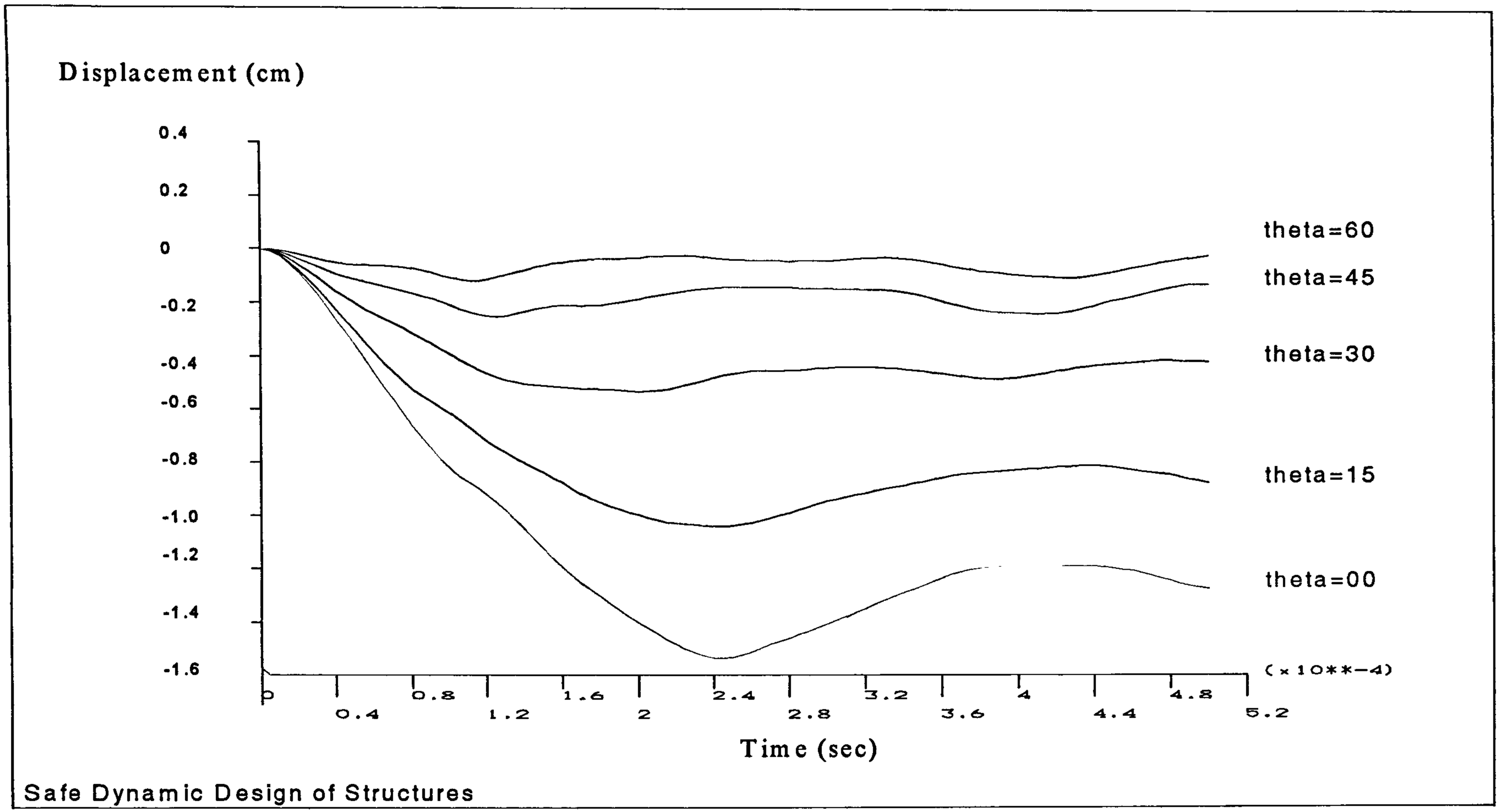

Fig.4.8. Transient responses for $z = l/2$ with different θ

4.2.3 Discussions

A case study has been carried out using ANSYS and the results have been compared to existing experimental, finite difference and finite strip results. The results obtained from the present finite element analysis are very close to the experimental results, whereas there are considerable discrepancies between both the finite difference and the finite strip results and the experimental results.

Differences may be due to the idealised analysis. In other words, the geometry and loading imperfections in both shell geometry and loading should be considered in the numerical analysis. However, as observed, the results of the present analysis are in reasonable agreement with the experimental ones.

4.2.4 Large structures

In order to extend the code validation process to vessels of chemical plant size experiencing pulse loading, numerical analysis is applied to one of the vessel designs associated with the Flixborough incident (Gugan, 1979).

The exponential modelling refers back to equations (4.2) and (4.3). 192 eight-noded shell elements were used for the analysis. The finite element model of the cylinder is quite similar to the one in Fig.4.4. The tank is made of carbon steel with the following parameters:

Material: Carbon steel, Length: l=609.6 cm., Radius: a=304.8 cm., Thickness: h=6.09 cm., Modulus of Elasticity: $E = 2.06\times10^5$ MPa, Tangent Modulus: $E_t = 0$ MPa, Yield

Stress: σ_y=3.44×10^2 MPa, Density: ρ=8200 kg/m^3, Poisson's Ratio: ν=0.3, P_R = 4.8 MPa, P_I = 1.03 MPa and t_0 = 3.1 msec.

As it can be seen from the above values, the stress-strain of the material is assumed to be elastic-perfectly plastic in this case too. Therefore the stress-strain curve of the material is similar to Fig. 4.3.

The modal analysis was first carried out and the fundamental frequency was determined to be 62.62 Hz. The transient response for the critical node (θ = 0 & z = l/2 = 304.8 cm.) is illustrated in Fig.4.9.

The main objective of the above analyses was to ensure the capability of ANSYS program to be used for dynamic analysis. The above aluminium and steel cases showed that by just simplifying the analyses without considering the imperfections ANSYS can present reasonable results compared to the experimental ones and also in the large and small case studies. Therefore ANSYS is to be used through the research here to study the dynamic behaviour of structures. The detailed experimental results for the large case are not available to discuss and compare with numerical results.

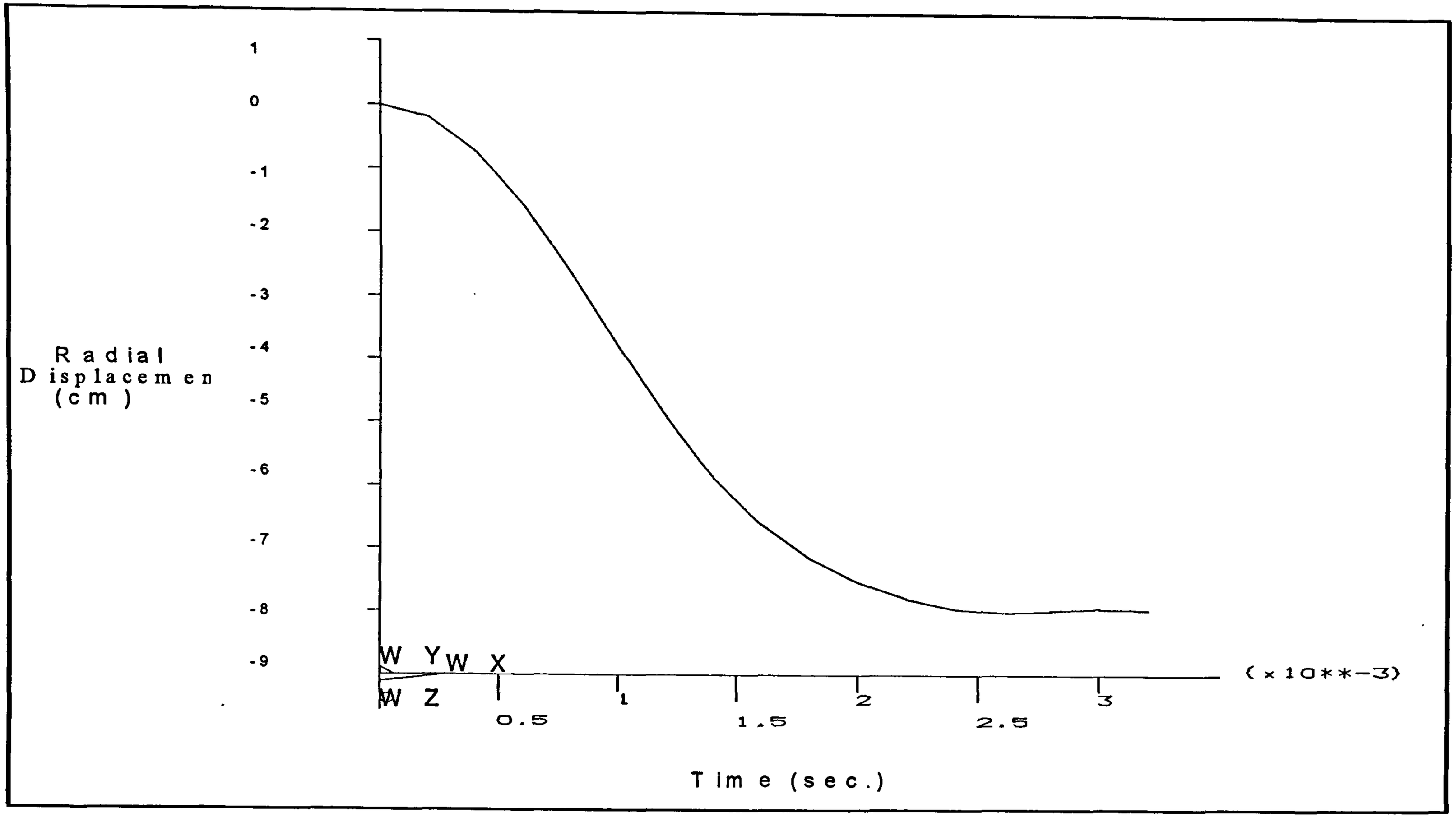

Fig.4.9. Transient response of the critical node

4.3 Pulse modelling and duration

In this section, the effect of different type of impulsive load modelling and load duration on the shell structural behaviour due to pressure transient loading are investigated. All analyses for this study are carried out for the plastic response of the shell which were performed in the last section on the aluminium case in section 4.2.1.1. (Fig. 4.4).

4.3.1 Pulse models

Various modelling techniques for explosion modelling are now discussed here. So far, the explosive loading has been modelled as an exponential curve. Triangular and rectangular modelling are now considered, and a comparison of the effects of these three types of load modelling, i.e. triangular, rectangular and exponential, on the response of the cylindrical vessel is made. In order to achieve this purpose, $P_0(t)$ requires to be changed in equation (4.4), so that 'I', which is the total impulse, is equal for all cases. In other words:

$$P_0(t) = \text{exp.}\,[-t/t_0] \qquad (4.5)$$

where $t_0 = 31\ \mu\text{sec.}$

$$I = P_0(t).dt = \text{exp.}[-t/t_0].dt = P_0(\text{max.}).t_0 \qquad (4.6)$$

The duration of the other two types of modelling namely rectangular and triangular were chosen so that the impulse, 'I', is equal for all cases.

These three shapes are illustrated in Fig.4.10.

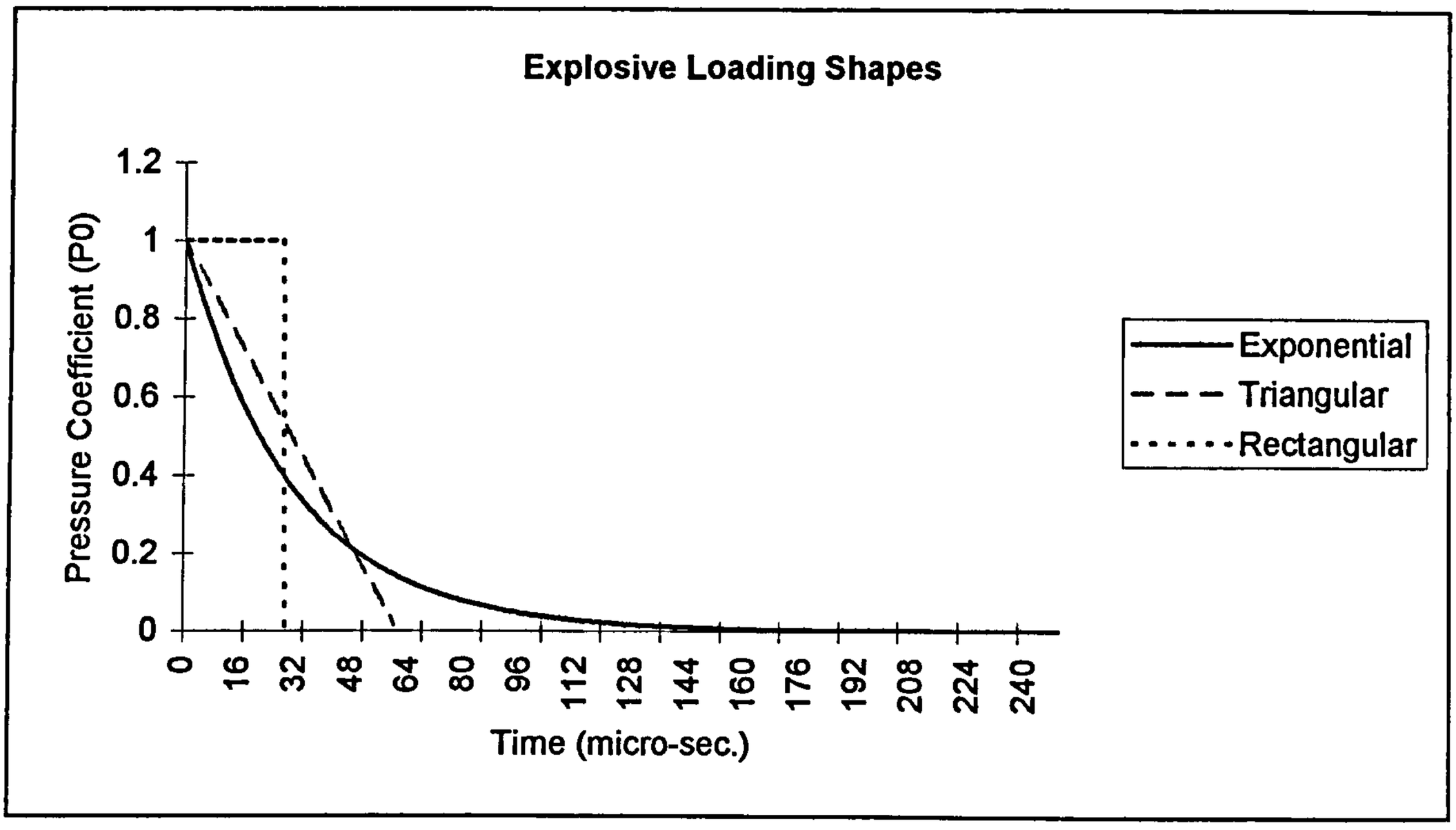

Fig.4.10. Explosive loading shapes

The above three shapes of explosive loading were applied to the small cylindrical vessel which was analysed in the last section (Section 4.2.2) with the plastic response, and consequently, the following transient displacements, for $\theta = 0$ and $z = l/2 = 7.62\ cm.$, were obtained. Fig.4.11. shows the comparison amongst the response of the shell to the different load types.

Changing the shape of explosion modelling does not change the behaviour of the structure in terms of plasticity however it does affect the final deflection of the structure which is shown in Fig.4.11.

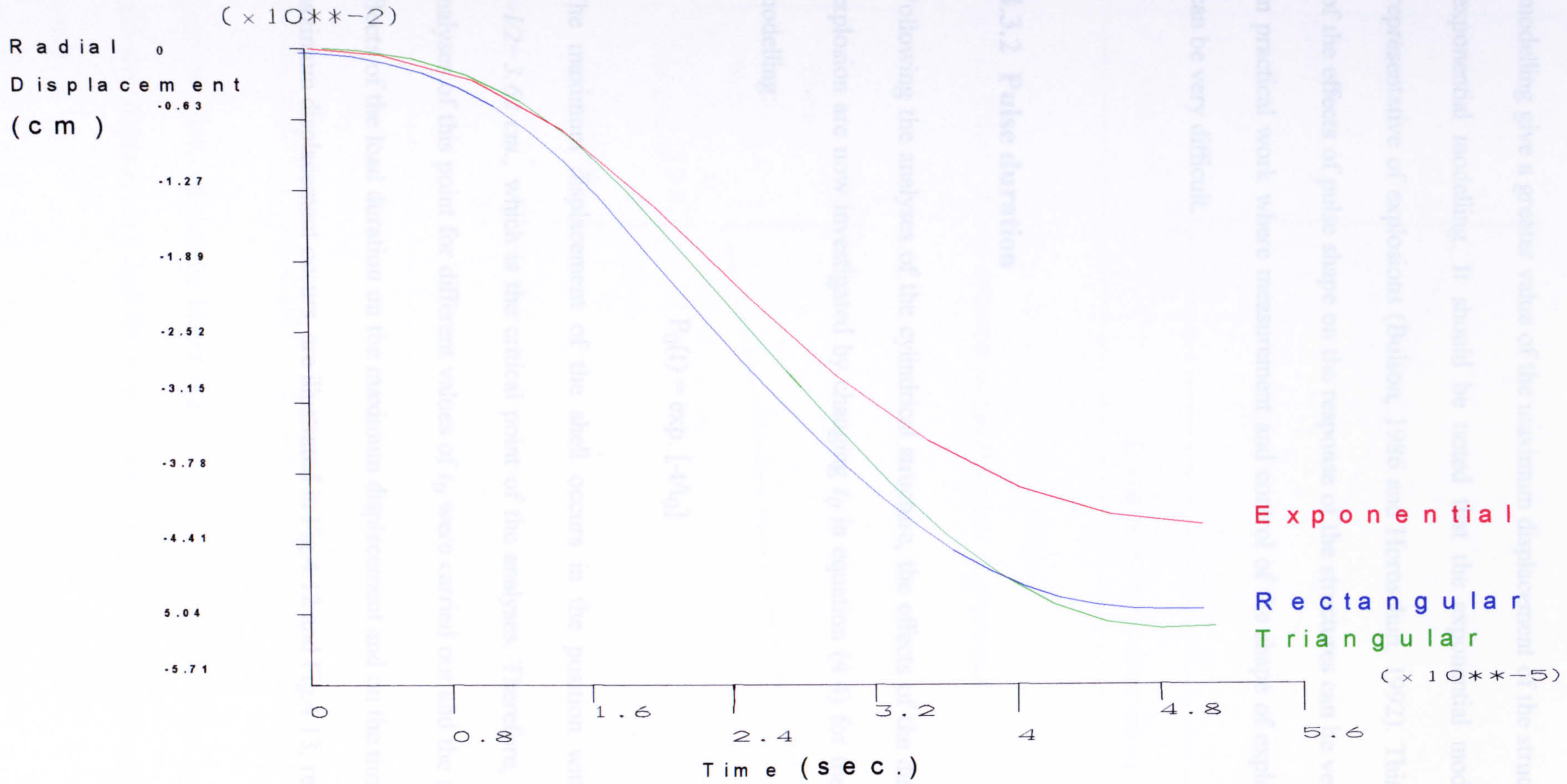

Fig.4.11. Transient deformation for different explosion load shapes

A comparison of the above results reveals that the triangular and rectangular modelling give a greater value of the maximum displacement of the structure than the exponential modelling. It should be noted that the exponential modelling is the representative of explosions (Bulson, 1986 and Horoschun, 1992). This comparison of the effects of pulse shape on the response of the structures can be very significant in practical work where measurement and control of the shape of explosive loading can be very difficult.

4.3.2 Pulse duration

Following the analyses of the cylindrical structure, the effects of the duration of the explosion are now investigated by changing t_0 in equation (4.4) for the exponential modelling:

$$P_0(t) = \exp.\ [-t/t_0] \qquad (4.7)$$

The maximum displacement of the shell occurs in the position with $\theta = 0$ & $z=l/2=3.62\ cm.$, which is the critical point of the analyses. Therefore, the transient analyses of this point for different values of t_0 were carried out and the results of the effects of the load duration on the maximum displacement and on the time during this maximum displacement occurs, are illustrated in Fig.4.12 and Fig.4.13, respectively.

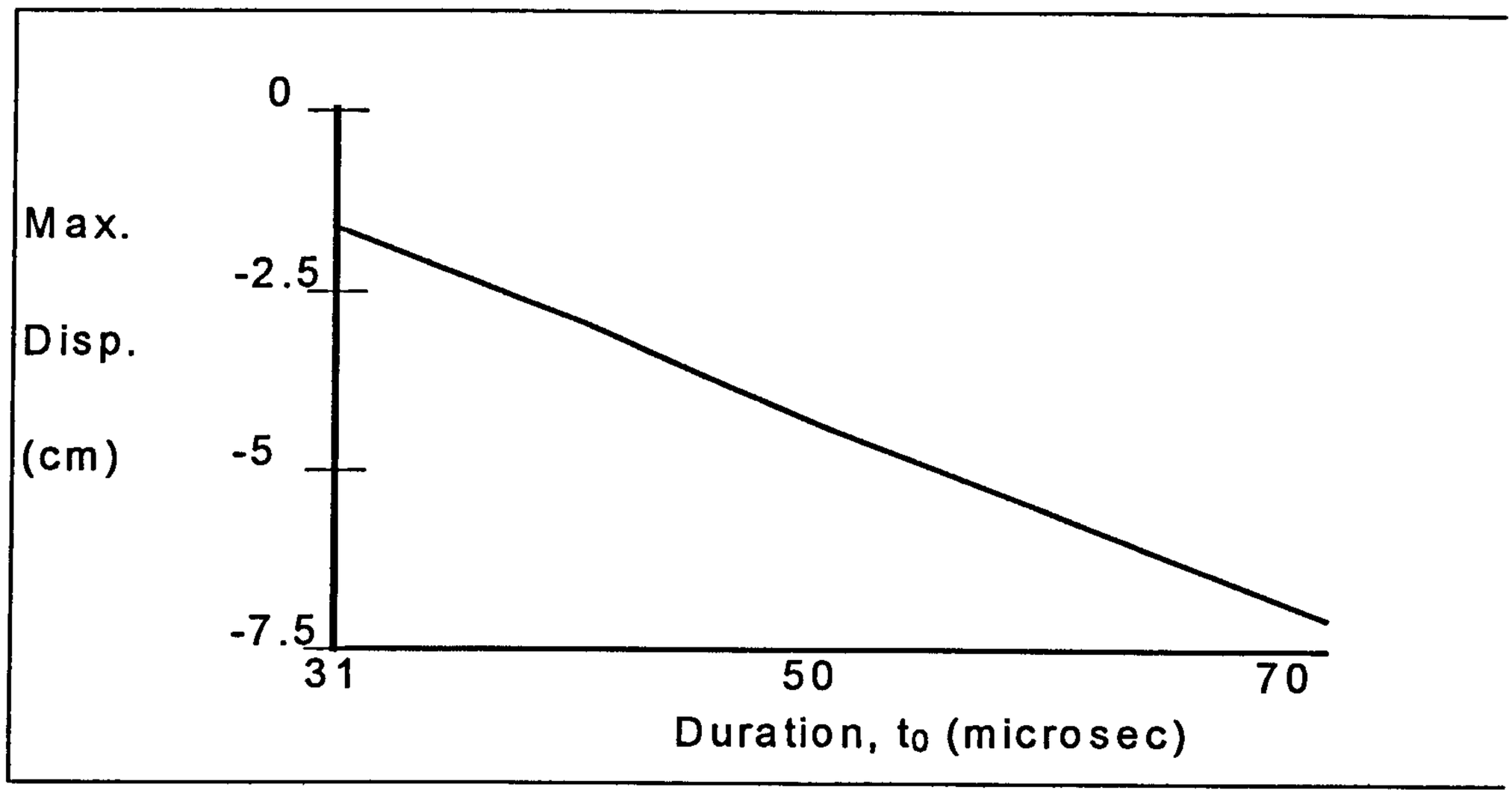

Fig.4.12. Effects of load duration on the maximum displacement

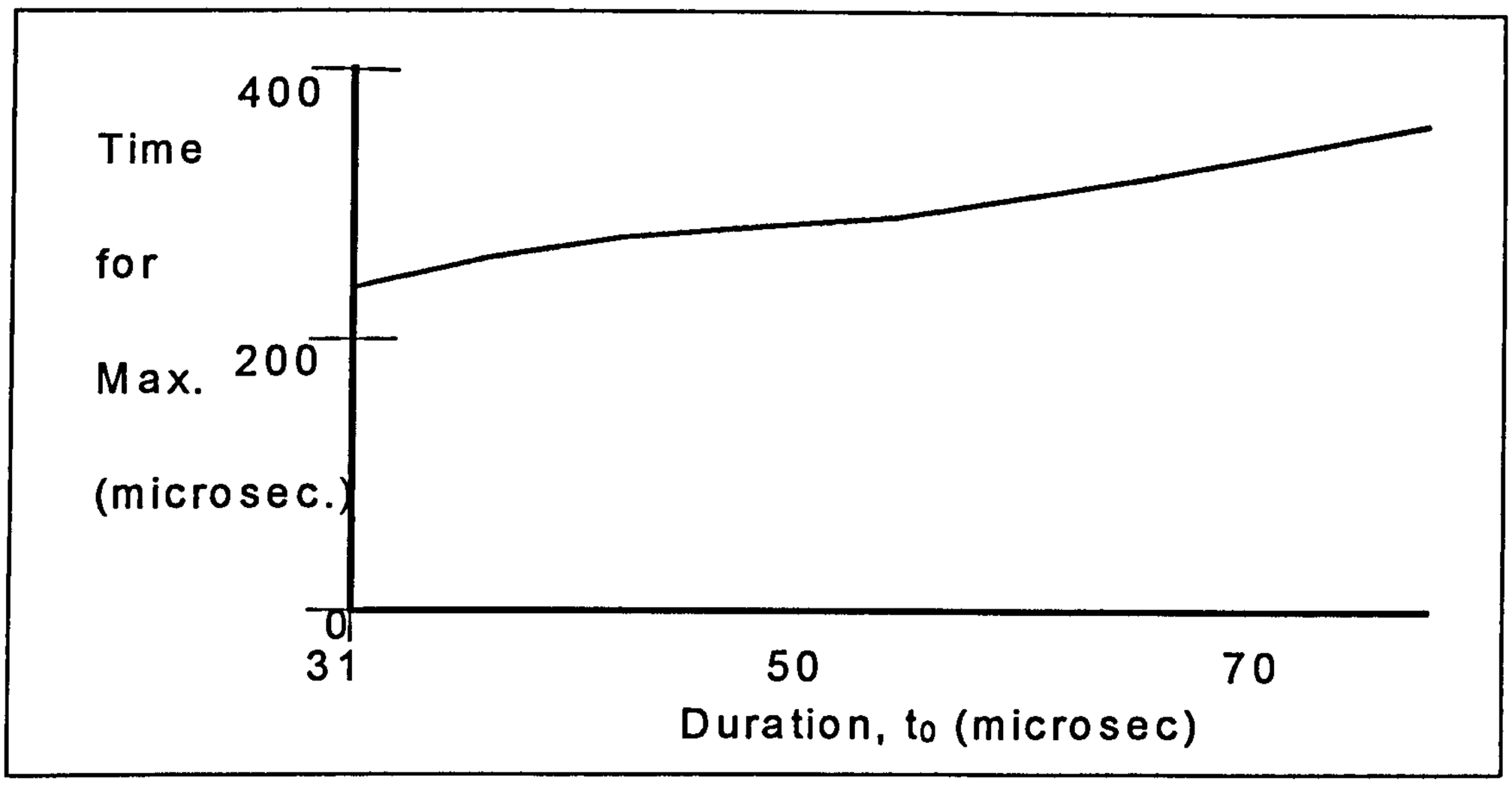

Fig.4.13. Effects of load duration on the time to the max. displacement occurs

It can be observed that by increasing the duration of the impulsive load, both the maximum displacement, and the time at which the maximum displacement occurs, increase.

It can be also seen that both above curves change approximately linearly. It is noted that the changes in Fig. 4.13. are of less significance as the curve is relatively flat. However Fig. 4.12. shows an increase of maximum displacement by increasing the pulse duration. This is consistent with an increase in impulse as the pulse duration increases.

4.4 Elastic response

The maximum pressure would be expected in process plant explosions around *1 bar* *(1×10^5 Pa.)*. The tanks which are used in process plants have very thin walls and consequently the radius to thickness ratio of them is likely to be higher than 60 which means the response of such structures to explosions is not plastic. A tank with flat head (*Radius=1.5 m., Length=3 m., Thickness=1 cm.*) was analysed under explosive loading *(P_{max}=1 bar)*. Only the bottom end of the tank is clamped. The material properties and loading are the same as the earlier case discussed on 4.2.1.1 and 4.2.1.1.The load applied from one side of the cylinder. The top head of the cylinder is closed with the flat head. The only difference here is to consider dampin which will be discussed shortly.

Results of the analysis will be shown in section 4.4.2. after discussing damping which is required for the analysis. (Fig.4.14 & Fig.4.15.)

4.4.1 Damping

The source of damping can be inherent or added. Only inherent damping need be considered in the current analysis. There are mainly two types of damping, i.e. frequency dependent (viscous and dry friction) and hysteretic (material damping).

In order to calculate the damping matrix of the system, *[C]*, the Rayleigh damping equation is used which is defined by

$$[C]=\alpha[M]+\beta[K] \tag{4.8}$$

where

[M]: mass matrix

[K]: stiffness matrix

The values of α and β are not generally known directly, but are calculated from modal damping ratios, ξ_i, which are defined by the ratio of actual damping to critical damping for the particular mode of vibration, i. If ω_i is the natural circular frequency of mode i, α and β satisfy the relation

$$\xi_i=\alpha/2\omega_i+\beta\omega_i/2 \tag{4.9}$$

In dynamic cases chosen should be the dominant ω_i frequencies to calculate α and β, otherwise the damping values will not be realistic.

4.4.2 Results and discussions

The modal analysis of the system, which the details were presented in the beginning of the section (section 4.4.), was first performed and the natural frequency was determined to be *0.343 Hz*. However higher modes of the structure are excited in response to pulse loading. When it is subjected to pulse loading, high modes of structures will be present. The fuller explanation will be covered later in results and discussion. The transient analysis of the structure in this case without considering damping, using ANSYS, showed that the range of response frequencies is *15-25 Hz.* Consequently, *15 Hz* and *25 Hz* are chosen to calculate α and β, using the above indicated equation (4.9) having a damping ratio of *0.05* for steel structures.

The transient dynamic analysis of the vessel was then carried out using the finite element model of the vessel shown in Fig.4.14. The transient response of the structure, for the middle point at one side which is the critical point, considering damping, is illustrated in Fig.4.15. As can be observed, the final deflection of the structure is zero. This means the structure does not fail if the failure criterion is considered to be based on final displacement.

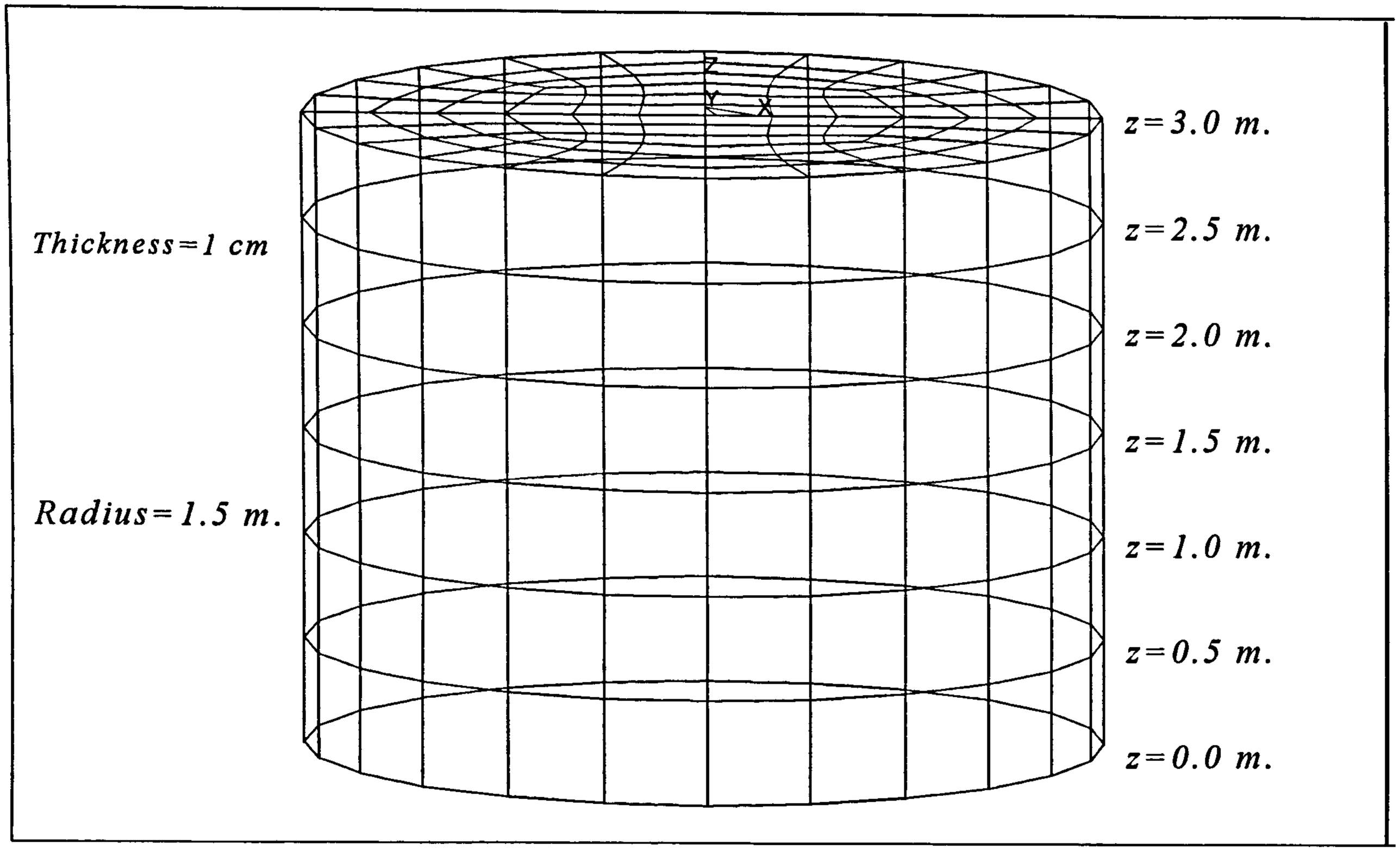

Fig.4.14. The meshed tank with the flat head and fixed bottom (loading as section 4.2.1.1 & 4.2.1.1)

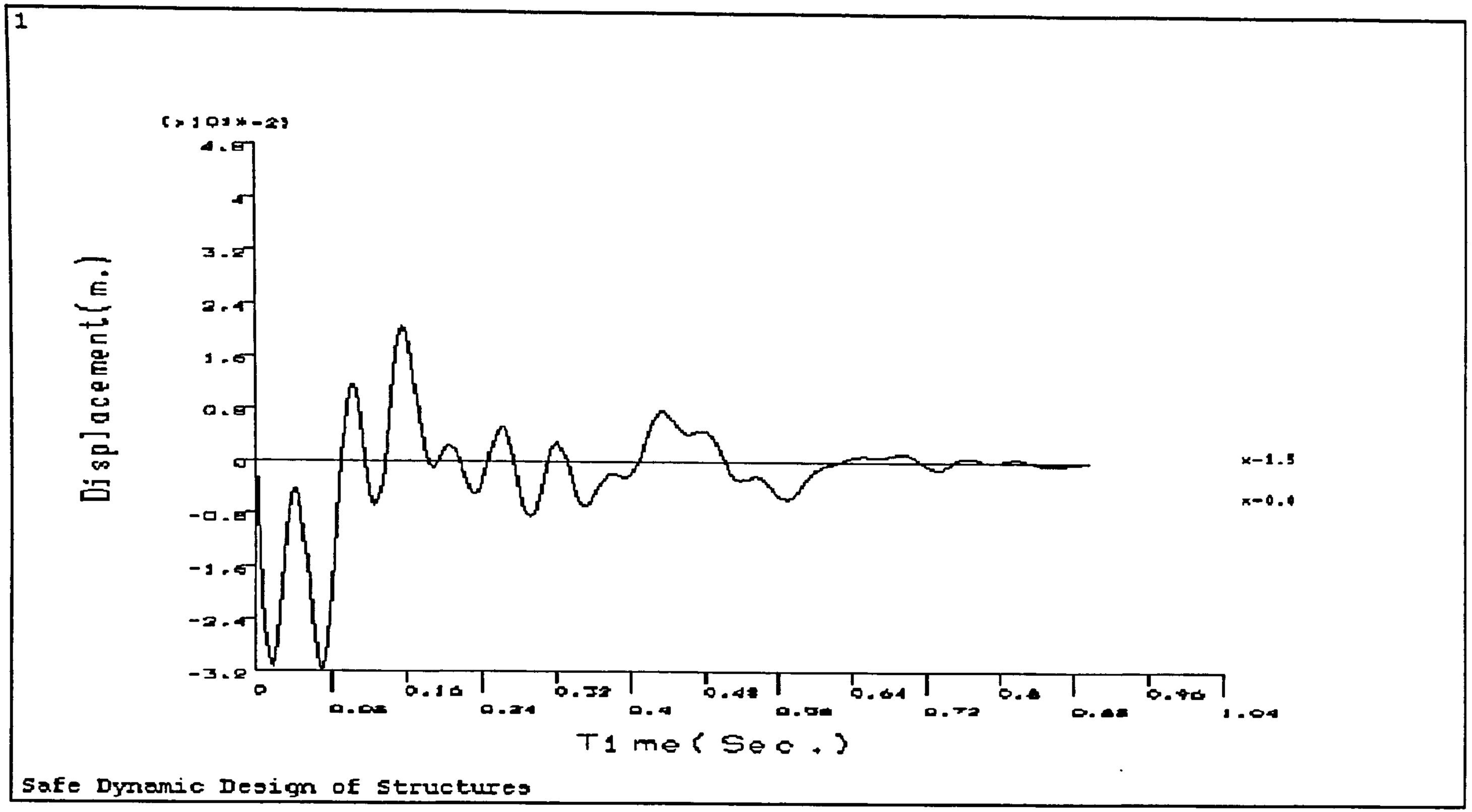

Fig.4.15. Transient response of the critical point of the tank

4.5 Elasto-plastic response

The transient analysis of a cylindrical structure subjected to internal impulsive spot loading, which gives elasto-plastic response, using the ANSYS is discussed in this section. To the knowledge of the author to the date, there is no work available on the response of cylindrical shell structures subjected to internal impulsive spot loading.

4.5.1 Descriptions

A 6-metre tube having a diameter of *1* metre made of steel (yield stress = 344 MPa), subjected to internal impulsive spot loading is analysed here. The spot, which has a diameter of *0.5* metre is located in one side on the middle of the tube. The tube was designed for *1* MPa internal static pressure under yield condition using the ASME boiler and pressure vessel code (ASME,1983). In order to model the structure in ANSYS, 1512 shell elements with plasticity, large deflection, and large strain capabilities are used as is illustrated in Figure 4.16. Both ends of the cylinder are assumed to be clamped. The internal pressure of 10 MPa for the duration of 10 ms was applied to the spot which is shown in Fig.4.16.

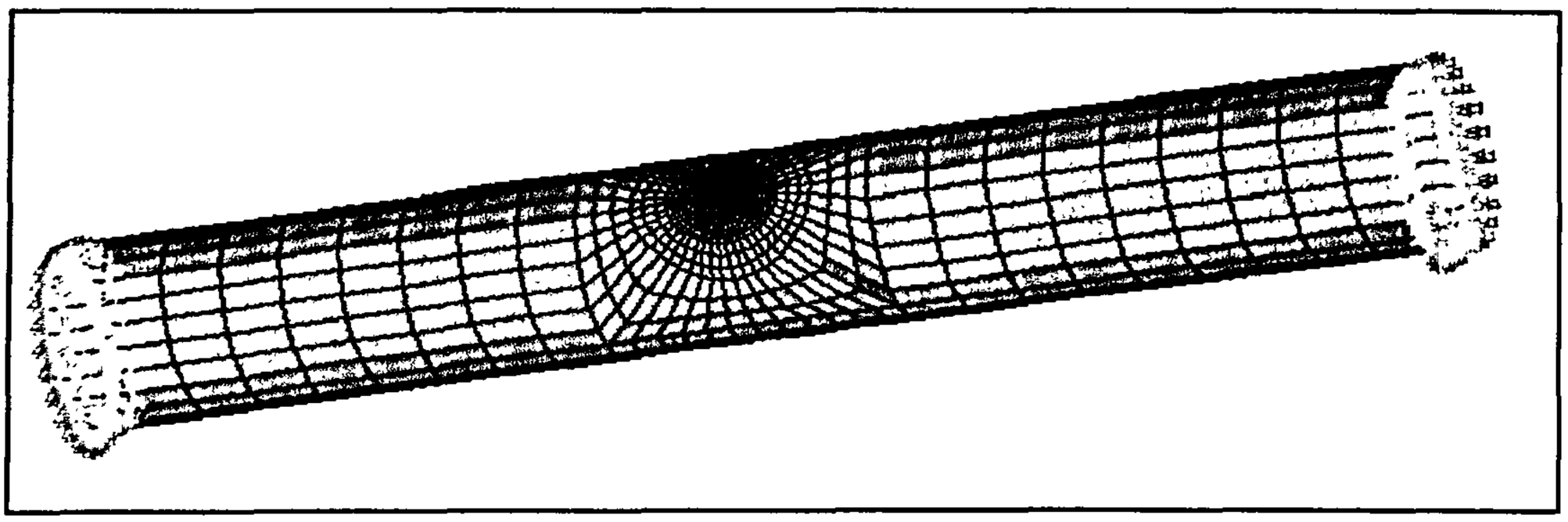

Fig.4.16. Finite element model of the circular cylindrical shell structure

The cylindrical vessel under impulsive loading is expected to have large deformations and thus large displacements and rotations which were taken into account by invoking the non-linear strain-displacement relationships where higher-order derivatives of displacements and rotations are included. Nonlinearity of the material is assumed to follow the bilinear isotropic hardening which means both elastic and plastic parts of stress-strain curve are linear. This option uses the Von Mises yield criterion, as explained earlier, to assess the failure of the structure under the specified loading conditions.

The modal analysis of the tube was first undertaken to determine the natural frequency of the structure. This enables the calculation of the proper integration time step for the transient analyses. Integration time step was then calculated by the ANSYS recommended *'1/20f'* formula where *"f"* is the natural frequency of the structure (Kohnke, 1992). Rectangular impulsive loading is used for the analysis so that the load suddenly increases to the maximum (4 MPa) value and then remains for the limited duration (10 msec) and finally returns to zero. The above value is just an

example of different values for pressure and duration used in the analysis to investigate the failure of the structure which will be discussed later in this chapter. Fig.4.17. shows the pressure-time profile for the analysis.

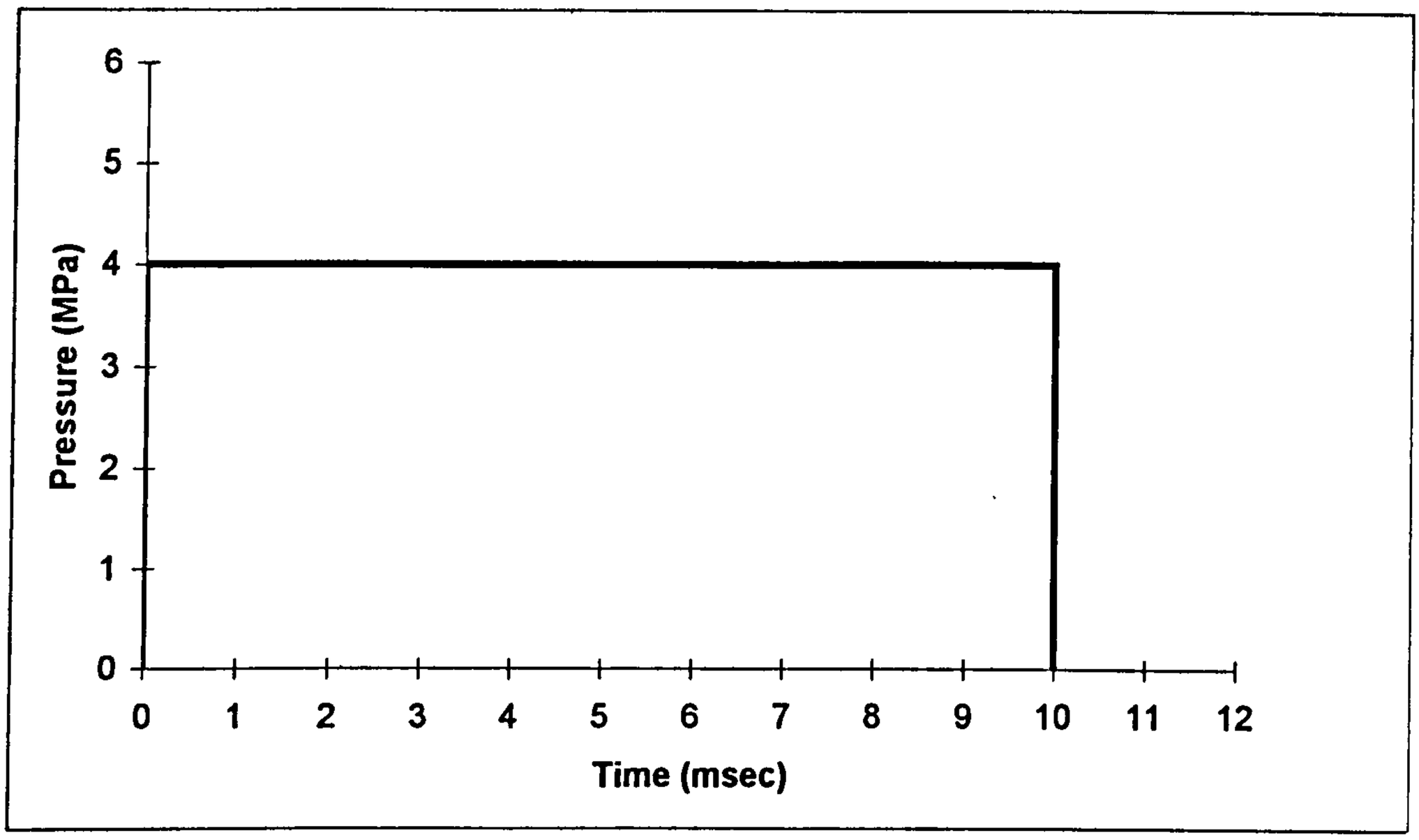

Fig.4.17. Pressure-time profile

4.5.2 Results and Discussions

The fundamental frequency of the structure was determined by modal analysis to be 66.7 Hz (Period: 15 msec) which leads to the calculation of the integration time step '1/20f' for the analysis which equals 0.75 msec.

The transient response of the centre of the spot, namely displacement and equivalent stress, obtained from the non-linear transient analysis with 4 MPa pressure and 10 msec duration, are shown in Fig.4.18. and Fig.4.19, respectively.

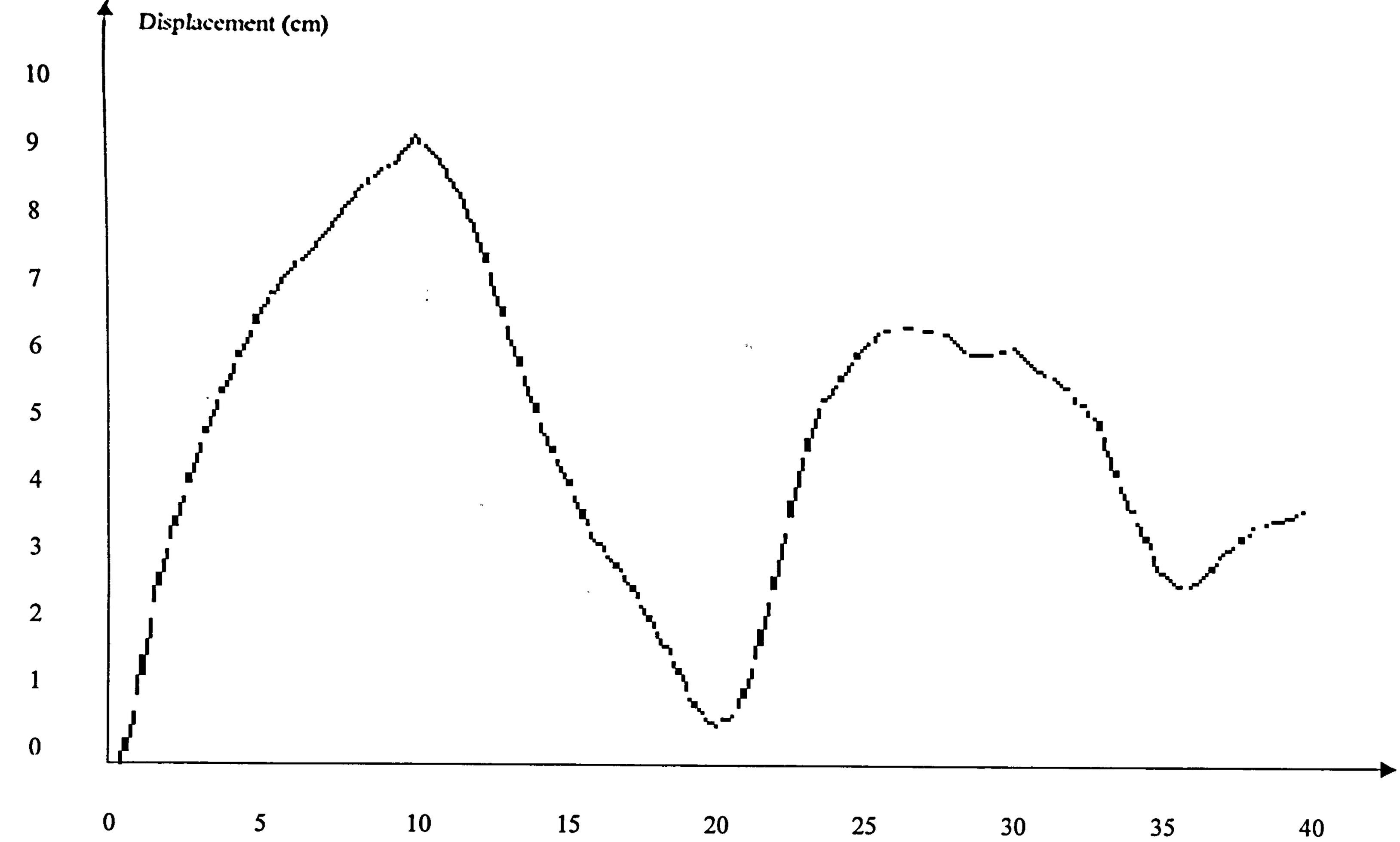

Fig. 4.18. Displacement-time relationship for the centre of the spot

Fig. 4.19. Equivalent stress-time relationship for the centre of the spot

As can be observed, Fig.4.18, the displacement of the point increases to a maximum value and then damps to a final deflection which is not zero. As the pressure is applied to the structure, the structure starts to responds in direction of the applied load. However the structural stability and damping push the elements back to stabilise the situation. This forward and backward of the elements around the reference line which is the final deflection will continue until the structure reaches the final stabilisation. As explained earlier, a combination of the structural modes are excited in dynamic response and the fundamental frequency of the structure plays an important role in the analyses. If the pulse duration is very short compared to the fundamental period, the response of the structure is perfectly plastic but a long pulse duration results in an elastic response (Abrahamson and Lindberg, 1971). For the present analysis, the duration is very close to the period of the structure so that the response is consequently elasto-plastic. The above explanation is correct when the structure is under the equal pulse in all cases.

The maximum stress, Fig.4.19, in the structure reaches a value which is higher than the yield stress. However the structure does not fail under this condition according to the ANSYS finite element code. The reason is that the pulse duration is too short to cause the failure so that the load is not categorised in static loading. It expresses that the structure can endure stresses higher than yield stress for less than a critical duration, in other words the dynamic yield criteria are different form the static ones.

In order to observe the effects of the duration of pulse loading on the response of the shell, a series of analyses on the model with different pulse duration have been carried out to indicate the relationship between the pulse loading duration with time at which the maximum displacement and stress occur. It was found that the maximum

displacement of the centre of the spot, which is the critical point of analyses, occurs at 10.6 msec regardless of the pulse duration as long as the response is in elasto-plastic region. Therefore, the maximum displacement in time, in elasto-plastic response, does not depend on the pulse duration, however the final deflection which occurs in the plastic region depends on the pulse duration which is due to the stress wave through the structure. Consequently, the role of the natural frequency of the structure is explored which basically provides the information on the structural response to indicate whether the response is elastic, plastic or elasto-plastic which is due to the pulse duration (Lindberg and Florence, 1987).

4.5.3 Failure Criterion

A series of analyses were then carried out to observe the response of the structure to internal impulsive spot loading with the value of 2-10 MPa and 2-50 msec duration. The failure of the structure, for each case, was checked by applying Von Mises criterion by calculating all principal stresses and checking Equation 2.1. to determine the failure point of the structure.

Von Mises failure criterion was applied to assess the structural failure for the present case. However the non-linear transient analyses of the shell structure under internal transient spot loading with different values for pressure and duration can produce a fail-safe curve which indicates a safe region for the cylindrical structure under impulsive spot loading without structural failure. This fail-safe curve for the present case is illustrated in Fig.4.20.

Duration (ms)	Presure (MPa)
2	10.1
10	5.8
30	4.2
50	2.3

Table 4.3. Fail-safe data for the cylindrical structure

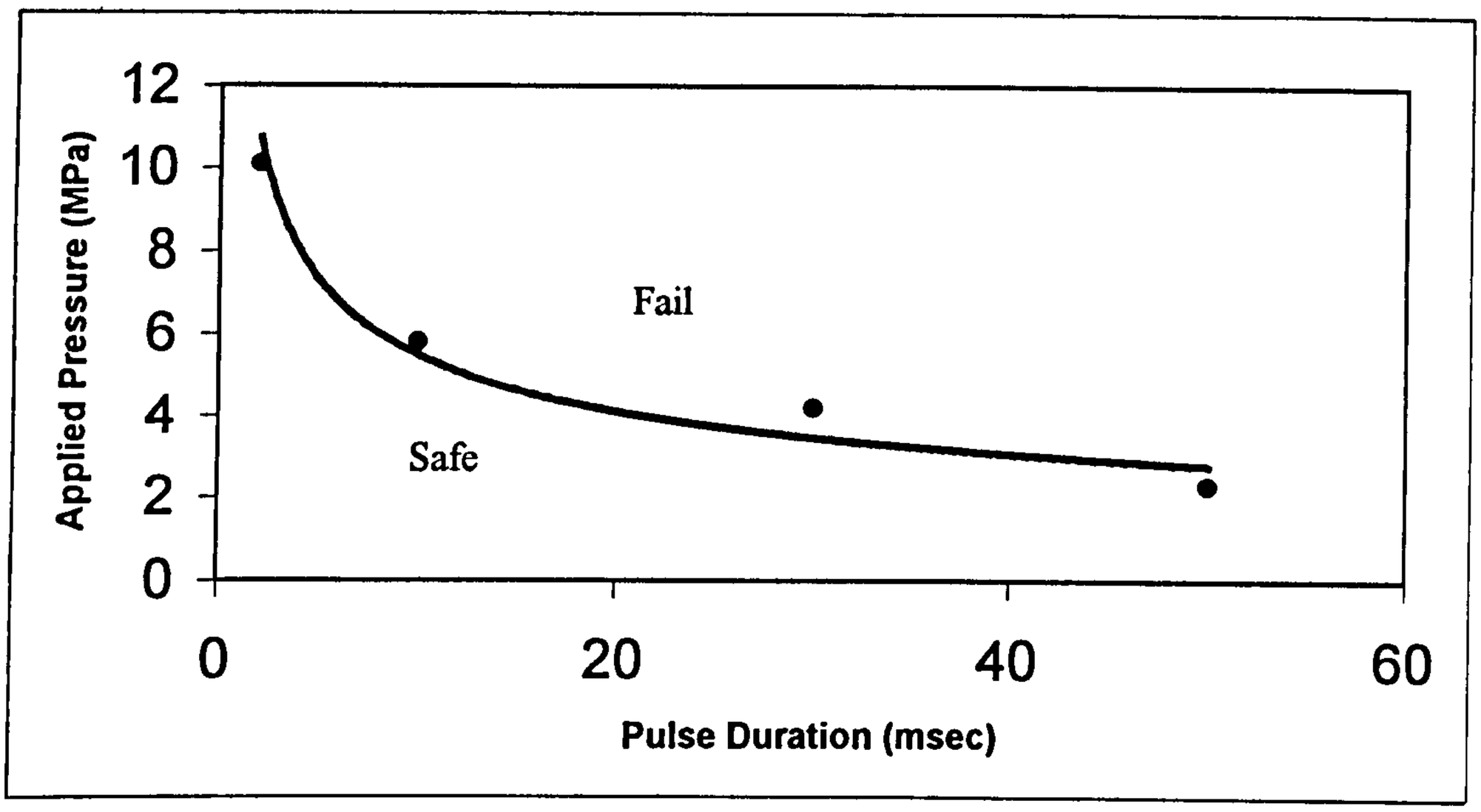

Fig.4.20. The fail-safe curve for the cylindrical structure

To obtain the fail-safe curve, the duration was assumed to be constant for example 10 ms and the applied pressure was increased for example from 4.5 MPa until the failure occurred. This procedure was carried out for a number of the duration to obtain the maximum allowable pressure for each duration. These are represenred in Table 4.3. and shown graphically in Fig. 4.20.

When the pulse duration is short the structural response will be different as the high mode are excited however when the pulse duration is long in the above curve the response is static and the static design pressure will be the maximum allowable pressure for the structure.

4.6 Conclusions

The plastic, elastic and elasto-plastic responses of cylindrical shell structures subjected to pressure transient loading were studied numerically.

In the plastic response, the response of the cylindrical vessel with the radius to thickness ratio equal to 24 whose response is perfectly plastic was analysed. The results were compared with existing experimental results as well as the finite difference and finite strip analyses results. It was found that comparison between the results from the present finite element analysis with the experimental results gave better agreement compared to the results from the other two methods, i.e. finite difference and finite strip, with the experimental one. Three different types of modelling for the explosion, i.e. triangular, rectangular and exponential, were also considered to investigate the effects of the explosion modelling on the structural response. It was found that the exponential modelling is more realistic, compared to the experiments, than the other two types of modelling considered in this chapter. The effects of impulsive loading duration on the response of the structure under external transient pressure loading in the plastic response region were also investigated. It was found that by increasing the duration of the transient pressure

loading, both the maximum displacement, and the time during the maximum displacement occurs, increase.

The elastic response of a large cylindrical structure was also investigated numerically and was found that the consideration of damping is so significant to allow the numerical analysis produce the correct results.

In elasto-plastic response of the shell structure, the non-linear transient analysis of a cylindrical shell structure due to an internal impulsive spot loading was carried out numerically. The response of the shell was found to be elasto-plastic since the pulse duration was close to the period of the structure. Von Mises failure criterion was applied to investigate the failure of the structure. According to the analysis carried out by ANSYS code, it was found that a dynamic pressure greater than the yield pressure can be applied to the structure without failure if the impulse duration is less than a critical value. The critical value must be determined for any structure under specific conditions. It was also observed that the maximum displacement of the structure occurs at a certain time regardless of the pulse duration as long as the structural response is elasto-plastic. A series of analyses for different values for the maximum pressure and its duration has also been carried out to find a safe-fail curve for the structure. It can be concluded that the design criteria under transient pressure are different since the dynamic yield criteria are different from static ones.

In the next chapter the experimental procedure will be explained and the failure criteria will be experimentally investigated in order to validate the finite element predictions for structures under high transient pressures.

5. Experimental procedure

5.1 Introduction

A series of experiments, using a shock tube, have been carried out to validate a number of aspects of the numerical analysis and demonstrate the numerical analysis ability to predict the structural response and behaviour due to pressure pulse loading. A simple shock tube provides a means by which gas flows and pressure can be generated for short periods of time by suddenly bursting a diaphragm (bursting disc) separating a high pressure gas from a low pressure section.

Shock tubes have been extensively been used to study different phenomena in physics, chemistry and aeronautics. The shock tube in the present experiments is used to generate the impulsive loading which can be applied to the structures.

In this chapter, the fundamentals of shock tube are first discussed, and then the experimental set up and instrumentation will be presented in detail. Finally, the procedure will be explained.

5.2 Shock tube

A simple shock tube consists of a high pressure driver section and a low pressure driven section of equal bore, separated by a diaphragm which can be burst by increasing the driver pressure. On removing the diaphragm, a compression wave is therefore formed and travels into the low pressure driven section. The shock tube is shown in Fig. 5.1.

The driver and driven sections are normally filled by gas. However for certain applications the driven section can be filled with water to provide the necessary pulse shapes. For low pressures required in the driven section the air is used. However to obtain high pulse pressures in the driven section water is used. The reason is that in the air-air case the air in the driven section is not compressed and therefore a big pressure drop will be observed when the diaphragm is ruptured due to the bursting pressure in the driver section.

A contact surface separating the expanding driver gas from the media in the driven section, follows the shock down the tube at a slower speed. Following behind the shock, the high pressure gas expands into the driven section, the contact surface in effect, pushing the air in the direction of the shock with the velocity depending on the

original pressure ratio across the diaphragm. The shock tube theories are explained by (Ferri, 1961).

Test pieces can be located at the downstream end of the driven section. Maximum pressure and pulse duration can also altered by some means which will be discussed later in this chapter.

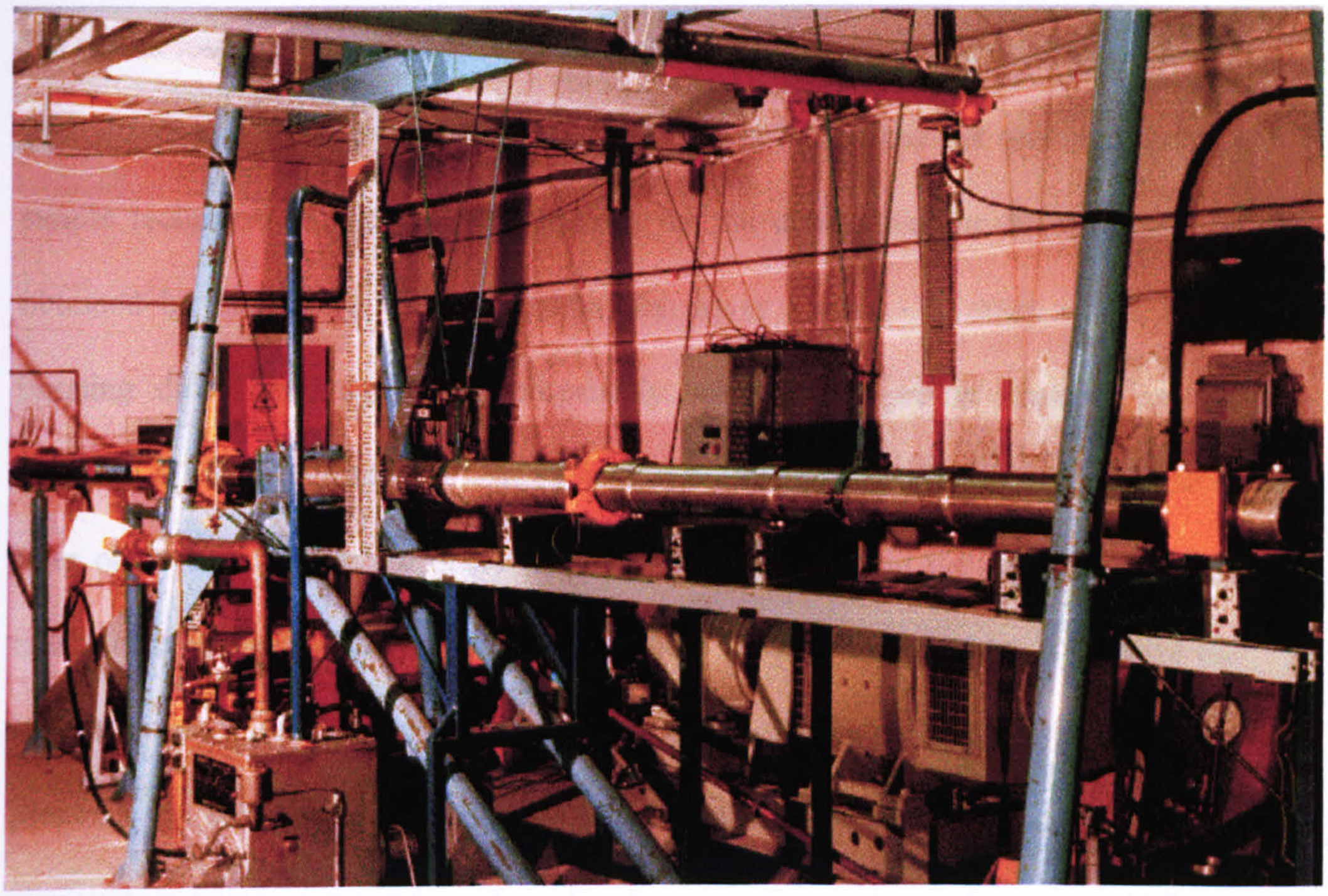

Fig. 5.1. Shock tube used for the present experiments

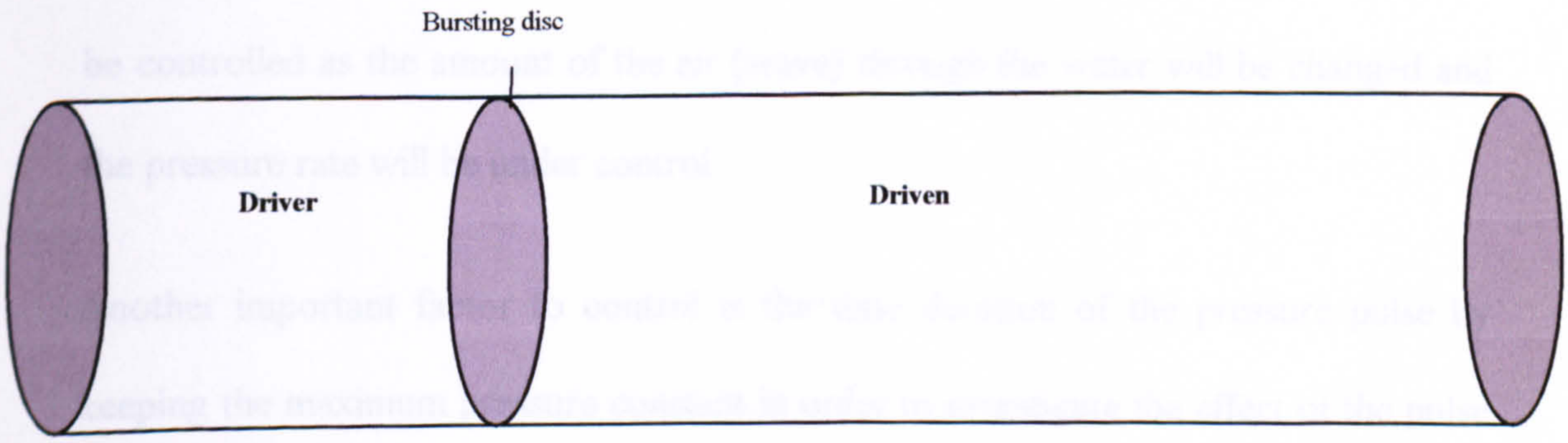

Fig. 5.2. Schematic diagram of shock tube

5.2.1 Pressure and duration control

Control of the pressure duration (Δt) and also the maximum pressure (P_0) are quite significant in the experimental work. Because the response of the structure due to a certain pressure with different duration or certain duration with different maximum pressure will be investigated in order to find out the failure condition.

To obtain low pressure in the driven section, the gas-gas system is used which means both driver and driven sections are filled with the air. From the last section, there is a simple technique to increase the pressure in the driven section. It can easily be obtained by increasing the pressure in the driver section. In other words if the bursting disk (diaphragm) is appropriately selected the proper pressure can be achieved in the driven section. The subject of bursting disks will be covered in depth later on in this chapter. In order to have higher pressure in the driven section, as mentioned before, the gas-water is used. There are two options here to control the maximum pressure in the driver section. First choice is to change the driver section pressure, by selecting an appropriate bursting disk, as the previous case. Another approach is to use a secondary disc after bursting disc with a hole in the middle of this disc whose hole diameter enables to control the pressure in the driven section. Therefore by changing the diameter of the hole, the pressure in the driven section can be controlled as the amount of the air (wave) through the water will be changed and the pressure rate will be under control.

Another important factor to control is the time duration of the pressure pulse by keeping the maximum pressure constant in order to investigate the effect of the pulse width on the structural response. In the gas-gas case, reducing the driver section

5.2.1 Pressure and duration control

Control of the pressure duration (Δt) and also the maximum pressure (P_0) are quite significant in the experimental work. Because the response of the structure due to a certain pressure with different duration or certain duration with different maximum pressure will be investigated in order to find out the failure condition.

To obtain low pressure in the driven section, the gas-gas system is used which means both driver and driven sections are filled with the air. From the last section, there is a simple technique to increase the pressure in the driven section. It can easily be obtained by increasing the pressure in the driver section. In other words if the bursting disk (diaphragm) is appropriately selected the proper pressure can be achieved in the driven section. The subject of bursting disks will be covered in depth later on in this chapter. In order to have higher pressure in the driven section, as mentioned before, the gas-water is used. There are two options here to control the maximum pressure in the driver section. First choice is to change the driver section pressure, by selecting an appropriate bursting disk, as the previous case. Another approach is to use a secondary disc after bursting disc with a hole in the middle of this disc whose hole diameter enables to control the pressure in the driven section. Therefore by changing the diameter of the hole, the pressure in the driven section can be controlled as the amount of the air (wave) through the water will be changed and the pressure rate will be under control.

Another important factor to control is the time duration of the pressure pulse by keeping the maximum pressure constant in order to investigate the effect of the pulse width on the structural response. In the gas-gas case, reducing the driver section

length is a good technique to control the pressure duration (pulse width) as there is an expansion wave after the shock which depends on the length of the driver section. Therefore by changing the length of the driver section the pulse width can be controlled as a shorter length gives a shorter pulse width. In the case of high maximum pressure which the gas-water system is used, changing the driver section volume to a very small sizes causes low pressure in the driven section of the shock tube. Therefore another technique is used which is to change the position of the test pieces to get different pulse durations. The control of the pulse width in this case is basically obtained by the expansion wave exit from the end of the tube. In other words an increase in the testing time (pressure duration) is available by using the expansion wave exit from the end of the driven section.

5.3 Instrumentation

In this section the facilities and instrumentation which were used for the present experiments are described. The schematic diagram of the overall experimental set-up is depicted in Fig. 5.3.

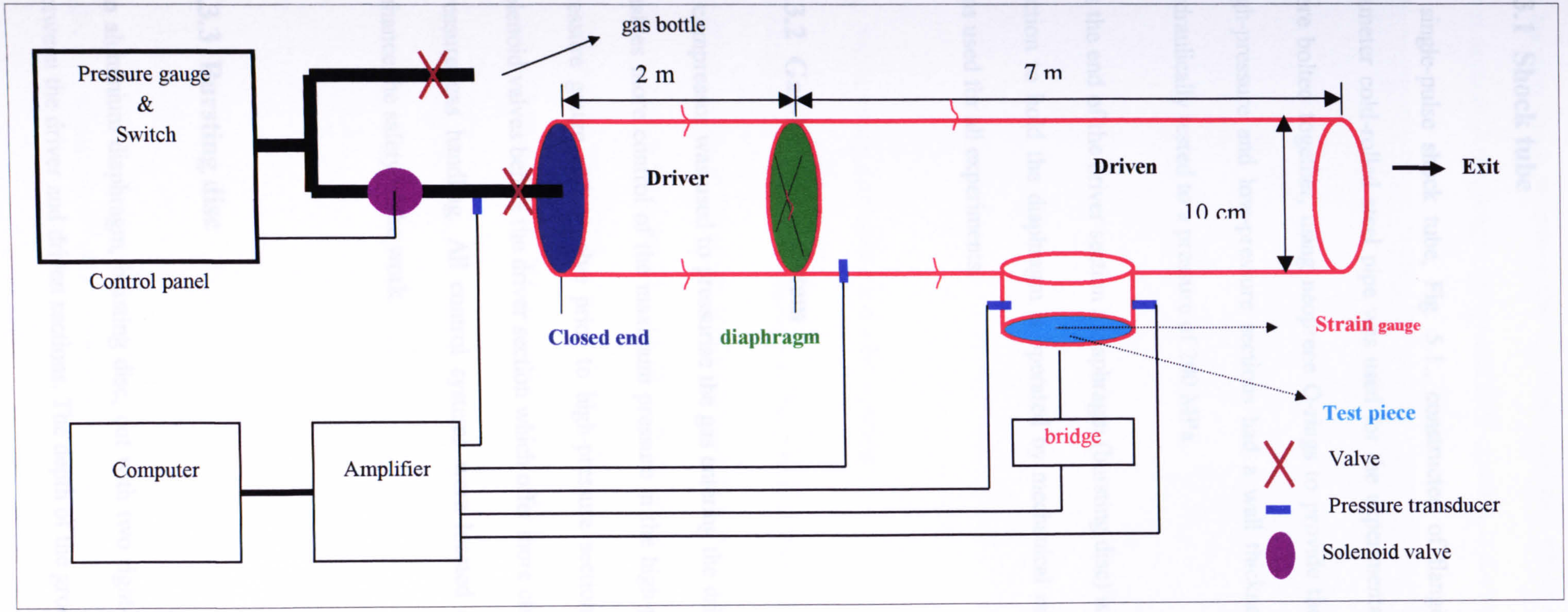

Fig. 5.3. The schematic diagram of the overall experimental set-up for the shock tube

5.3.1 Shock tube

A single-pulse shock tube, Fig. 5.1., constructed of flanged sections of 10 cm. diameter cold-rolled steel pipe was used for the experimental studies. The sections were bolted together, using neoprene O-rings to provide the necessary seals. Both high-pressure and low-pressure sections had a wall thickness of 3 cm. and were hydraulically tested to a pressure of 200 MPa.

At the end of the driver section a diaphragm (bursting disc) is installed. The clamping section to hold the diaphragm is operated by mechanical means. High-pressure air was used for all experiments.

5.3.2 Gas-handling system

A compressor was used to pressurise the gas entering the driver section. This facility enables more control of the maximum pressure in the high-pressure section using a pressure gauge and a valve prior to high-pressure section. There were also two solenoid valves before the driver section which offer more control and safety of high-pressure gas handling. All control systems were located in the control room to enhance the safety of the work.

5.3.3 Bursting disc

An aluminium diaphragm, bursting disc, cut with two right-angle grooves was used between the driver and driven sections. The depth of the grooves and the thickness of

the bursting discs determine the maximum pressure which can be reached in the driver section. A diaphragm, before and after opening, is shown in Fig. 5.4.

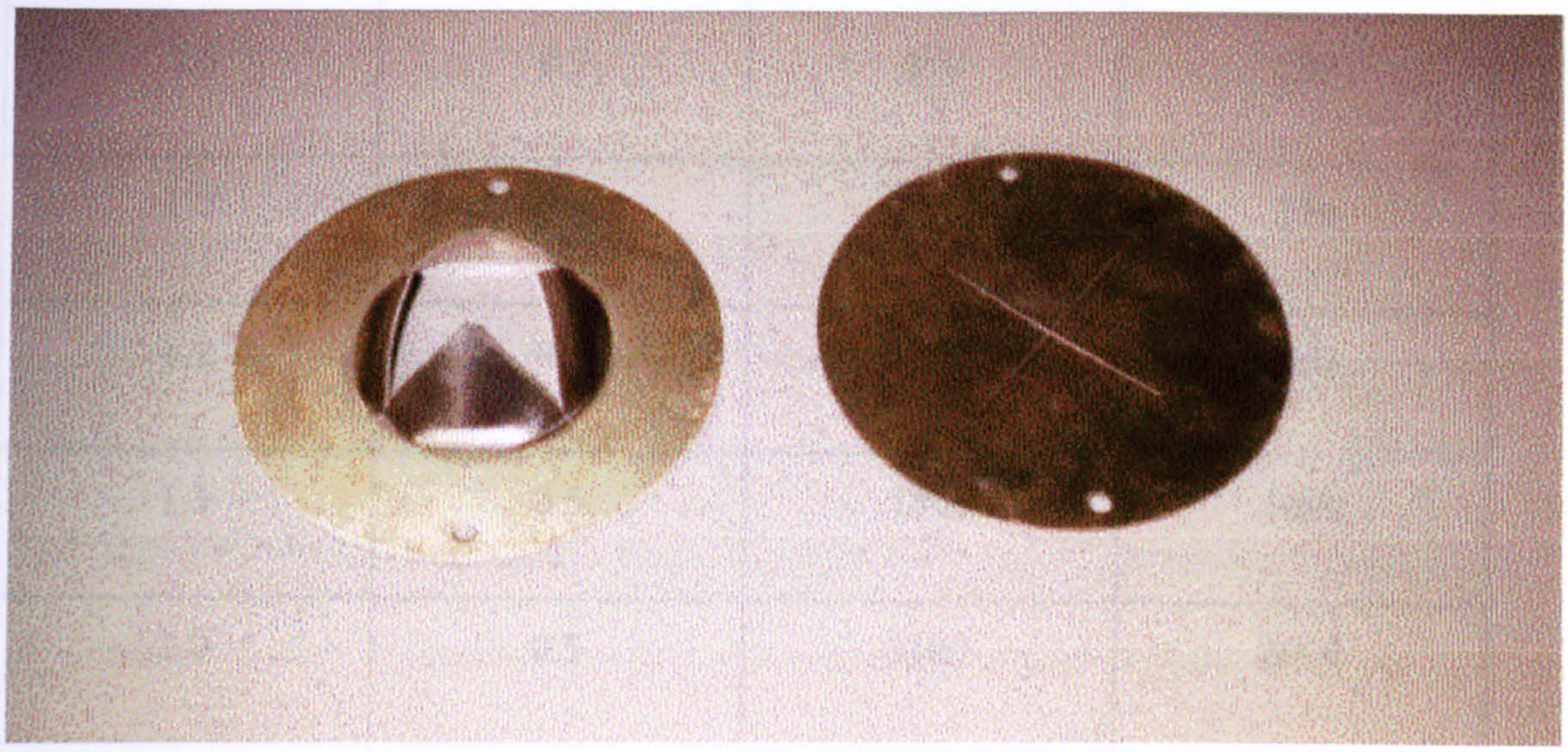

Fig. 5.4. Bursting disc before and after opening

To obtain a very low peak pressure in the driven section due to the low pressure in the driver section in the air-air configuration, very thin aluminium foils were used. In this case there was no need for the cross in the middle of the bursting sheets as the thickness value was already small. The following table shows the experimental results for this case where aluminium sheets were used as the bursting disk.

Sheet thickness (mm)	Bursting pressure (kPa)	Peak pressure (kPa)
0.3	413	150
0.6	813	250
0.9	1210	400

Table 5.1. Experimental data for bursting sheet characterisation (air-air system)

Disk thickness (mm)	Cross depth (mm)	Bursting pressure (kPa)	Peak pressure (kPa)
0.5	0.3	690	200
1.0	0.3	900	300
1.2	0.5	1650	800
1.3	0.5	1800	1000
2.0	0.5	3100	2000
2.0	0.66	2400	1400
2.6	0.86	3380	2500
3.2	1.0	4800	2800
3.2	0.8	5500	3800
3.2	0.6	6200	4000
6.4	0.58	15800	8000
6.4	0.92	14000	7000

Table 5.2. Experimental data for bursting disk characterisation (air-water system)

As mentioned earlier, to obtain a high peak pressure in the driven section air-water system was implemented. Bursting disks, all made from aluminium, with different thickness and cross depth were experimented to find out the bursting pressure and

obtained peak pressure in the driven section. The results from these experiments are summarised in Table 5.2.

5.3.4 Test section

A T-section was made and located in the driven section. The test piece was placed at the end of T-section. Having the T-section also allows this to be located in different positions in the driven section in order to control the pulse duration as previously discussed. Fig. 5.5. shows the T-section which is already attached to the shock tube.

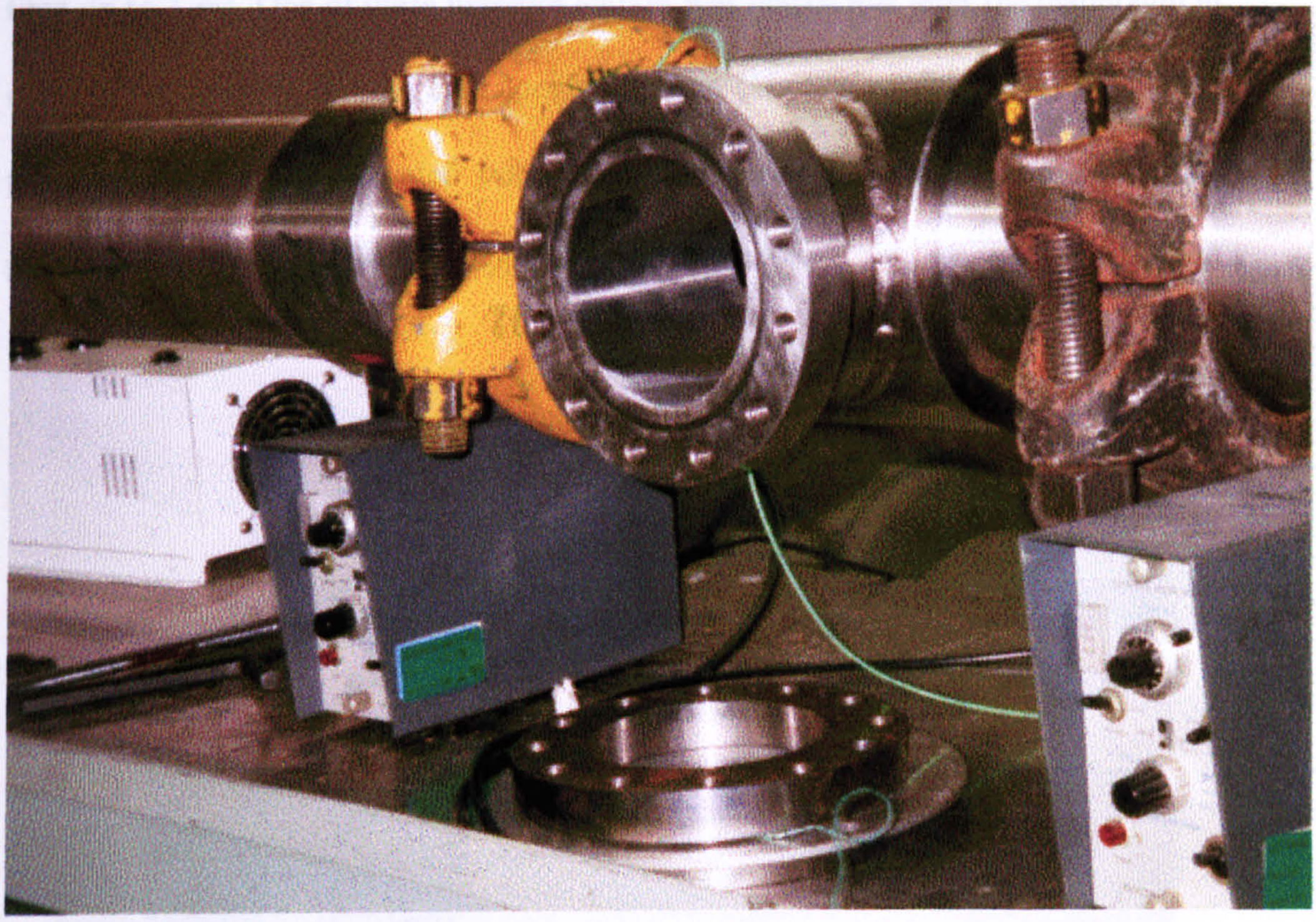

Fig. 5.5. Test section

5.3.5 Pressure determinations

Since the available testing time for the shock tube is quite short, all instrumentation must consequently be designed for the fast response time. Four piezoelectric pressure gauges were used to measure the pressure in different points in the driven section. The sensing elements, in these gauges, are quartz. One static pressure transducer was located in the entrance of the driver section to trace the bursting pressure of the diaphragm. This static pressure transducer is made by Entran Ltd and its pressure range is 0-17 MPa. The other pressure transducers are made by Kistler Ltd for the dynamic cases. The pressure range for these transducers is 0-15 MPa for a very short time up to 1 ms. One of these pressure gauges was placed just after the diaphragm in order for triggering for the data logging system (On-line reading) and finally two pressure sensors were located both sides of the end of T-section to obtain the pressure-time profile which was applied to the test-piece.

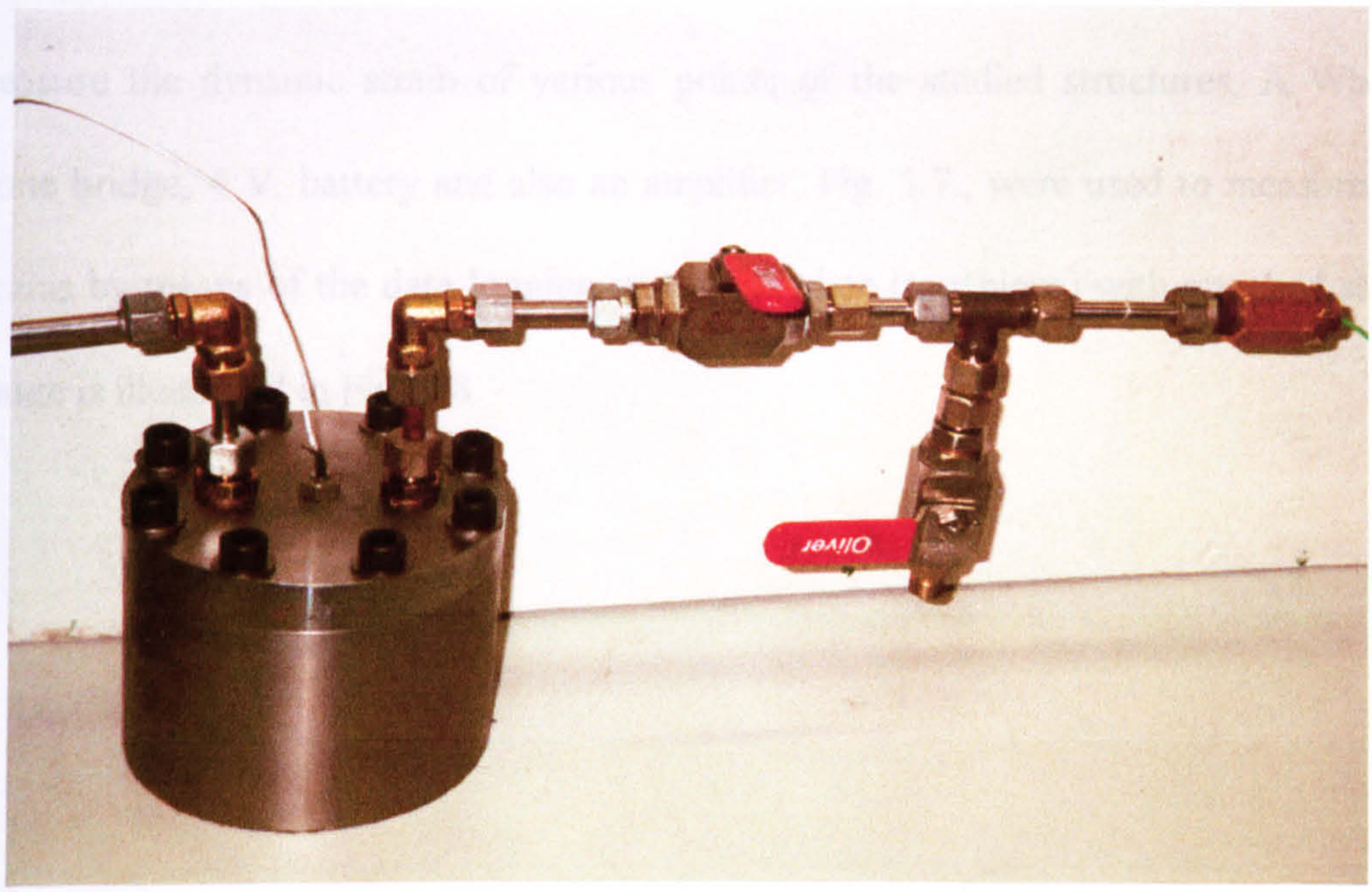

Fig. 5.6. Dynamic pressure transducer calibrator

An instrument, which is shown in Fig. 5.6., was designed in order to calibrate the dynamic pressure transducers to give the correct results. To calibrate the fast transducers, first, by opening the first valve the storage was pressurised up to a certain pressure which can be read by the static pressure gauge. Then the second valve was suddenly opened to allow the dynamic pressure transducer to read. The first data value read by dynamic pressure transducer within first 1 ms (as the Kistler pressure transducers are designed for the dynamic measurement up to 1 s.) should be the same as the value that the static pressure gauge obtained. All fast (dynamic) pressure transducers were calibrated by this facility.

5.3.6 Strain measurement

The plastic deformation was expected in the experiments since the study is concerned with the failure of the structures. Therefore very short post-yield gauges were used to measure the dynamic strain of various points of the studied structures. A Wheat-stone bridge, 4 V. battery and also an amplifier, Fig. 5.7., were used to measure the strains by means of the data logging system. A plate (test piece) with attached strain gauge is illustrated in Fig. 5.8.

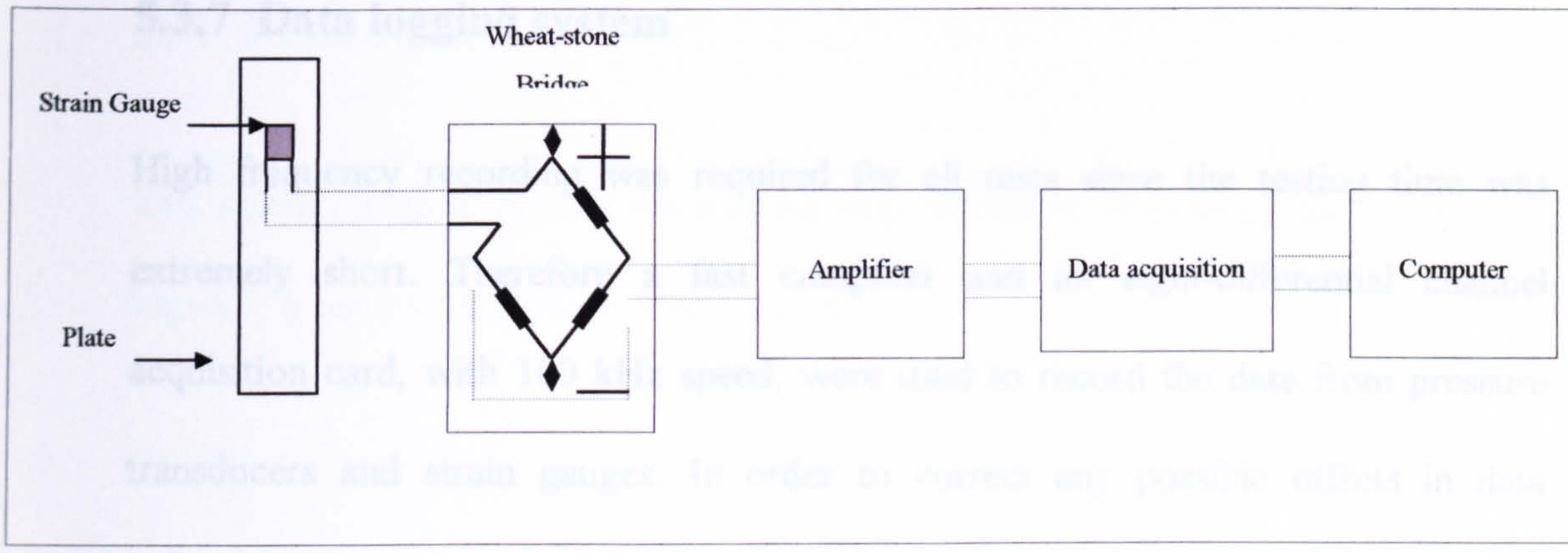

Fig. 5.7. Schematic diagram of strain measurement

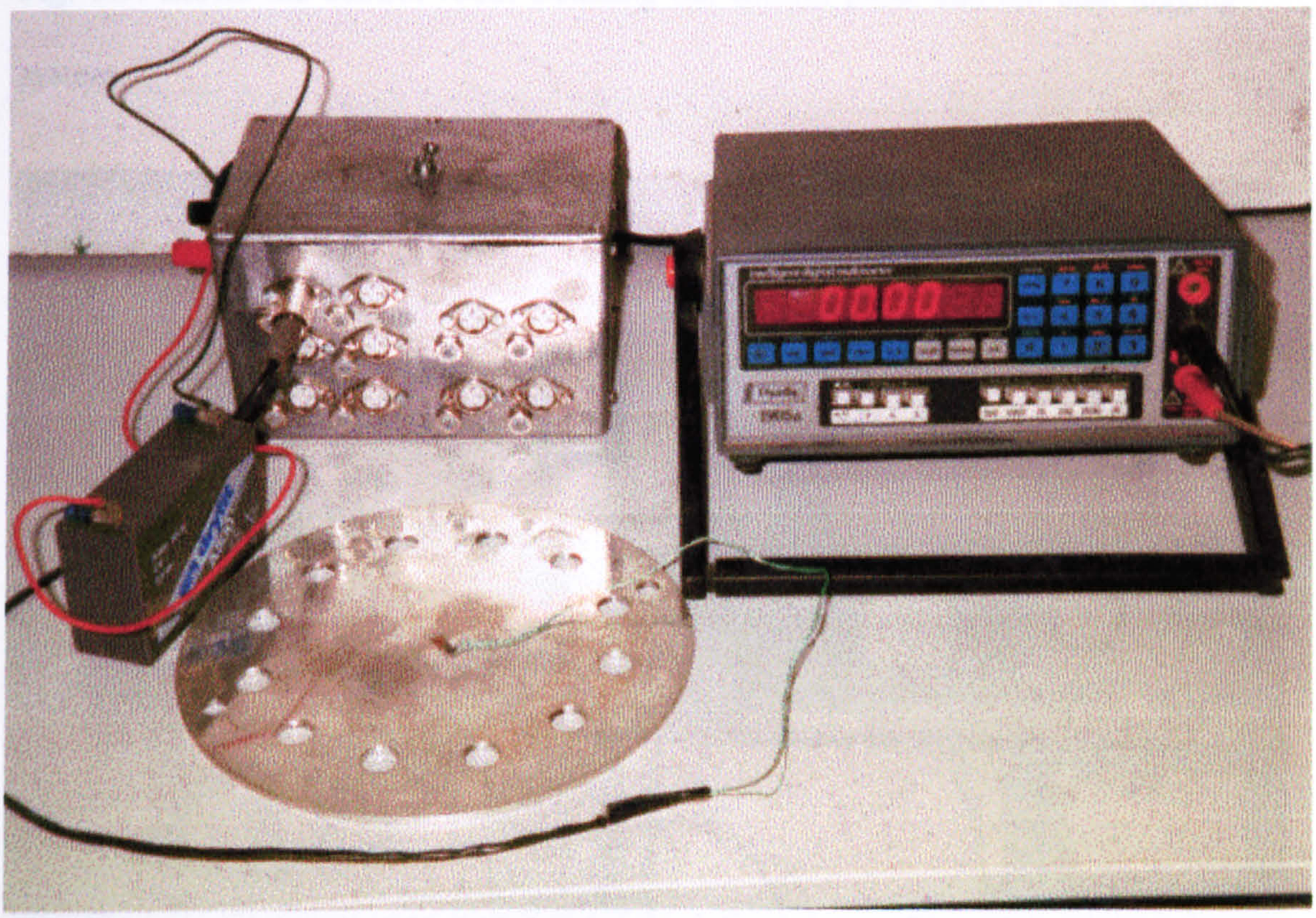

Fig. 5.8. Strain gauge set-up

5.3.7 Data logging system

High frequency recording was required for all tests since the testing time was extremely short. Therefore a fast computer and an eight-differential channel acquisition card, with 100 kHz speed, were used to record the data from pressure transducers and strain gauges. In order to correct any possible offsets in data collection processing, pre-triggering was also used. It means that 25% of the data was collected prior to the actual trigger point. Amplifiers were also used, which were connected to the strain gauges and pressure transducers, before the acquisition card.

Fig. 5.9. shows the control room including the control panel and the data logging system.

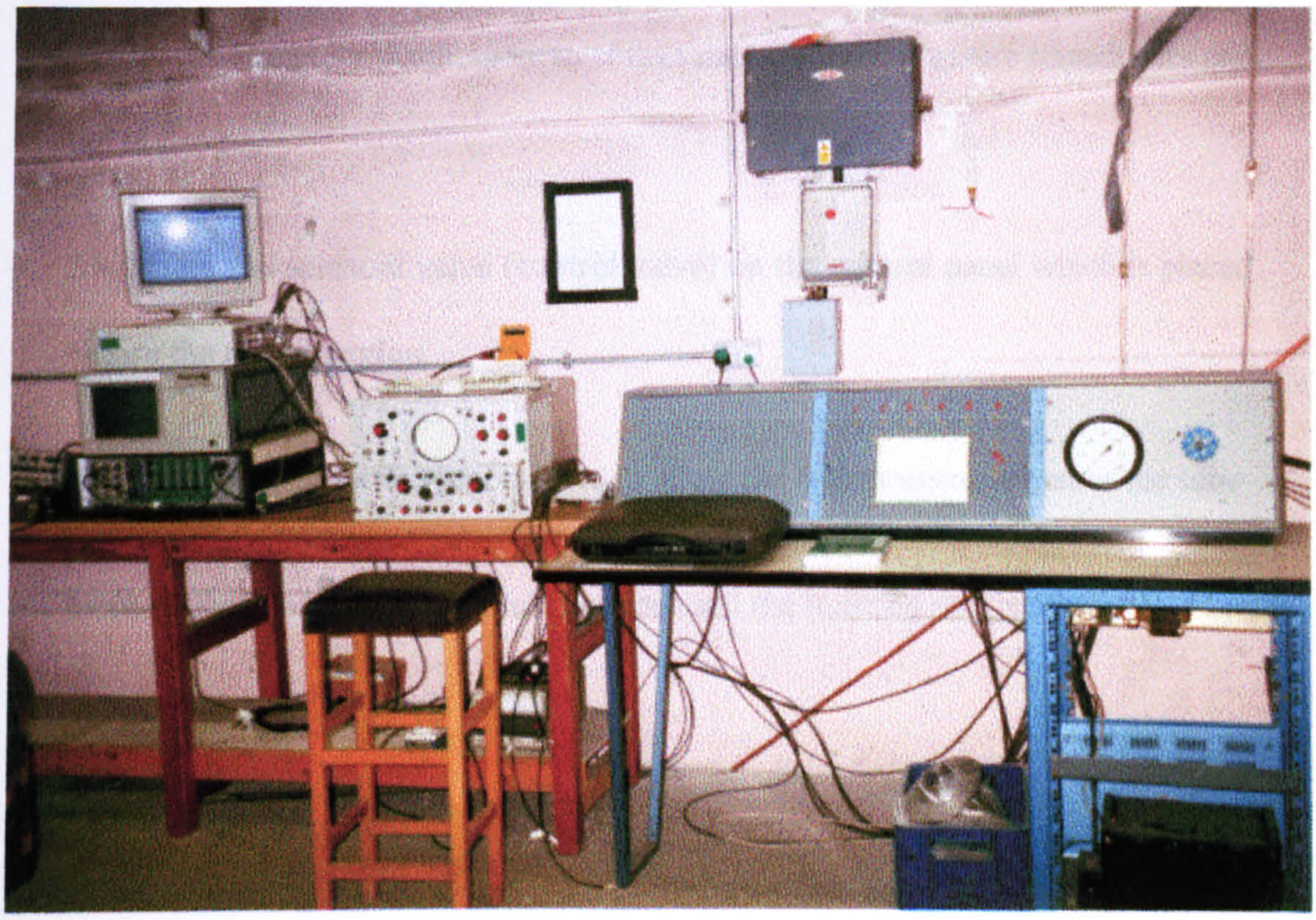

Fig. 5.9. Control room

5.4 Procedure

This section aims to explain the step by step procedure of running the shock tube.

Fig. 5.3. is used with the following procedure.

5.4.1 Start-up procedure

- Place the bursting disc between the driver and driven section
- Close the pressure relief valve in the driver section
- Attach the strain gauge to the test piece and then locate it at the end of T-section
- Set up the computer programme to collect data from the pressure transducers and strain gauges
- Switch on the solenoid valve (control valve) on the control panel which is placed before the driver section.
- Open the manual driver section valve to allow the high pressure air enter the tube
- Increase the pressure in the driver section until the bursting disc ruptures.

5.4.2 Shut down procedure

- Turn off the control valves
- Open the driver section relief valve

- Close the air bottle

- Transfer the data for analysis

5.5 Conclusions

The experimental procedure and some aspects of the principles of the shock tube were described in this chapter. The experimental set-up was designed to achieve the objective of the experiments which is to apply impulsive loading with various peak pressures and duration.

The results of the experiments, carried out using the described facilities, will be presented in the next chapter. The comparisons between the obtained experimental results and calculated numerical ones will also be made and discussed in the following chapter.

6. Results and Discussion

6.1 Introduction

Understanding of the complex structural behaviour under the spatial pressure pulse loading requires the primary analysis and practice on the simple geometry. In order to build up the proper investigation of cylindrical structures subjected to pulse loading, a simple geometry is first used to explore the relations of the pulse width and the maximum pressure and the structural natural frequencies.

In order to validate the results of the numerical analyses, a series of experiments were first performed on a simple geometry (circular plates) to explore the failure of the structure and more complicated cylindrical structures under pulse loading were then investigated and this chapter also presents a general approach to structural failure due to pressure pulse loading.

6.2 Circular plate

The first step was to determine the accuracy of the numerical work in reproducing the experimental results. Therefore, a circular plate under pressure pulse loading was first investigated as a first step before further investigation on more complex structures such as cylindrical vessels.

Therefore a comparison of the experimental and numerical work on a circular plate under pulse loading will first be made, and then the relation between the pulse width and the fundamental frequency of the plate will be explored and finally an experimental fail-safe curve for a circular plate will be presented.

Circular plate structures made of aluminium with the diameter of 10 cm and various thicknesses were made and placed in the T-section of the experimental set-up which was explained earlier.

6.2.1 Experimental and numerical Validation

As discussed in the preceding chapter, the applied peak pressure and also the pressure pulse width can be controlled by some means such as changing the bursting disk thickness and the location of T-section.

An example of pressure-time profile, which was produced by the shock tube, using pressure transducer, is plotted in Fig. 6.1. As can be observed, the pressure rises quickly to the maximum value and then decays to the very low pressure that can be chosen to be zero by making suitable venting arrangements.

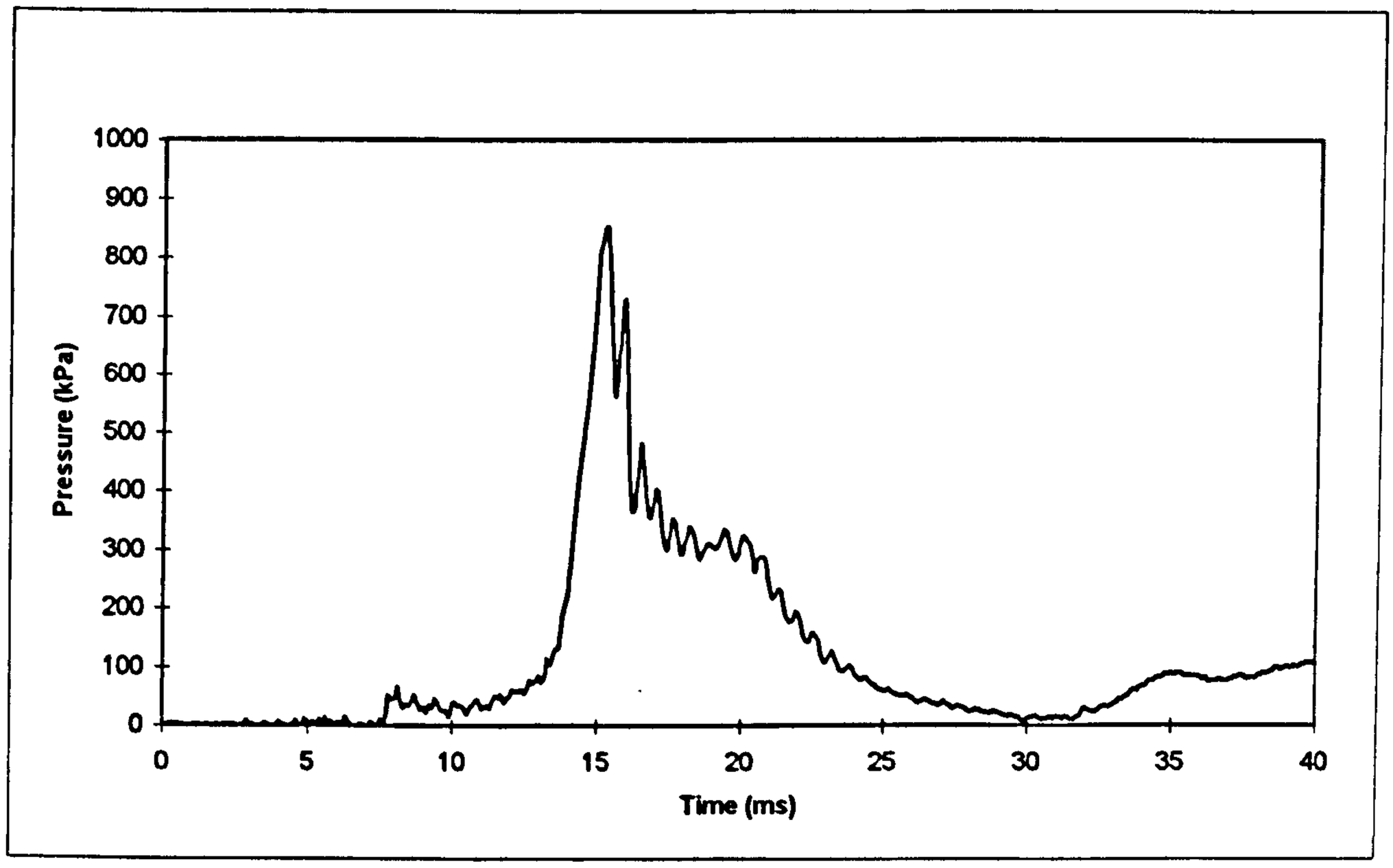

Fig. 6.1. Pressure-time profile produced by the shock tube.

Pressure pulses obtained in this way and similar to Fig. 6.1. were applied to the plate located in the T-section and the displacement of the centre of the plate was measured by means of attached strain gauge.

In order to compare the results of the above experiment with the numerical analysis, the stress-strain curve of the material is also needed. Therefore, the tensile test of the available aluminium plate which was used for the experimental work, was first carried out. The test involves straining the test piece by tensile force, generally to fracture, for the purpose of determining the stress-strain curve.

Four test pieces under tensile testing standards (British Standard Institution, 1990) was made which is shown in Fig. 6.2. According to the above standard (BS EN 10 002-1) the test piece has gripped ends which are wider than the parallel length. The

parallel length shall be connected to the ends by means of transition curves with a radius of at least 12 mm. The width of these ends shall be at least 20 mm and not more than 40 mm. Test pieces were cut in the university laboratory and Mayes tensile machine was used to carry our four tests. The results of stress-strain curves for the experiments are shown in Fig. 6.3.

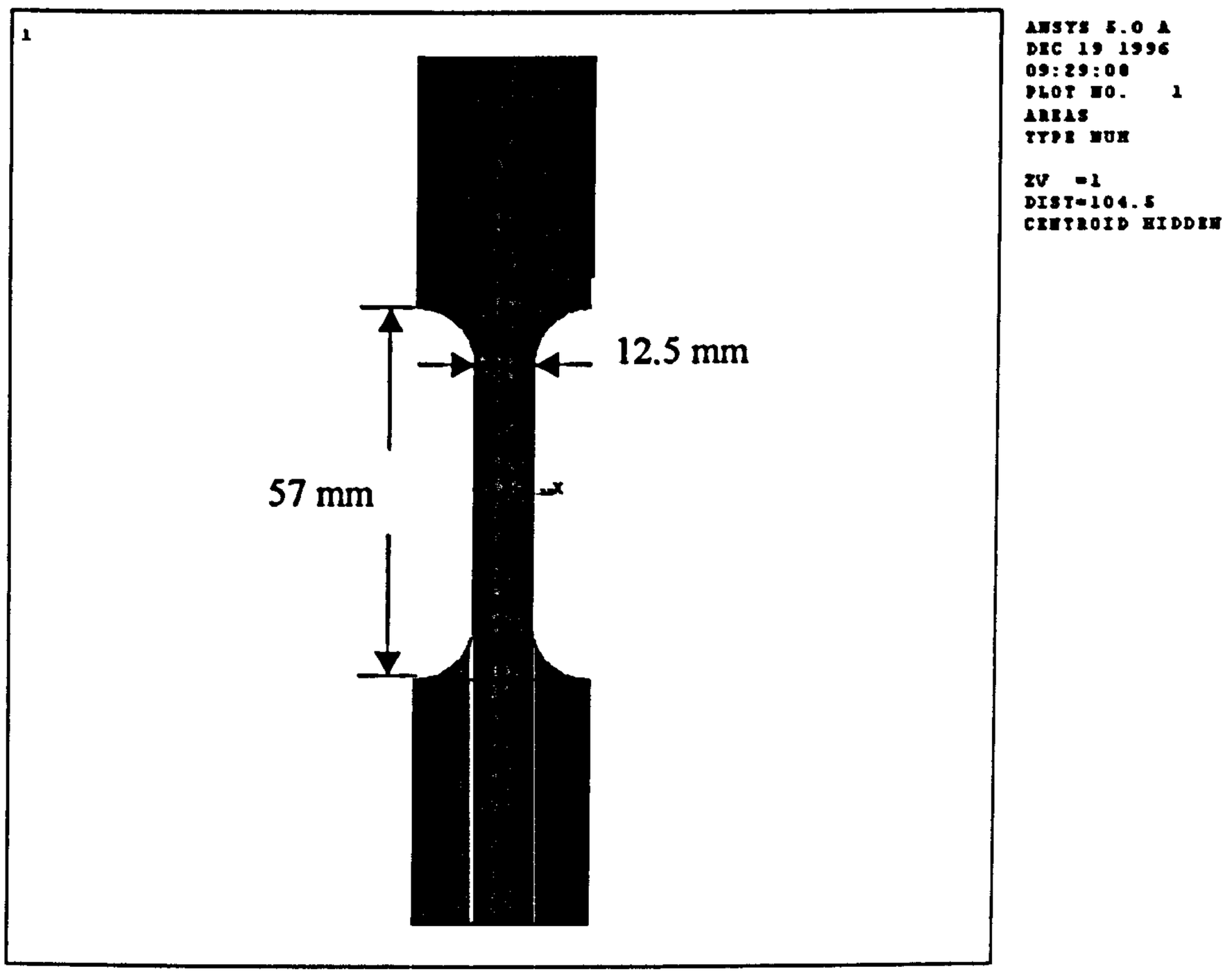

Fig. 6.2. test piece for the tensile test

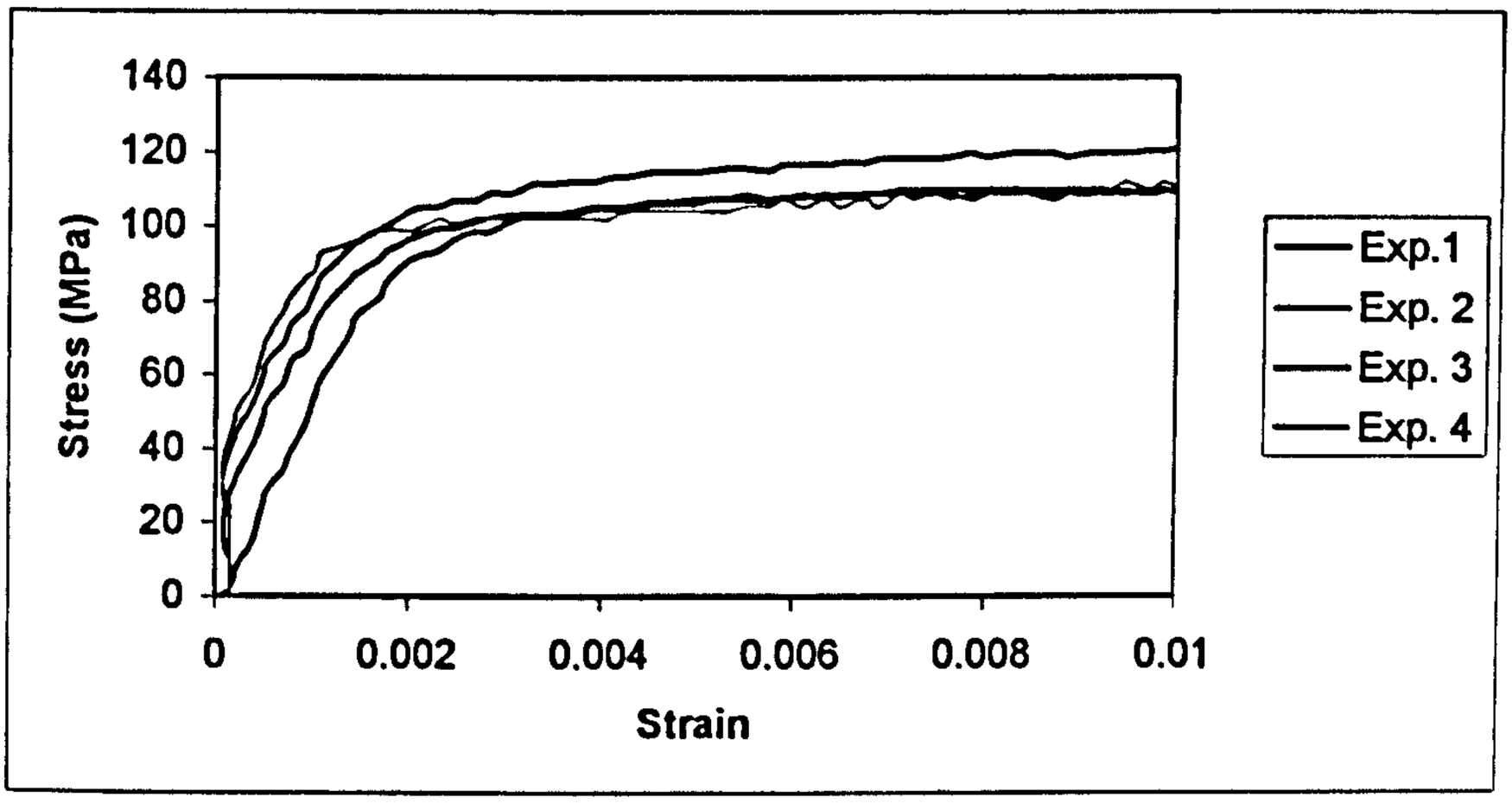

Fig. 6.3. Experimental stress-strain curves for aluminium.

A series of experiments, using the shock tube facilities which were explained in the preceding chapter, was then carried out to observe the response of the aluminium plates to the pulse pressure loads. Three examples with the plastic, elasto-plastic and elastic response are presented here and compared with the numerical results. The reason for choosing different response regimes of the plate for the experiments and analyses was to determine if the present numerical work based on finite element method is capable of predicting the actual behaviour of the structure due to pressure pulse loading. The results of each case will be compared to the experimental ones.

The elastic response in the plate case means that the final deflection of the centre of the plate after applying the pressure pulse will be zero. In other words there will be no final deflection in the elastic case. The elasto-platic case means that the response of the plate is somewhere in the transition part of the stress-strain curve where, after removing the pressure pulse from the structure a residual remains. In the plastic case, the response behaviour of the structure is well into the plastic region as by removing

the applied pressure from the plate structure there will be no changes in the final deflection.

In order to model the structure in ANSYS, 2352 shell elements with plasticity, large deflection, and large strain capabilities are used as illustrated in Fig. 6.4.

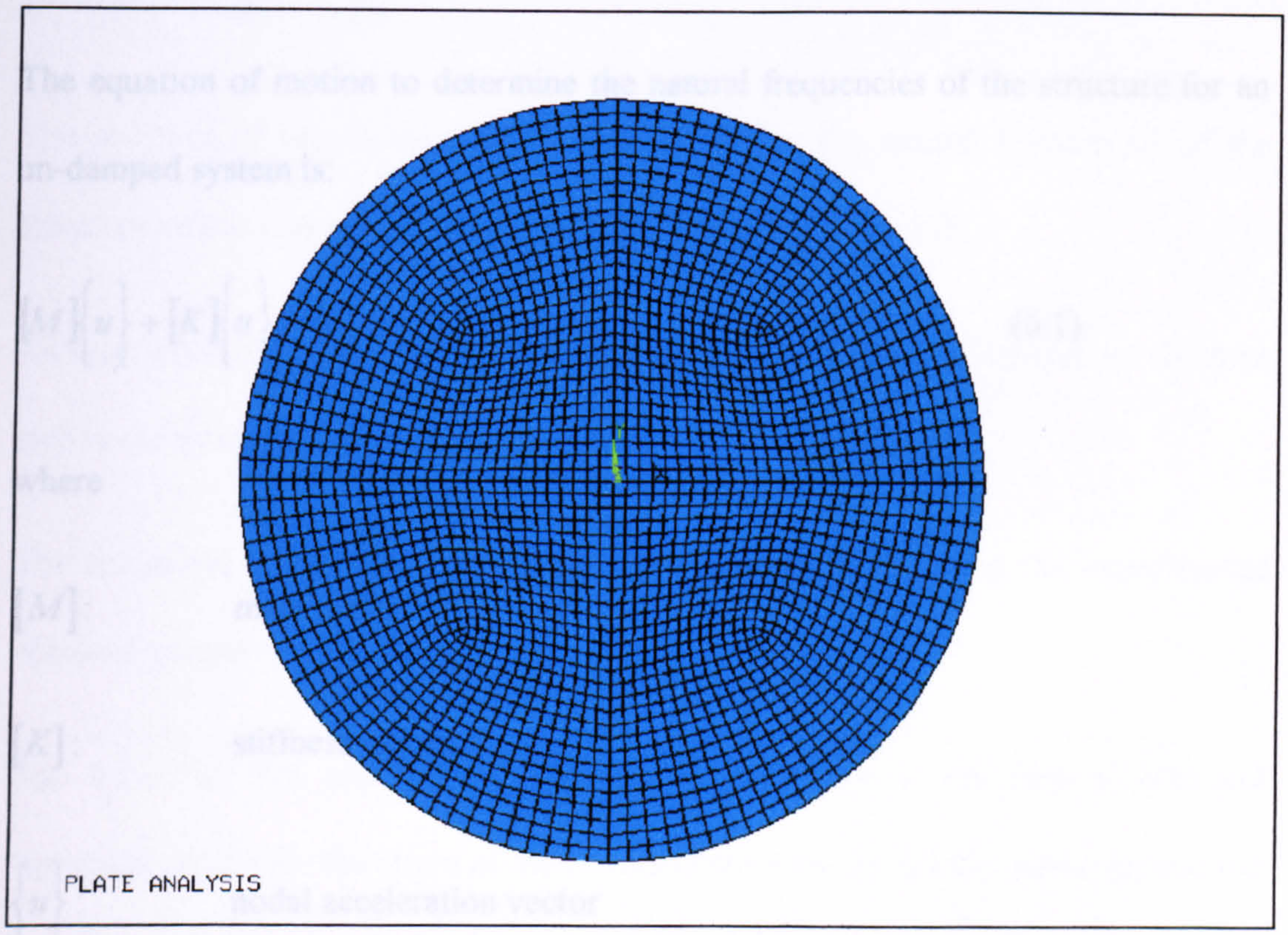

Fig. 6.4. Finite element model of plate.

In order to perform the numerical transient analyses for the plates, the fundamental frequencies of the plate for three different thickness namely 1.2 mm, 2 mm and 3.25 mm, using ANSYS and the measured density, 2276.5 kg/m^3, were first determined by modal analyses to be 1149.4 Hz, 1910.3 Hz and 3084 Hz, respectively. These determinations lead to the calculation of the integration time step *'1/20f'* for the transient analyses.

The modal analysis is basically used to determine the natural frequencies and mode shapes of a structure. The natural frequencies and mode shapes are important parameters in the design of a structure for dynamic loading as explained in the literature review. Modal analysis helps in determining vibration characteristics of structures.

The equation of motion to determine the natural frequencies of the structure for an un-damped system is:

$$[M]\{\ddot{u}\}+[K]\{u\}=\{0\} \tag{6.1}$$

where

$[M]$: mass matrix

$[K]$: stiffness matrix

$\{\ddot{u}\}$: nodal acceleration vector

$\{u\}$: nodal displacement vector

For a linear system, free vibration will be harmonic of the form:

$$\{u\}=\{\varphi\}_i \cos\omega_i t \tag{6.2}$$

where,

$\{\varphi\}_i$: eigenvector representing the mode shape of the *i*th natural frequency

ω_i : ith natural circular frequency (radius per unit time)

t: time

Therefore equation (6.1) becomes:

$$\left(-\omega_i^2[m]+[K]\right)\{\varphi\}_i = \{0\} \qquad (6.3)$$

The solution of the above equation will determine the natural frequencies of the structure which was performed using ANSYS numerical analysis.

As mentioned above the modal analysis here will lead to the calculation of the time step in the dynamic analysis.

The numerical analysis for each case was then carried out using the experimental obtained pressure-time profile for each case.

Fig. 6.5., Fig. 6.6. and Fig 6.7. show the comparison of the experimental and numerical results for the strain of the middle of the plate for plastic, elasto-plastic and elastic response, respectively, where 'D' is the diameter, 'h' is the thickness and 'T' is the period of the structure.

As can be observed in Fig. 6.5., Fig. 6.6. and Fig. 6.7. good agreements are met between experimental and numerical results.

There is a small discrepancy between experimental and numerical results in Fig. 6.6., which is the transition case. As in the elastic region, the strain follows the load trace, this discrepancy may be caused by the experimental error in determining the mechanical properties i.e. stress-strain curve of the available aluminium as the

transition part of the curve plays a very important role in the structural behaviour in the elasto-plastic case.

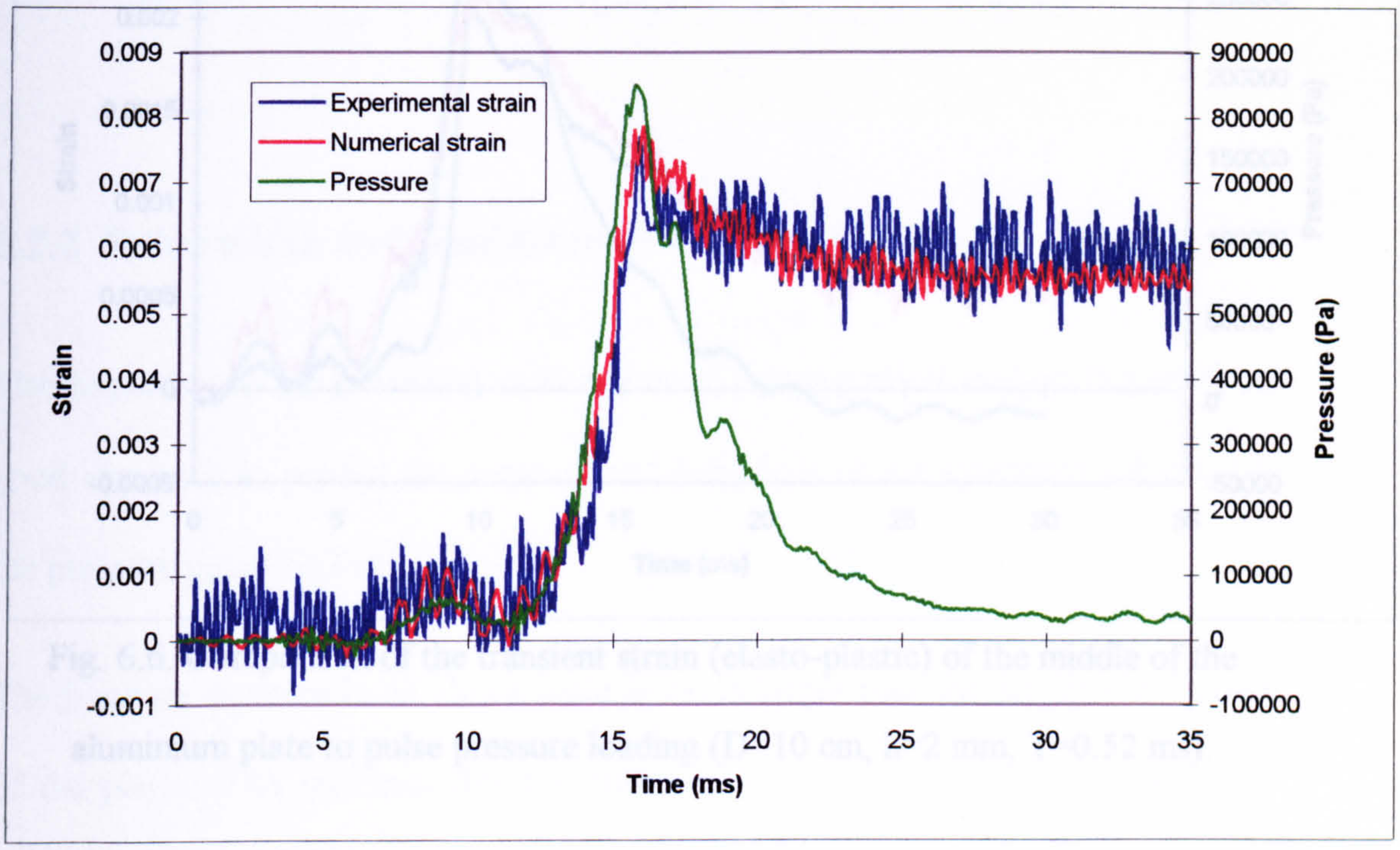

Fig. 6.5. Comparison of the transient strain (plastic response) of the middle of the aluminium plate to pulse pressure loading (D=10 cm, h=1.2 mm, T=0.87 ms).

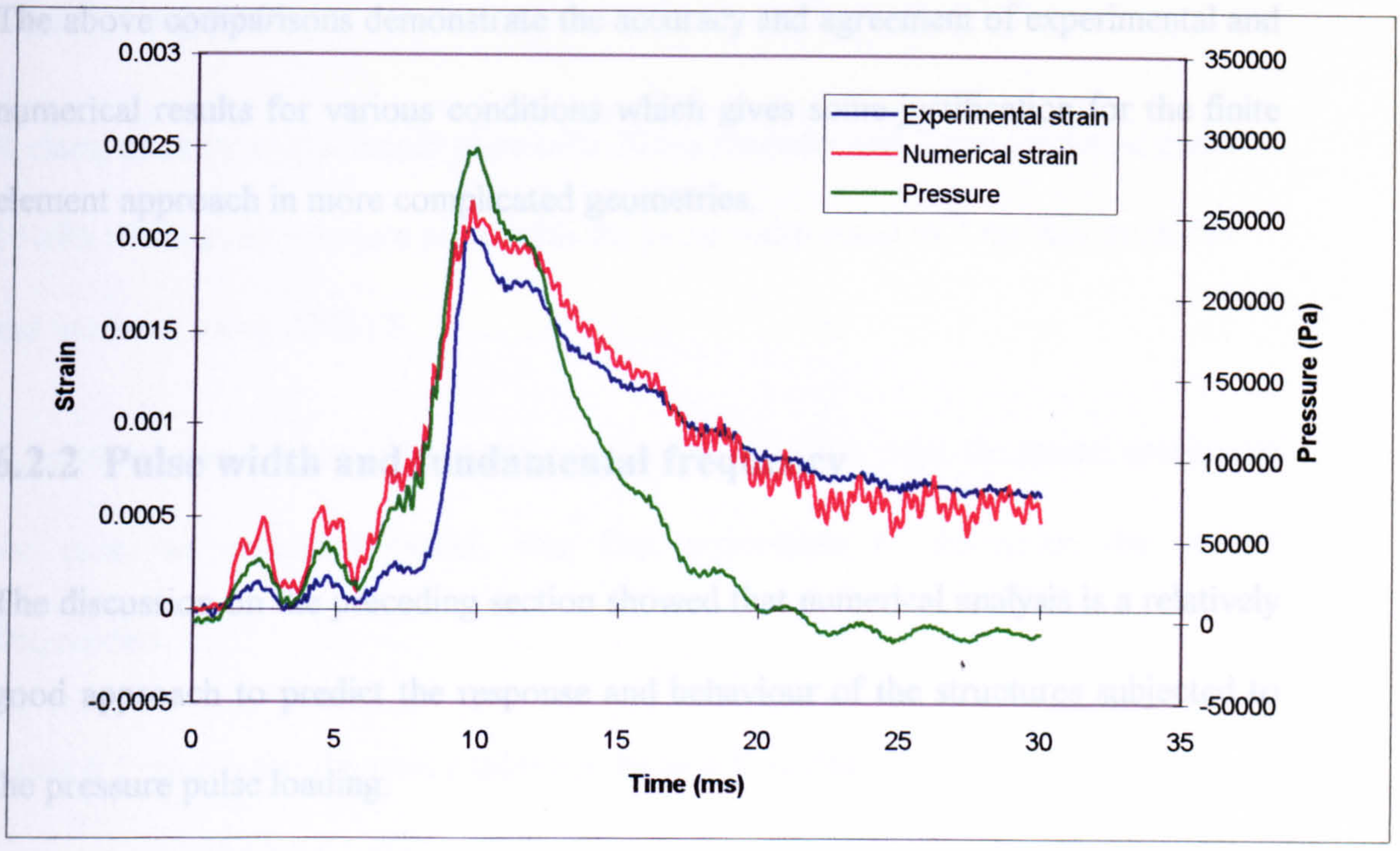

Fig. 6.6. Comparison of the transient strain (elasto-plastic) of the middle of the aluminium plate to pulse pressure loading (D=10 cm, h=2 mm, T=0.52 ms).

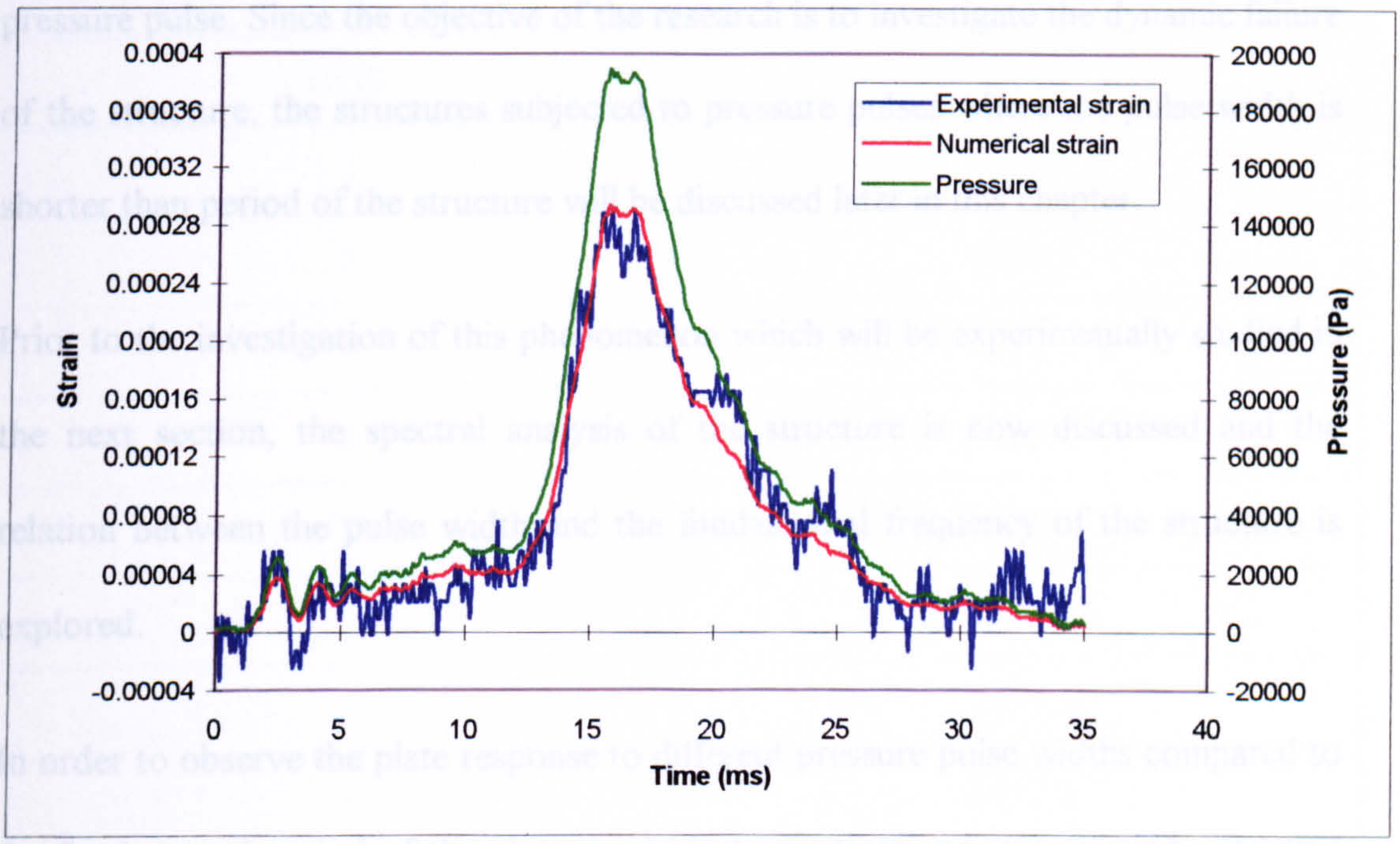

Fig. 6.7. Comparison of the transient strain (elastic response) of the middle of the aluminium plate to pulse pressure loading (D=10 cm, h=3.25 mm, T=0.32 ms).

The above comparisons demonstrate the accuracy and agreement of experimental and numerical results for various conditions which gives some justification for the finite element approach in more complicated geometries.

6.2.2 Pulse width and fundamental frequency

The discussion on the preceding section showed that numerical analysis is a relatively good approach to predict the response and behaviour of the structures subjected to the pressure pulse loading.

The pressure duration in all above cases is much larger than the fundamental period of the plates. This indicates that the structure has enough time to respond to the pressure pulse. Since the objective of the research is to investigate the dynamic failure of the structure, the structures subjected to pressure pulses where the pulse width is shorter than period of the structure will be discussed later in this chapter.

Prior to the investigation of this phenomenon which will be experimentally studied in the next section, the spectral analysis of the structure is now discussed and the relation between the pulse width and the fundamental frequency of the structure is explored.

In order to observe the plate response to different pressure pulse widths compared to the fundamental period of the plate, numerical investigations were carried out using two examples with long and short pulse widths.

6.2.2.1 Long pulse

A clamped circular aluminium plate with 20 cm diameter and 2 mm thickness under 10 kPa rectangular pressure pulse with the pulse width equal to 2 ms was modelled and analysed using ANSYS.

In order to compare the pulse width and the period of the plate, the modal analysis of the case, as explained earlier, was first undertaken to determine the natural frequencies.

Table 6.1. shows the frequency table for the first 8 modes.

MODE	FREQUENCY (Hz)
1	543.3
2	1038.7
3	1038.7
4	1686.8
5	1713.
6	1975.3
7	2477.2
8	2477.2

Table 6.1. Plate frequencies of the clamped circular aluminium plate with 20 cm diameter and 2 mm thickness.

The spectra of the centre of the plate under the defined condition is shown in Fig. 6.8. As can be observed the fundamental frequency of the plate is mainly excited and the reason is the pressure pulse width (2 ms) is long and in this case the same as the period of the structure (2 ms).

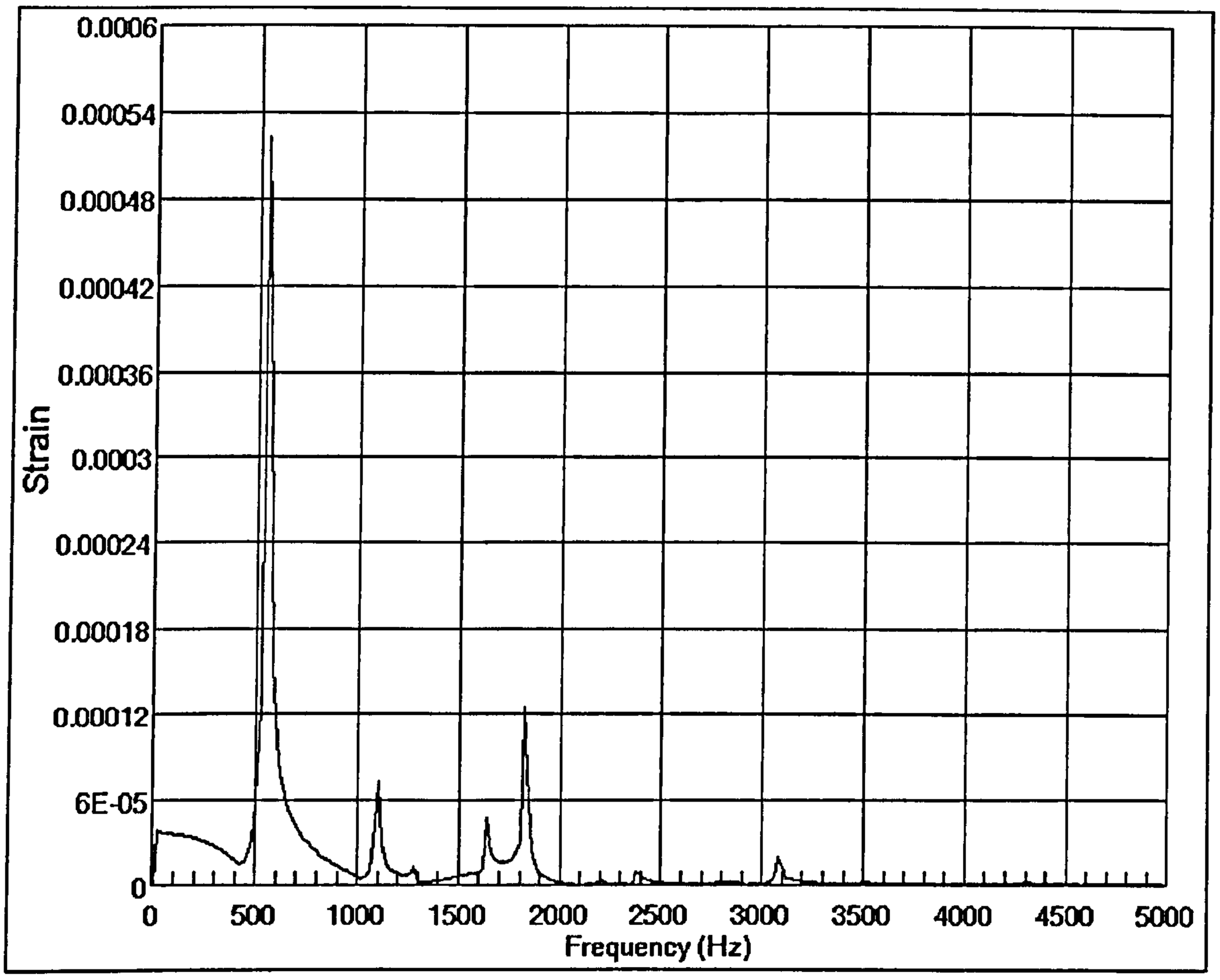

Fig. 6.8. The spectra of the strain in the middle of the aluminium plate (diameter: 20 cm, thickness: 2 mm, period: 2 ms) under rectangular pressure pulse (pressure: 10 kPa, pulse width: 2 ms)

6.2.2.2 Short pulse

To observe the response to the short pulse, a clamped circular aluminium plate with 20 cm diameter and 0.5 mm thickness under 1 kPa rectangular pressure pulse with the pulse width equal to 1 ms was also modelled and analysed using ANSYS.

In order to compare the pulse width and the period of the plate, the modal analysis was also first undertaken for this case. Table 6.2. shows the frequency table for the first 18 modes for this case.

MODE	FREQUENCY (Hz)
1	124.4
2	260.0
3	260.0
4	422.7
5	429.4
6	495.1
7	621.4
8	621.4
9	763.0
10	763.0
11	841.6
12	852.2
13	1046.0
14	1077.4
15	1103.2
16	1103.2

17	1146.6
18	1385.5

Table 6.2. Plate frequencies of the clamped circular aluminium plate with 20 cm diameter and 0.5 mm thickness.

The spectra of the centre of the plate under defined condition is shown in Fig. 6.9. As can be observed the higher frequency of the plate is excited and the reason is the pressure pulse width (1 ms) is very short compared to the period of the structure (8ms).

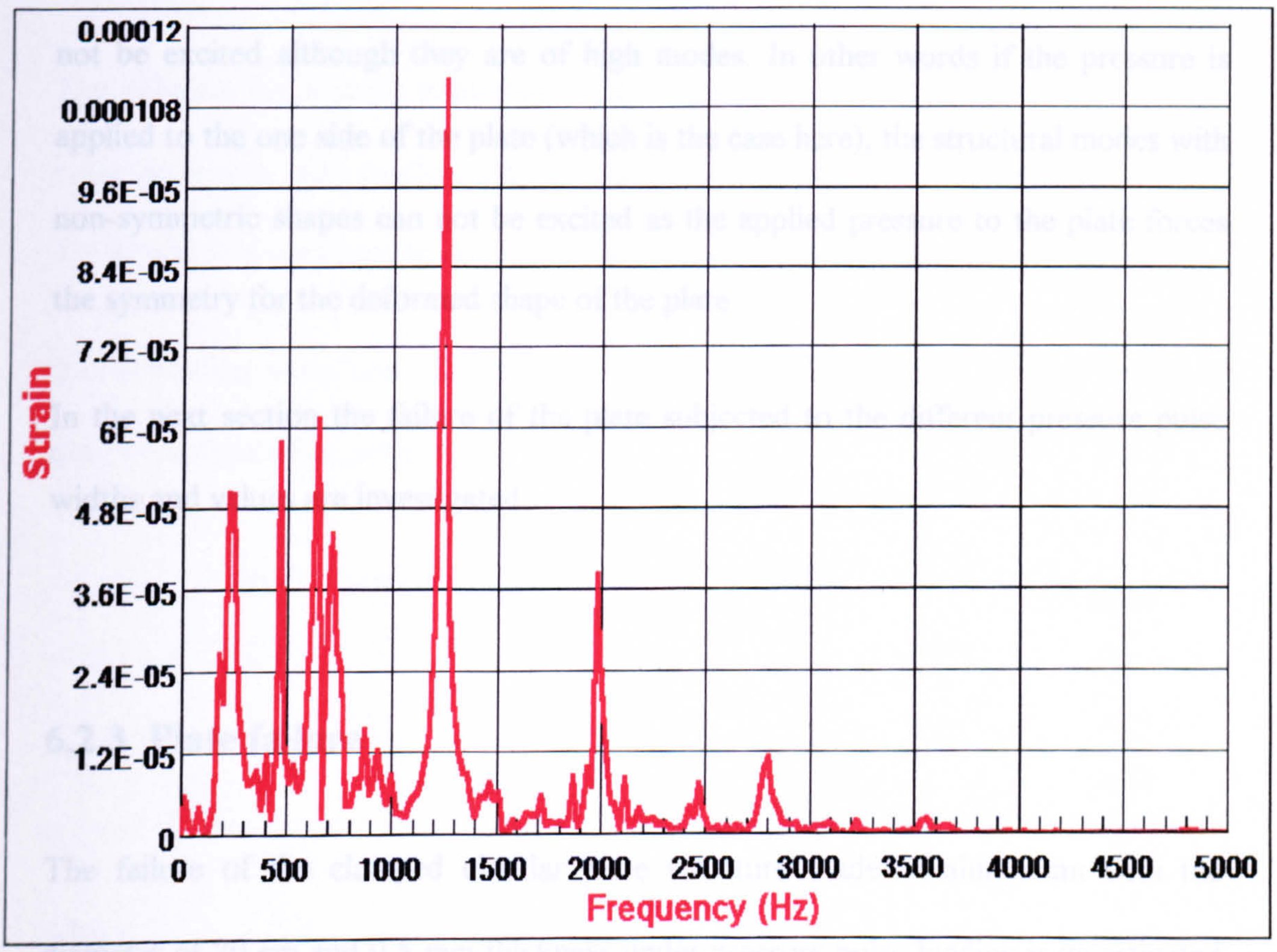

Fig. 6.9. The spectra of the strain in the middle of the aluminium plate (diameter: 20 cm, thickness: 0.5 mm, period: 8 ms) under rectangular pressure pulse (peak pressure: 1 kPa, pulse width: 1 ms)

6.2.2.3 Conclusions

It was observed that by decreasing the pressure pulse width to very short pulses compared to the period of the plate structure, the higher modes are excited. It must also be mentioned that the excited modes in spectra must follow that symmetry of the pressure pulse shape and therefore the plate modes with non-symmetric shapes will not be excited although they are of high modes. In other words if the pressure is applied to the one side of the plate (which is the case here), the structural modes with non-symmetric shapes can not be excited as the applied pressure to the plate forces the symmetry for the deformed shape of the plate.

In the next section the failure of the plate subjected to the different pressure pulse widths and values are investigated.

6.2.3 Plate failure

The failure of the clamped circular plate structure made of aluminium with the diameter of 20 cm and 0.5 mm thickness under pressure pulse loading is investigated here.

The static design pressure of the plate is first determined and then a comparison of experimental and numerical results for the plate under a pressure pulse loading with a pulse width well under the period of the plate is made and finally an experimental fail-safe curve for the plate subjected to the pressure pulse loading is generated.

6.2.3.1 Static design pressure

The static allowable pressure for the aluminium plate first needs to be determined in order to observe if the plate can withstand pressures higher than this static pressure under pulse loading later in this chapter.

The solution for a static uniformly loaded circular plate with a clamped edge with large deflection was studied and presented (Timoshenko and Woinowsky-Krieger, 1959) which is used here to determine the allowable static pressure for the case.

The following equations (Timoshenko and Woinowsky-Krieger, 1959) are used to determine the design pressure.

$$\frac{w_0}{h} + 0.471\left(\frac{w_0}{h}\right)^3 = 0.171\frac{p}{E}\left(\frac{a}{h}\right)^4 \tag{6.4}$$

$$\sigma_y = 0.976E\frac{w_0^2}{a^2} \tag{6.5}$$

where,

w_0: final deflection in the middle of the plate

h: thickness p: pressure

E: modulus of elasticity a: radius

σ_y : yield stress

and in the present case,

$h = 5\times10^{-4}$ m $E = 69\times10^{9}$ Pa

$a = 0.1$ m $\sigma_y = 146\times10^{6}$ Pa

Using equations (6.3) and (6.4), the maximum allowable static pressure to yield is:

$$p = 9827.6 \text{ Pa} \tag{6.6}$$

Therefore the maximum allowable static pressure for the clamped aluminium plate is 9827.6 Pa. The response of the plate under a higher pulse pressure will be discussed and compared in the next section.

6.2.3.2 Comparison

As can be observed in the last section, the maximum allowable static pressure is 9827.6 Pa. However pressure around 30000 Pa was experimentally applied to the plate within about 2 ms and no failure occurred according to the plastic deformation of the middle of the plate which can be observed in Fig. 6.11. Therefore it can be seen that the pressure as high as 3 times of the static design pressure can be applied to the structure without failure.

In order to show the capability of ANSYS in analysing transients where the pulse width is less than the fundamental period of the structure, the numerical response of

the plate under the defined conditions are also shown in Fig. 6.10. As small discrepancy between numerical and experimental results exists which may be due to the error in the material properties in terms of stress-strain curve. However the delay of the structural response in respect to the loading is very well predicted by using the numerical analysis. This gives some confidence that the numerical analysis can be used to investigate the failure of structures under the pressure pulse loading and present a viable alternative to large scale experimental tests.

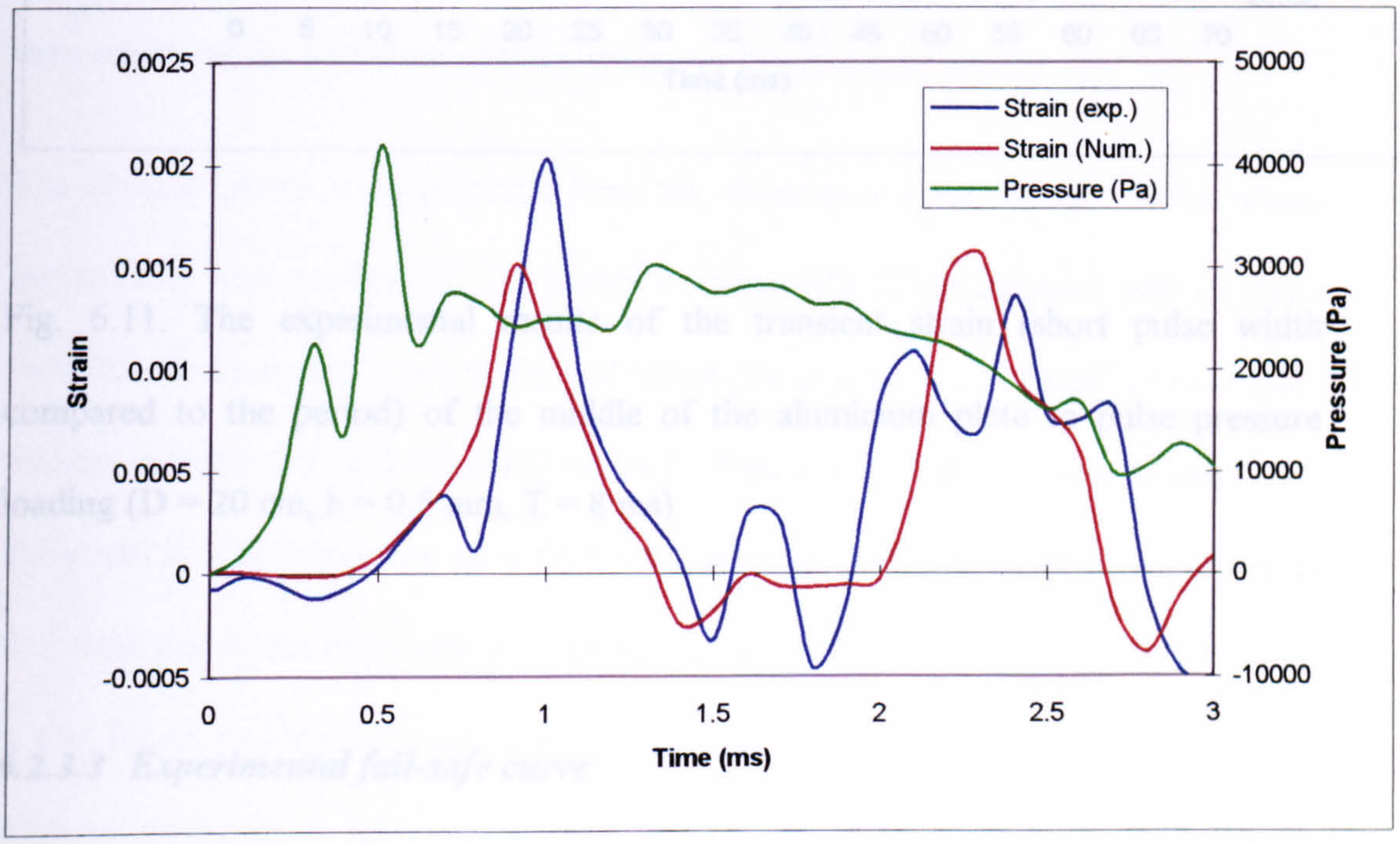

Fig. 6.10. Comparison of the transient strain (short pulse width compared to the period) of the middle of the aluminium plate to pulse pressure loading (D = 20 cm, h = 0.5 mm, T = 8 ms)

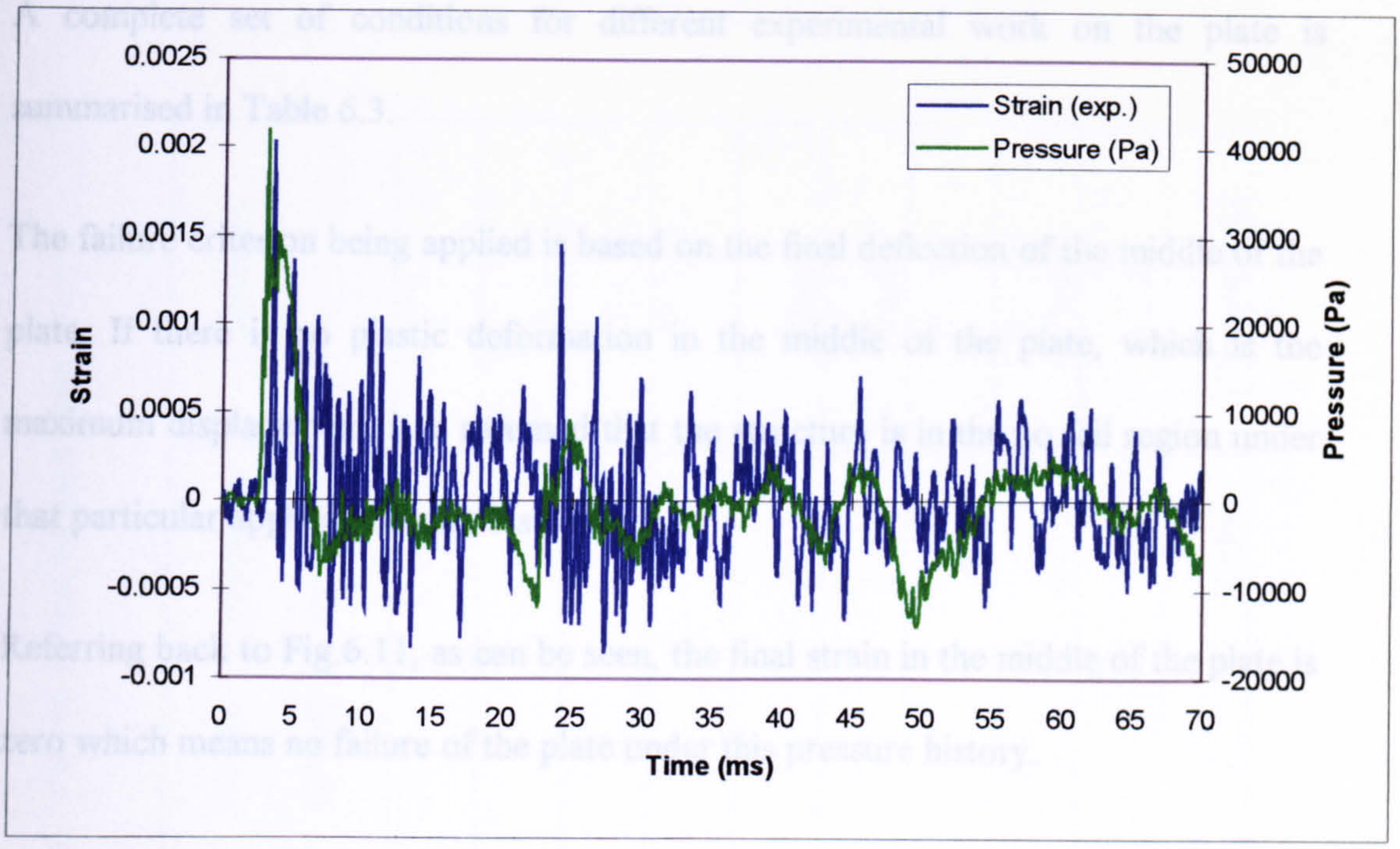

Fig. 6.11. The experimental results of the transient strain (short pulse width compared to the period) of the middle of the aluminium plate to pulse pressure loading (D = 20 cm, h = 0.5 mm, T = 8 ms)

6.2.3.3 Experimental fail-safe curve

A number of experiments have been carried out with different peak pressures and duration to investigate the failure of the plate under pressure pulse loading. As mentioned and observed, the plate structure can withstand pressures higher than the static limit pressure. This is now determined by experiment in this section.

Choosing various thicknesses of diaphragm (bursting disc) gives the freedom for the maximum peak pressure applied and also by changing the driver section length, the pressure duration can also be altered.

A complete set of conditions for different experimental work on the plate is summarised in Table 6.3.

The failure criterion being applied is based on the final deflection of the middle of the plate. If there is no plastic deformation in the middle of the plate, which is the maximum displacement, it is assumed that the structure is in the no fail region under that particular applied pressure history.

Referring back to Fig.6.11, as can be seen, the final strain in the middle of the plate is zero which means no failure of the plate under this pressure history.

The circular plates were prepared from the aluminium sheet (Grade: 1050) whose tensile tests were performed. 22 plates, 6 plates with 10 cm diameter and 16 plates with 20 cm diameters, were made and tested. Each plate is identified with the plate number in Table 6.3. and a few test on each of them were carried out until the plastic deformation was performed or a fault was detected. The test number of each plate was indicated in the table with the alphabetical order e.g. a, b. From the experiments, it was found that the fail –safe curve can not be produced for the plate with 10 cm diameter as the shock tube was not able to create the enough pressure within a short time to fail the plate. However the fail-safe date for 20 cm. Plate is shown in Table 6.4.

Table 6.3. Summary of the experimental works on the plate under pressure pulse loading. 'a' refers to 1st test on each plate

Test Number	Plate thickness (mm)	Plate diameter (cm) & media	Bursting Disc Thickness (cm)	Cross (mm)	Bursting Pressure (kPa)	Peak Pressure (kPa)	Pulse Width (ms)	Blocks (plugs)	Maximum Strain (μ)	Comments
Plate1-a	-	10-water	-	-	47532	500	8	-	-	
Plate1-b	-	10-water	-	-	47532	400	6	-	-	
Plate1-c	-	10-water	-	-	47532	800	4	-	-	
Plate1-d	-	10-water	-	-	47532	900	7	-	-	
Plate1-e	3.2	10-water	-	-	47532	800	4	-	7000	Plastic
Plate2-a	-	10-water	0.33	0.02	47532	400	15	-	4000	Faulty
Plate3-a	2.0	10-water	0.20	0.02	23766	15	5	-	90	
Plate3-b	2.0	10-water	0.33	0.02	47532	700	4	-	4500	Plastic
Plate4-a	2.0	10-water	0.33	0.02	47532	1000	30	-	40	Faulty
Plate5-a	2.0	10-water	0.20	0.02	23766	300	7	-	2000	Elasto-plastic

Plate6-a	3.2	10-water	0.307	0.012	9506.49	180	7	-	250	Elastic
Plate6-b	3.2	10-water	0.307	0.012	9506.49	190	7	-	280	Elastic
Plate7-a	-	10-air	0.307	0.012	9506.49	120	12	-	-	Faulty
Plate8-a	-	10-air	0.307	0.012	9506.49	200	3	-	-	Reduced driver
Plate8-b	-	10-air	0.307	0.012	9506.49	200	3	-	-	Reduced driver
Plate8-c	-	10-air	0.307	0.012	9506.49	120	1	-	-	Closer TEE section
Plate8-d	-	10-air	0.307	0.012	9506.49	100	1	-	-	Closer TEE section
Plate8-e	3.2	10-air	0.307	0.012	9506.49	100	1	-	2000	
Plate8-f	3.0	10-air	0.307	0.012	9506.49	100	1	-	10000	Plastic plate
Plate9-a	3.0	10-air	0.307	0.012	9506.49	80	1	-	90000	Plastic plate
Plate10-a	2.0	20-air	0.307	0.012	9506.49	160	3	-	12000	Large plate
Plate10-b	2.0	20-air	0.17	0.02	173593	200	4	-	1200	Aluminium plate
Plate10-c	2.0	20-air	0.30	0.02	47532	450	6	-	2500	Plastic
Plate11-a	0.5	20-air	0.307	0.02	7129.8	150	3	-	-	Faulty strain

Plate12-a	0.5	20-air	0.05	0.012	4753.24	80	3	-	1200	Plastic
Plate13-a	1.0	20-air	0.05	0.012	4753.24	80	3	-	1500	Plastic
Plate14-a	0.5	2-air	0.05	0.012	4753.24	40	3	-	1000	Plastic
Plate15-a	1.0	20-air	0.17	0.020	14259.7	55	5	-	800	Plastic
Plate16-a	1.0	20-air	0.307	0.020	14259.7	25	3	4 cm plug	-	
Plate16-b	1.0	20-air	0.17	0.020	14259.7	25	3	4 cm plug	-	
Plate16-c	1.0	20-air	0.05	0.012	4753.24	25	3	1.3 cm plug	-	
Plate16-d	1.0	20-air	0.05	0.012	4753.24	17	2	4 cm plug	-	
Plate16-e	1.0	20-air	0.05	0.012	4753.24	15	3	4 cm plug	-	
Plate16-f	1.0	20-air	0.05	0.012	4753.24	28	2	1.3 cm plug	-	
Plate16-g	1.0	20-air	0.05	0.012	4753.24	30	2	1.8 cm plug	-	
Plate16-h	1.0	20-air	0.05	0.012	4753.24	23	3	2.3 cm plug	-	
Plate16-i	1.0	20-air	0.10	0.012	6151.5	34	3	4.5 cm	-	

								plug		
Plate16-j	1.0	20-air	0.307	0.012	7129.86	27	3	4.5 cm plug	-	
Plate16-k	0.5	20-air	0.05	0.012	4277.5	20	2	4.0 cm plug	1500	Elastic
Plate16-l	0.5	20-air	0.05	0.012	4753.24	41	2	-	2000	Close to plastic
Plate17-a	0.5	20-air	0.05	0.012	4277.5	26	2	4.0 cm plug	2000	
Plate17-b	0.5	20-air	0.05	0.008	4277.5	26	2	4.0 cm plug	-	
Plate17-c	0.5	20-air	0.05	0.004	4277.5	48	4	4.0 cm plug	1400	Elastic
Plate17-d	-	20-air	0.10	0.028	4277.5	120	8	70 cm plug	-	Increased driver
Plate17-e	-	20-air	0.10	0.028	4277.5	140	8	140 cm plug	-	
Plate17-f	-	20-air	0.10	0.028	4277.5	125	12	-	-	
Plate17-g	0.02	20-air	Plastic	-	35703.3	140	13	-	-	Faulty strain-plastic

Plate18-a	-	Air	Plastic	-	4753.24	140	12	-	-	
Plate18-b	-	Air	Plastic	-	4753.24	160	12	-	-	
Plate18-c	-	Air	Plastic	-	3327.27	65	12	-	-	
Plate18-d	-	Air	Plastic	-	3564.58	70	12	-	-	
Plate18-e	-	Air	Foil-0.015	0.003	3916.22	12	15	-	-	Not fully opened
Plate19-a	-	Air	Foil-0.015	0.001	35703.3	100	13	-	-	Burst from edge
Palte20-a	-	Air	Foil-0.015	0.002	4990.28	100	12	-	-	Burst from edge
Plate21-a	-	Air	Foil-0.015	0.004	3327.27	20	12	-	-	Half opened
Plate22-a	-	Air	One foil	-	2851.94	17	12	-	-	
Plate22-b	-	Air	One foil	-	2851.94	19	13	-	-	
Plate22-c	-	Air	Two foils	-	-	32	12	-	-	
Plate22-d	-	Air	Three foils	-	-	50	12	-	-	

Plate22-e	0.5	20-air	One foil	-	-	20	5	140 cm plug	1000	
Plate23-f	0.5	20-air	Two foils	-	-	14	4	170 cm plug	700	
Plate23-g	0.5	20-air	Three foils	-	-	23	4	170 cm plug	1200	
Plate22-h	0.5	20-air	Two foils	-	-	17	8	70 cm plug	850	

Table 6.3. Summary of the experimental works on the plate under pressure pulse loading

Duration (ms)	Presure (MPa){numerical)
2	30 {28)
4.5	22 {23}
7	18 {21}
10	15 {12}
16	9 {8}

Table 6.4. Experimental and numerical fail-safe data for 20 cm. Aluminium plate

A fail-safe curve can also be introduced from Table 6.3. based on the final deflection of the middle of the plate. The variables in the curve are the maximum applied pressure (peak pressure) and the pressure duration (pressure pulse width).

The fail-safe curve for the plate structure under specified conditions is shown in Fig. 6.12. It is obvious from the fail-safe curve that pressures as high as around 2.5 times the static designed pressure can be applied without failure.

It should be noted that an experimental fail-safe curve for 10 cm. Plate could not be produced as the shock tube was not able to generate high pressures to fail the small plate.

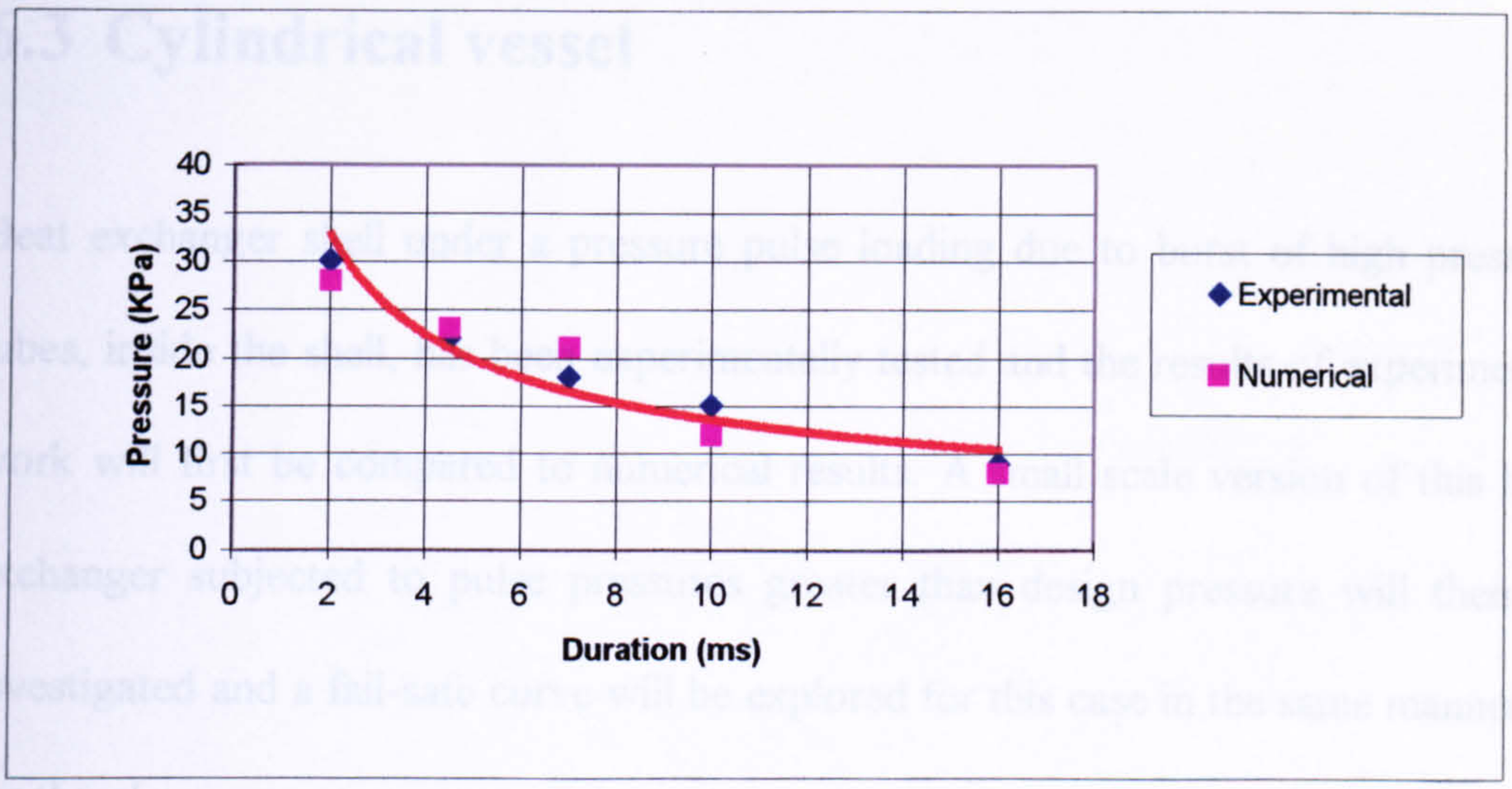

Fig. 6.12. The experimental fail-safe curve for the aluminium plate (D=20 cm, h=0.5 mm) under pressure pulse loading

6.3 Cylindrical vessel

Heat exchanger shell under a pressure pulse loading due to burst of high pressure tubes, inside the shell, has been experimentally tested and the results of experimental work will first be compared to numerical results. A small scale version of this heat exchanger subjected to pulse pressures greater than design pressure will then be investigated and a fail-safe curve will be explored for this case in the same manner as for the plate geometry.

6.3.1 Heat exchanger

The heat exchanger used is shown in Fig.6.13 and was of a shell and tube construction, with a 10 mm thick, 740 mm diameter shell and with a yield pressure of 80 bar. The tube bundle, shown in Fig.6.14 contained 564 tubes with 19.06 mm diameter and straight length of approximately 3600 mm. A large scale heat exchanger filled with water, made of steel which is depicted in Fig. 6.13. This was experimentally tested under pressure pulse loading by the induced failure of high pressure pipes inside the shell, Fig. 6.14, up to 150 bar to the burst. The shell was fitted with a 6 inch nominal bore nozzle to carry a graphite bursting disc with a 10±5% bar burst pressure, and a single 8 inch nominal bore nozzle to simulate part of the water system.

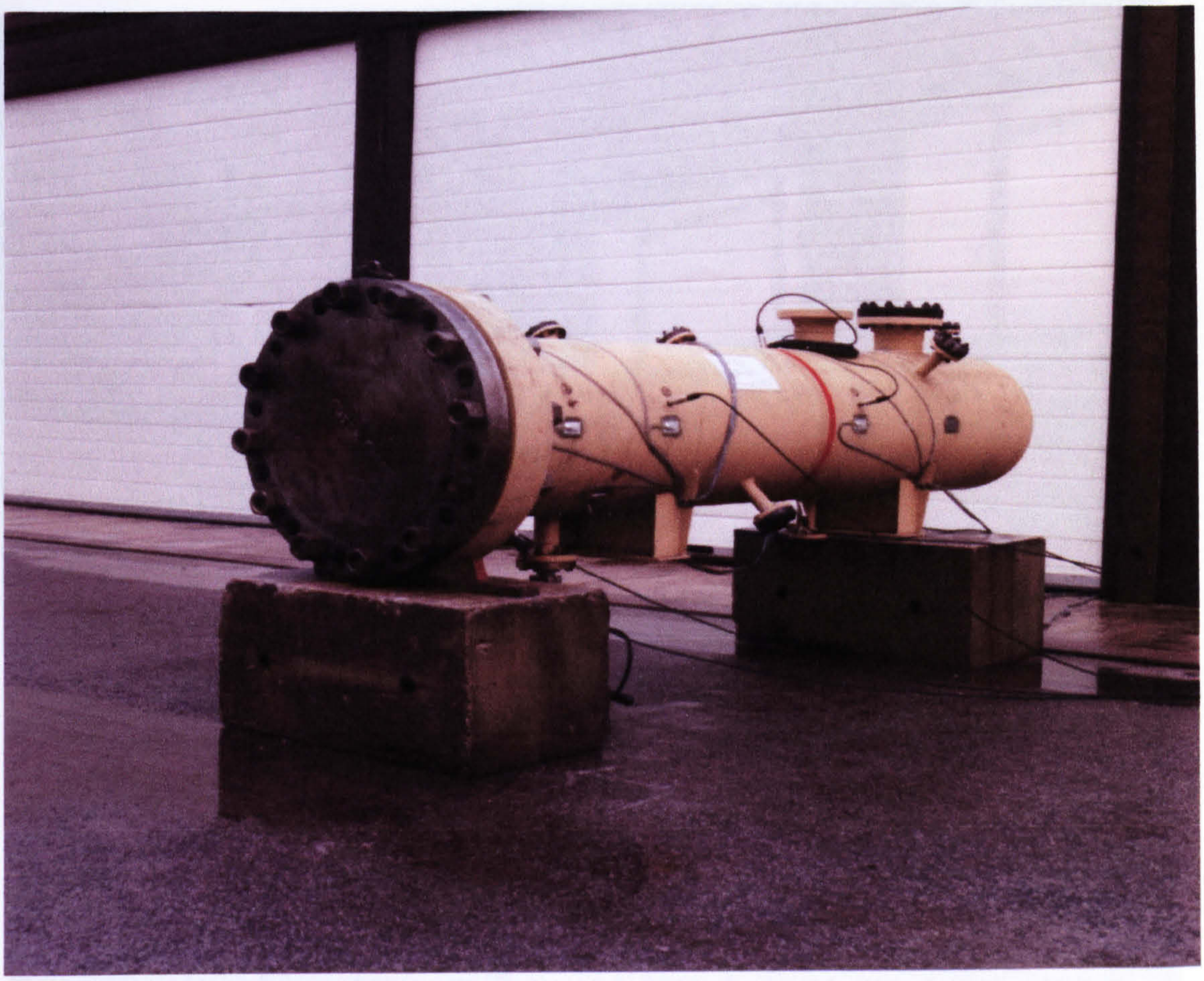

Fig. 6.13. Heat exchanger

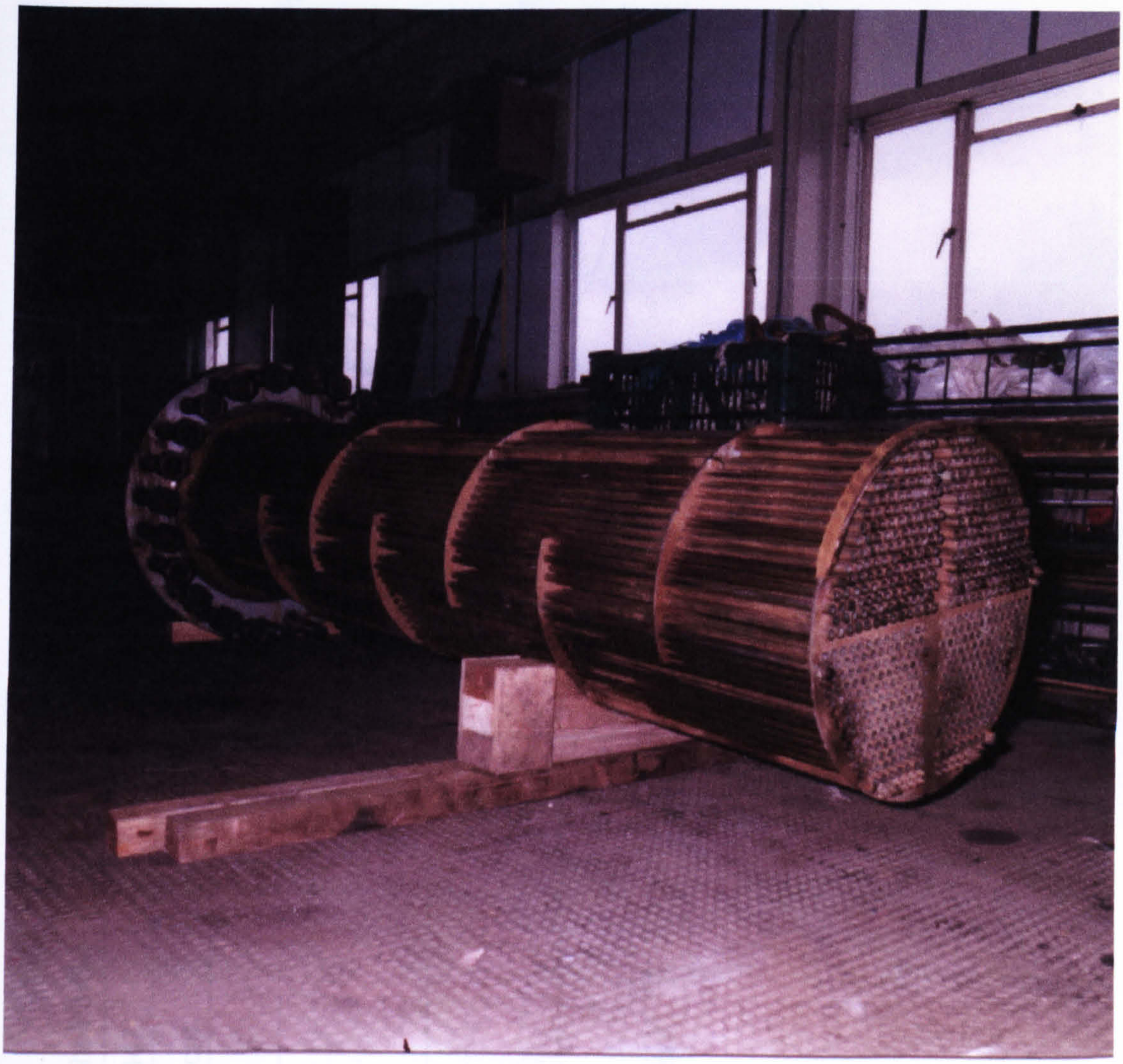

Fig. 6.14. High pressure pipes inside the heat exchanger

The pressure traces in different points close to the shell were then measured which are used to model the heat exchanger in order to compare the numerical and experimental results. Fig. 6.15. shows the dimensions of the shell and associated pipe work and Fig. 6.16. shows the positions of the internal pressure transducers and strain gauges used to monitor pressures and strains in the experiment.

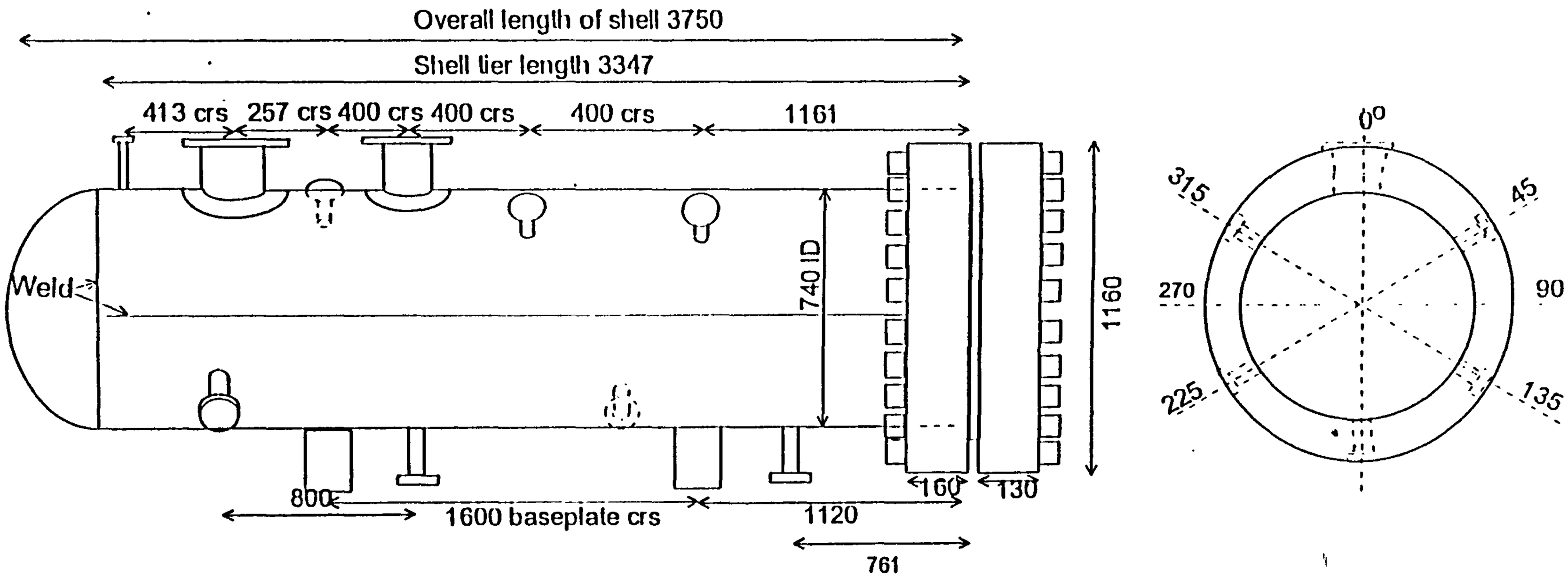

Fig. 6.15. Dimensions of the heat exchangers (in millimetres)

Instrument positions shown as a dotted circle are on the reverse face of the shell

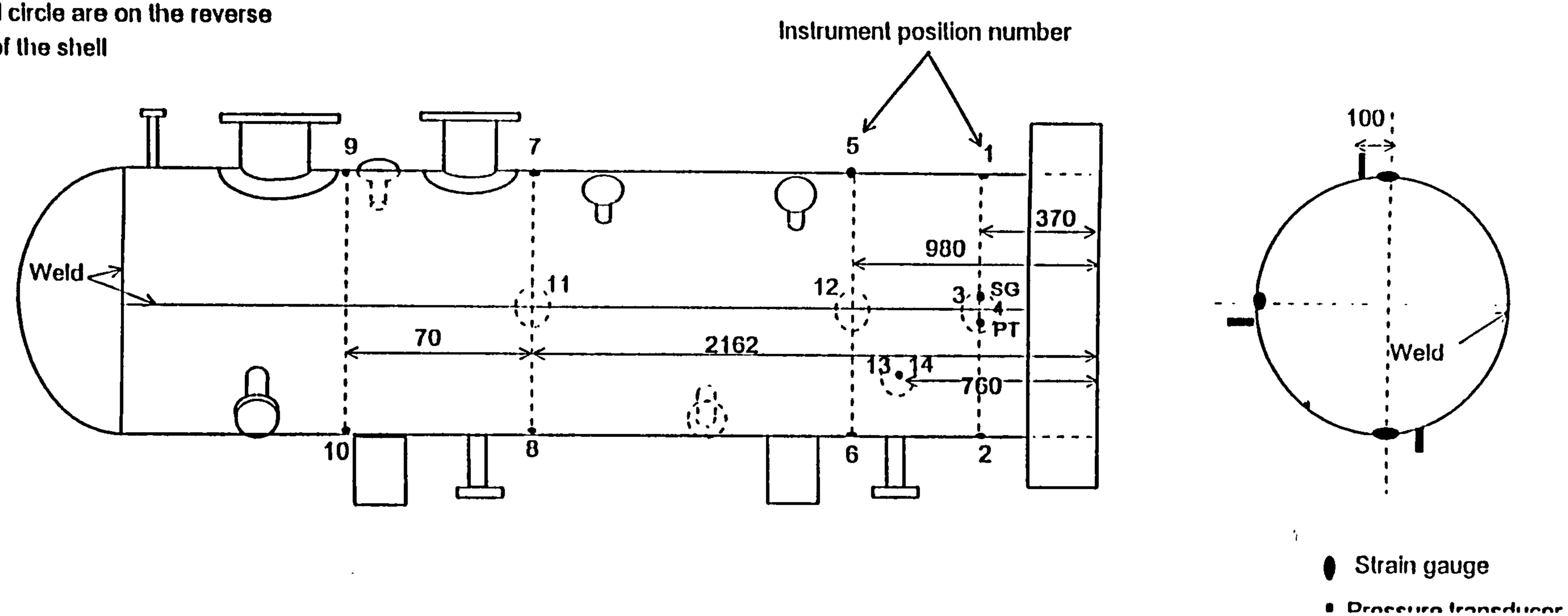

Fig. 6.16. Positions of the pressure transducers and strain gauges

A series of experiments were carried out by HSE (Health and Safety Executive) for different tube side pressures and the pressure and strain history were monitored at the points indicated in Fig. 6.16. The results were then given to analyse using the finite element method. The finite element modelling for one of these cases corresponding to a tube pressure of 146 bar in which the failure location was 0.7 m from the header end of the shell and 0.05 m from the wall is now presented in the next section.

6.3.1.1 Numerical modelling

The finite element model of the heat exchanger with 2592 shell elements with plasticity and large deflection effects is shown in Fig. 6.17. The dynamic model of experimental pressure profiles which are changing in amplitude and duration along the heat exchanger were modelled to obtain the numerical strains and responses of various points in the shell.

The following material properties were used for the analysis:

Modulus of elasticity: $E = 206 \times 10^9$ Pa

Tangent modulus: $E_t = 0$ Pa

Yield stress: $\sigma_y = 335 \times 10^6$ Pa

Density: $\rho = 8242.4$ kg/m^3

Poisson's ratio: $\nu = 0.3$

The pressure-time profile for a point 10 in Fig. 6.16., close to the head of the heat exchanger, as an example, is plotted in Fig. 6.18.

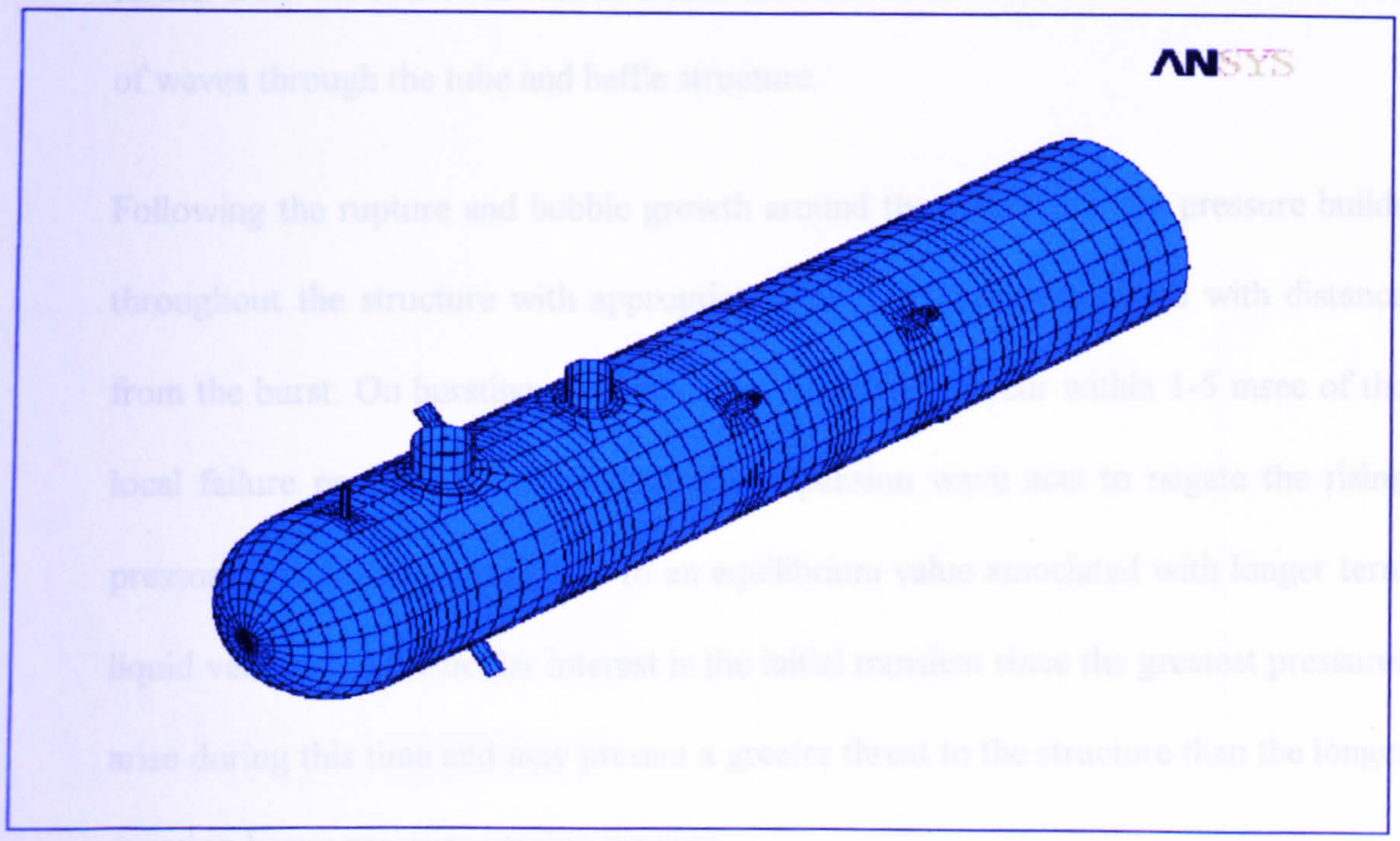

Fig. 6.17. Finite element model of heat exchanger

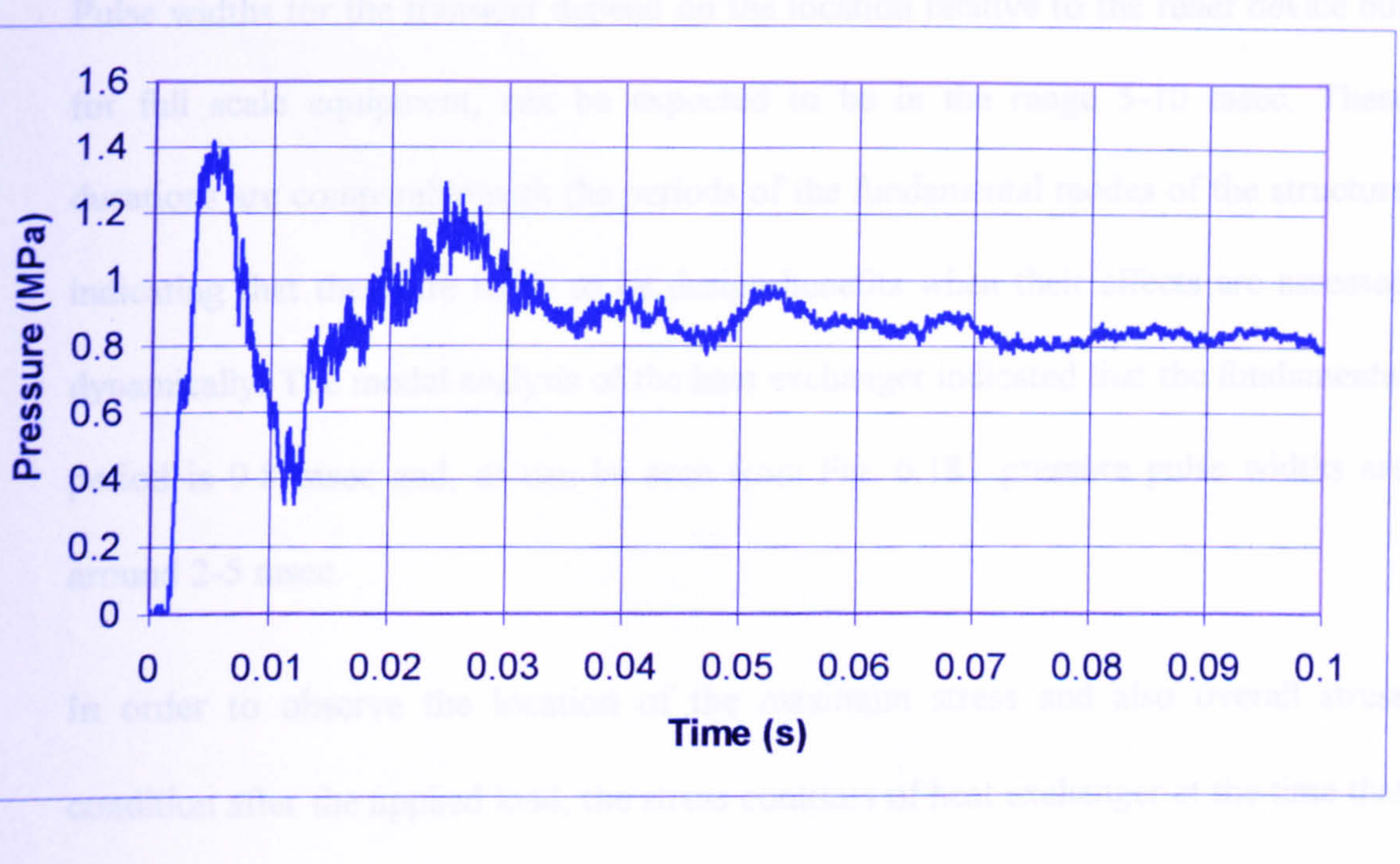

Fig. 6.18. Pressure-time profile in heat exchanger

It should be again reminded that the pressure time profiles decrease in peak pressure further from the source as well as a time shift associated with the finite transient time of waves through the tube and baffle structure.

Following the rupture and bubble growth around the failure site, the pressure builds throughout the structure with appropriate time differences associated with distance from the burst. On bursting disc operation, believed to occur within 1-5 msec of the local failure pressure being reached, the expansion wave acts to negate the rising pressure, resulting in a rapid fall to an equilibrium value associated with longer term liquid venting. Of particular interest is the initial transient since the greatest pressures arise during this time and may present a greater threat to the structure than the longer duration lower pressure venting process.

Pulse widths for the transient depend on the location relative to the relief device but for full scale equipment, can be expected to be in the range 5-10 msec. These durations are comparable with the periods of the fundamental modes of the structure indicating that there are likely to be design benefits when their effects are assessed dynamically. The modal analysis of the heat exchanger indicated that the fundamental period is 9.8 msec and, as can be seen from Fig. 6.18., pressure pulse widths are around 2-5 msec.

In order to observe the location of the maximum stress and also overall stress condition after the applied load, the stress contours of heat exchanger at the time that the maximum pressure is applied which is 5 ms are shown in Fig 6.19. and Fig. 6.20.

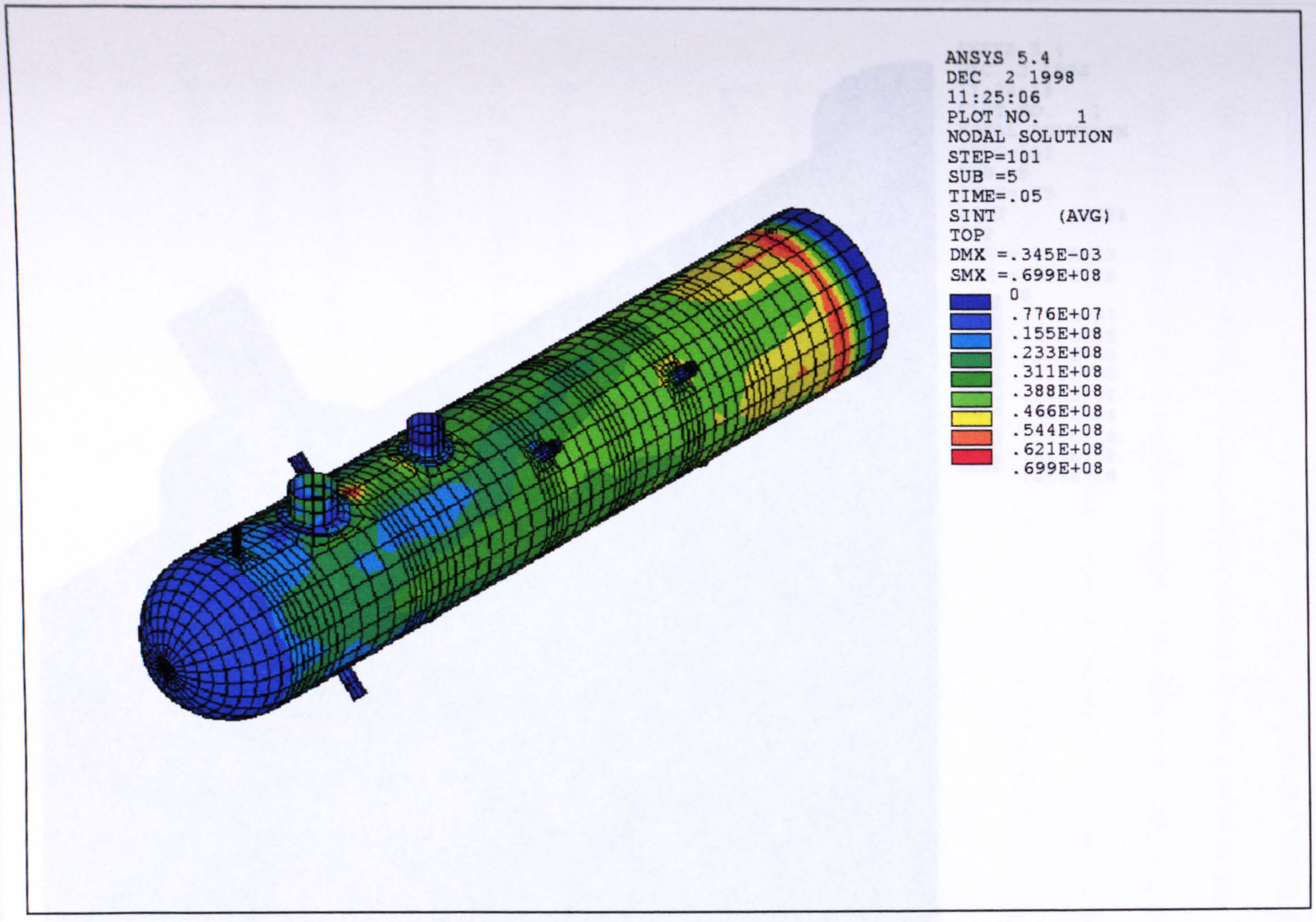

Fig 6.19. Equivalent Stress contour of heat exchanger (Pa)

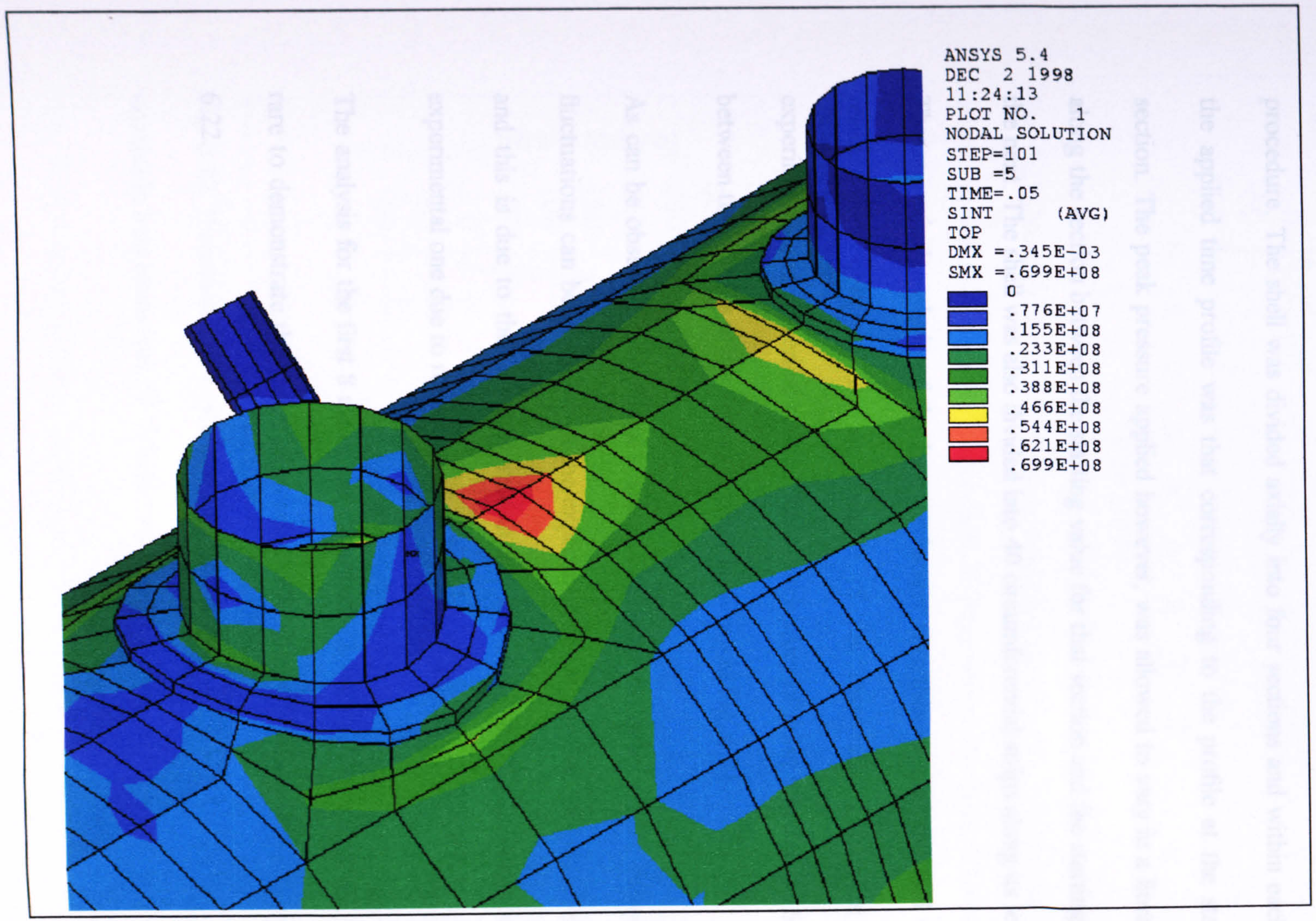

Fig. 6.20. Maximum equivalent stress in heat exchanger shell (Pa)

6.3.1.2 Experimental and numerical comparison

In order to have a realistic comparison between the experimental and numerical results, the applied surface pressure in the numerical work was allowed to vary with distance along the shell for each element and with time according to the following procedure. The shell was divided axially into four sections and within each section, the applied time profile was that corresponding to the profile at the start of the section. The peak pressure applied however, was allowed to vary in a linear manner along the section between the starting value for that section and the starting value for the next. The shell was also divided into 40 circumferential strips along its length.

The numerical analysis of the heat exchanger was then carried out and the strain results were obtained. As an example of the reasonable agreement between experimental and numerical results, the strain history of point 9 in Fig. 6.16. which is between the nozzles in the heat exchanger is shown in Fig. 6.21.

As can be observed the general shape of the traces are quite similar, however more fluctuations can be observed in the experimental compared to the numerical results and this is due to the sampling rate in the numerical calculation being 2% of the experimental one due to reduction of the CPU time in analysis.

The analysis for the first 8 ms of the experiment was modelled with higher sampling rare to demonstrate the above expression. The results for this case is shown in Fig. 6.22.

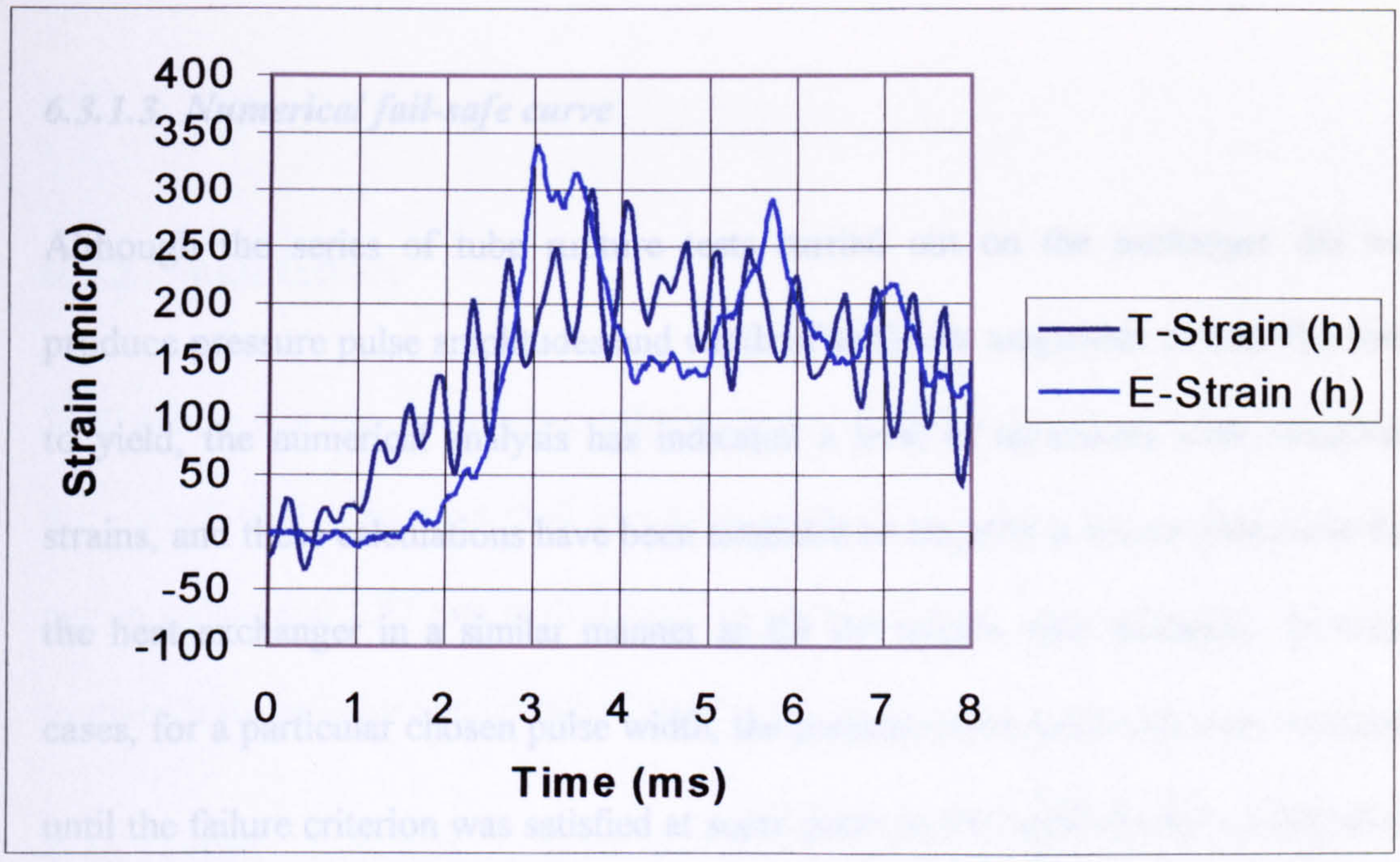

Fig. 6.21. Numerical and experimental strain history of point 9 (Fig. 6.16.) between nozzles in heat exchanger (T: Theoretical, E: Experimental, h: hoop, l: longitudinal)

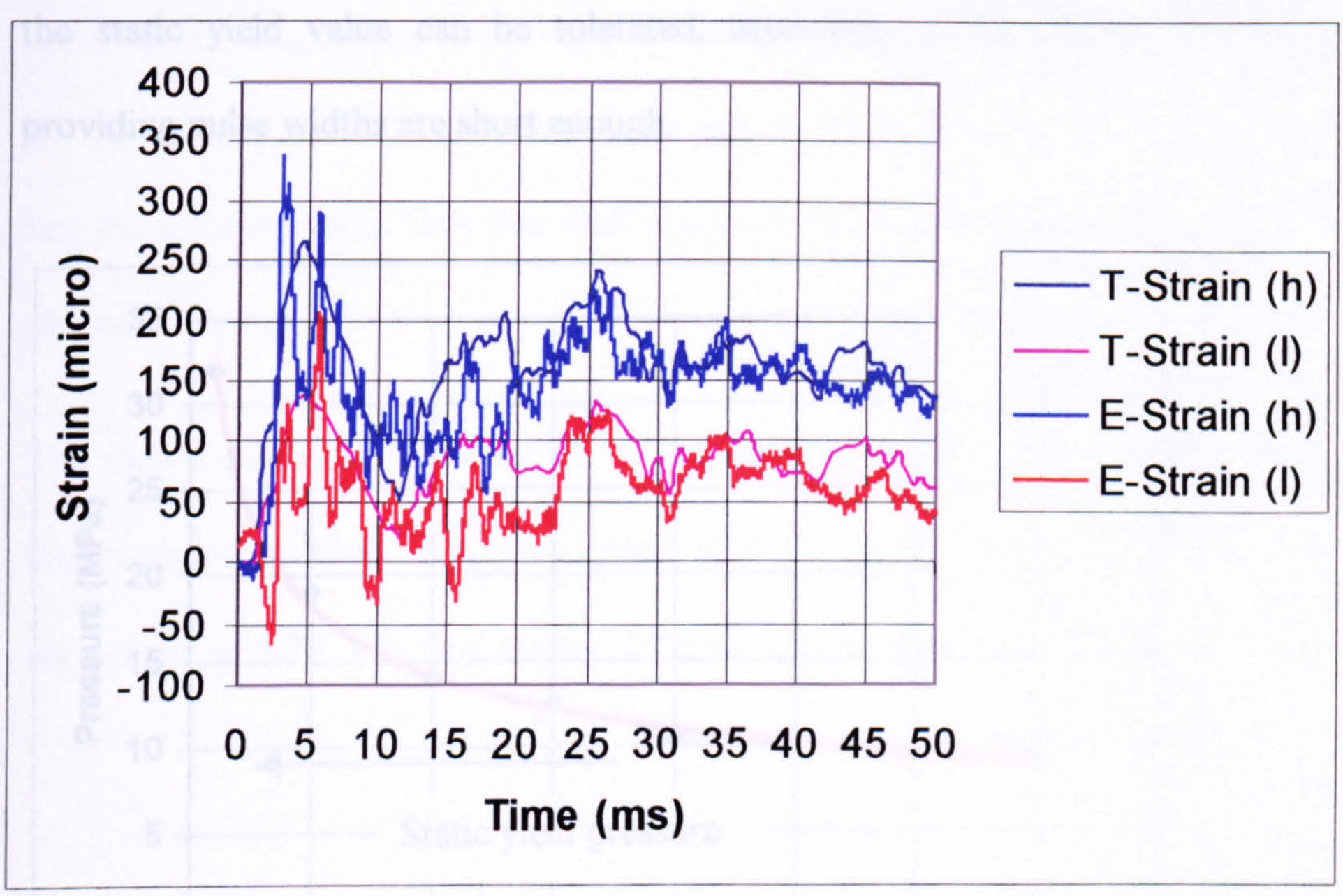

Fig. 6.22. Numerical and experimental strain history of point 9 (Fig. 6.16.) between nozzles in heat exchanger (T: Theoretical, E: Experimental, l: longitudinal)

6.3.1.3 Numerical fail-safe curve

Although the series of tube rupture tests carried out on the exchanger did not produce pressure pulse amplitudes and width of sufficient magnitude to take the shell to yield, the numerical analysis has indicated a level of agreement with measured strains, and these calculations have been extended to establish a failure limit curve for the heat exchanger in a similar manner as for the simple plate geometry. In these cases, for a particular chosen pulse width, the pressure pulse amplitude was increased until the failure criterion was satisfied at some point on the shell and this combination was then chosen as one pair of coordinates on the limit curve. The resulting limit curve is shown in Fig. 6.23. for a selected number of pulse widths. The behaviour is similar to the plate case and indicates that pressure pulses of amplitude several times the static yield value can be tolerated, according to the chosen fail criterion, providing pulse widths are short enough.

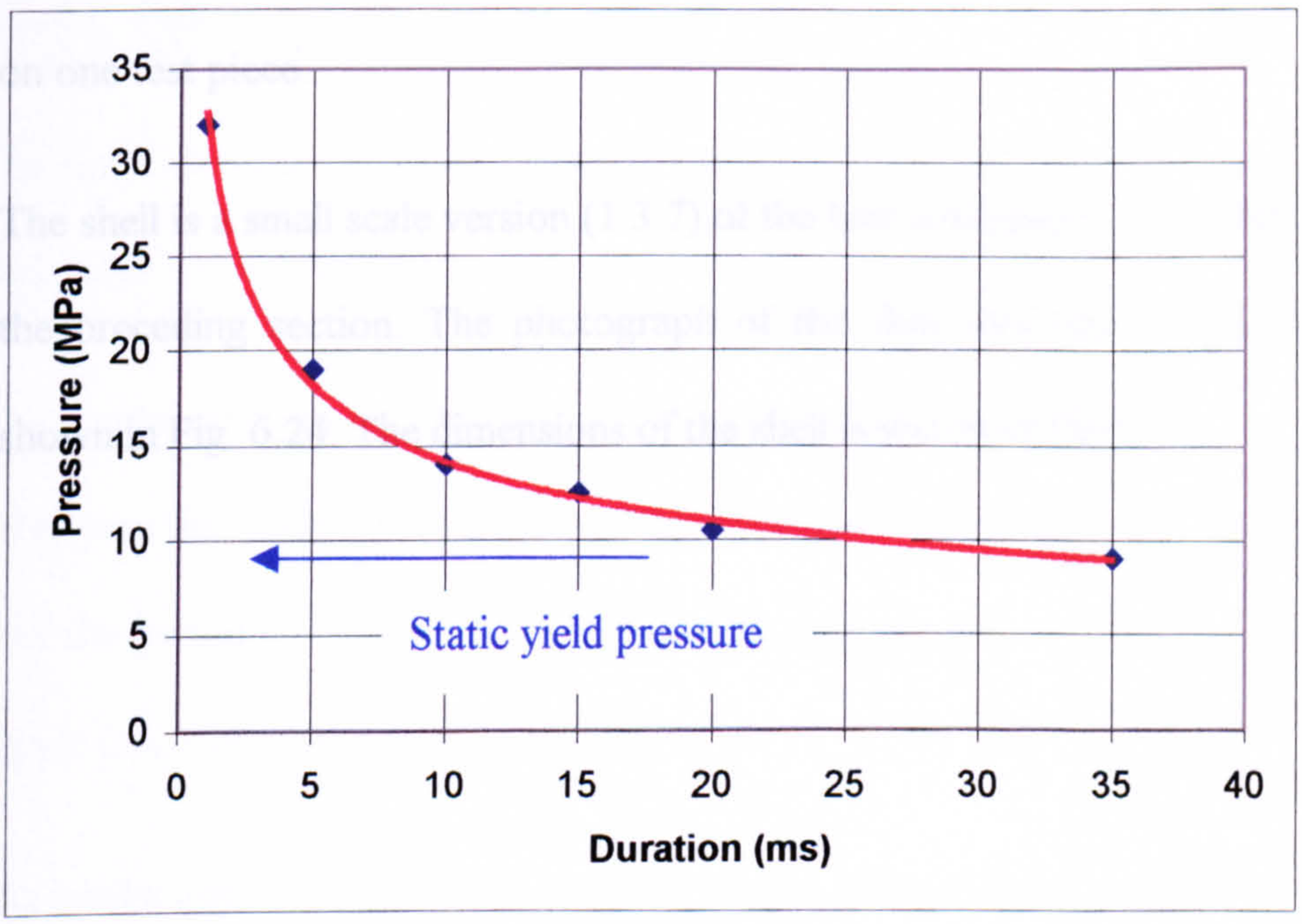

Fig. 6.23. Numerical limit curve for the heat exchanger

6.3.2 Shell failure

Shell failure was also investigated experimentally to determine the fail-safe limit curve for a small shell. The small shell was made of aluminium with 1.34 m in length, 100 mm in radius and 2.87 mm in thickness was attached to the T-section of shock tube to investigate its failure under pulse loading.

Whole length = 1340 mm Conical length = 100 mm Diameter = 200 mm

Thickness = 2.87 mm

The shell was made from a tube for the straight part and a conical part was constructed using a plate under no heat treatment. The manufacturing was stress free for the whole process. The conical shape part was welded to the tube to complete the test piece for the tests. Only one shell was made and all experiments were carried out on one test piece.

The shell is a small scale version (1:3.7) of the heat exchanger which was described in the preceding section. The photograph of the shell attached to the shock tube is shown in Fig. 6.24. The dimensions of the shell is shown in Fig.6.25

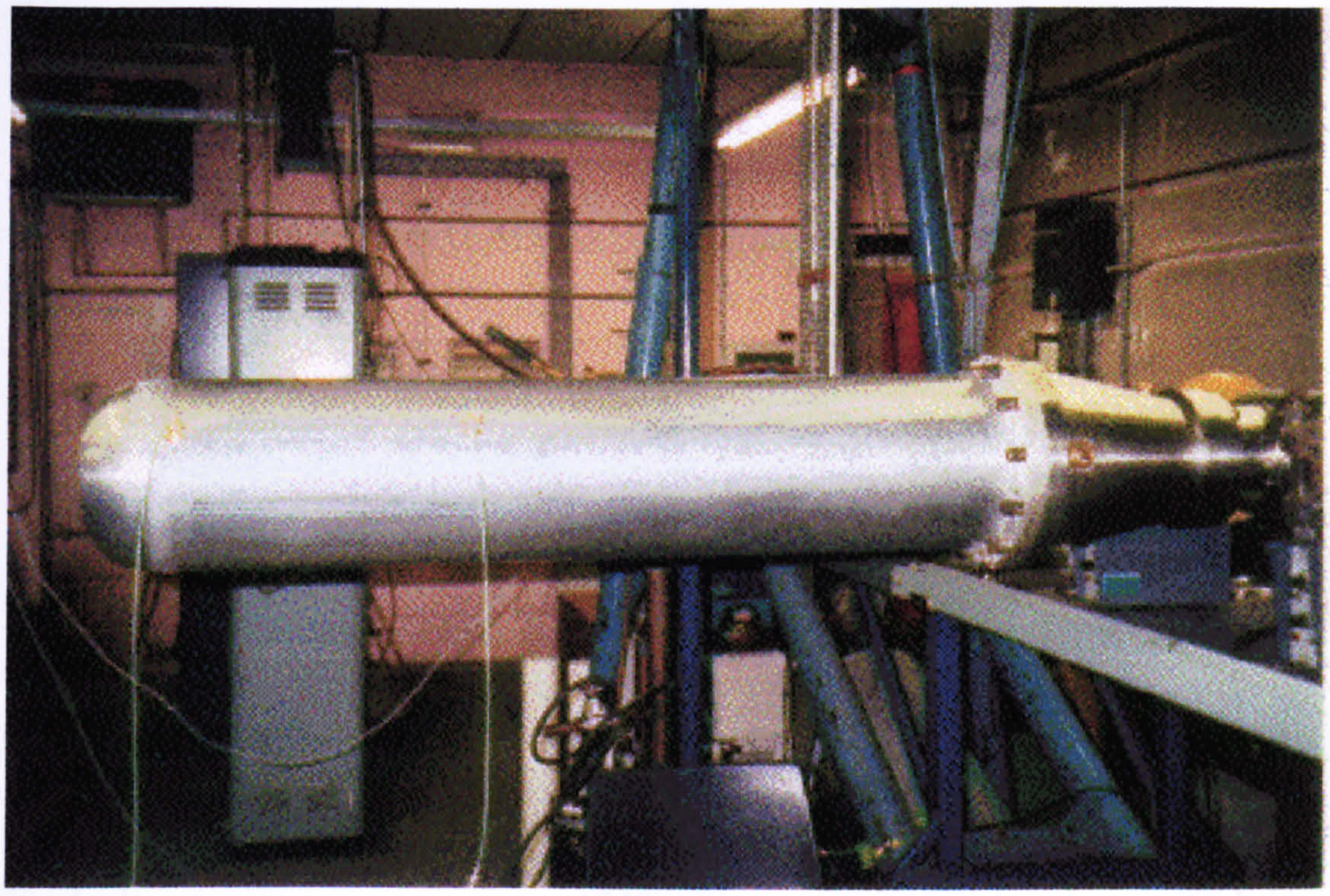

Fig. 6.24. Small scale of heat exchanger

6.3.2.1 F.E. modelling

The finite element model of the shell, clamped at the end, with 2592 shell elements with large deformation and non-linearities is shown in Fig. 6.25.

The modal analysis of the shell was carried out using finite element method to determine the fundamental period of the shell. The pulse width should be chosen less than the period of the shell to investigate the failure of the shell with pulse pressures higher than the static design pressure.

The modal analysis of the shell showed that the fundamental frequency of the shell is 165 Hz, corresponding to a fundamental period of 6 ms.

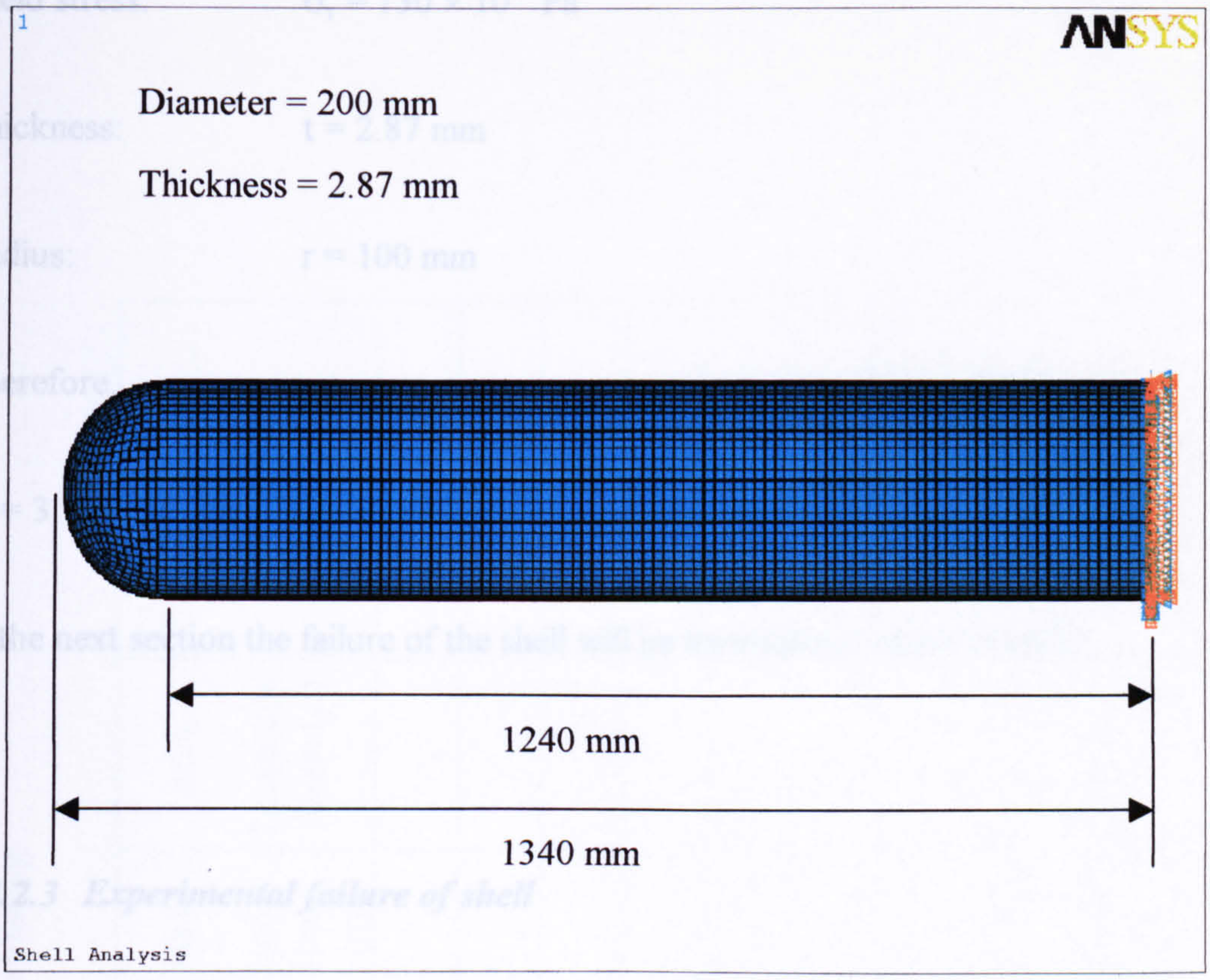

Fig. 6.25. Finite element model of the shell

6.3.2.2 Static design pressure

In order to investigate the shell response to the pulse loading for the pressures higher than the static design pressure, the static design load should be first determined.

The following formula is used to determine the static design pressure (Spenece and Tooth, 1994):

$$P_0 = \frac{\sigma_y t}{r} \tag{6.7}$$

where,

Yield stress: $\sigma_y = 130 \times 10^6$ Pa

Thickness: t = 2.87 mm

Radius: r = 100 mm

Therefore,

$P_0 = 3.731\ 10^6$ Pa

In the next section the failure of the shell will be investigated experimentally.

6.3.2.3 Experimental failure of shell

A series of experiments have been also carried out using the shock tube facilities to observe the effect of the pressure pulse loading on the shell and its failure. The operating conditions and main results of the experimental work are summarised in Table 6.5.

From the above results the fail-safe curve for the shell has been made which is shown in Fig. 6.26. As there was only one shell (test piece) available for the experimental works and the shell was deformed under the final tests, therefore only five experimental data points could be obtained to construct the fail-safe curve for this case.

Table 6.5. Summary of the experimental works on the shell under pressure pulse loading

Test Number	Orifice Diameter (in)	Bursting Disc Thickness (mm)	Cross (mm)	Bursting Pressure (kPa)	Peak Pressure (kPa)	Pulse Width (ms)	Max. Hoop Strain (μ)	Max. Longitude Strain (μ)	Comments
1	2	0.95	0.5	1378.95	800	5	-	-	-
2	2	0.95	0.5	1378.95	500	6	-	-	
3	2	0.95	0.5	1378.95	800	4	-	-	
4	2	0.95	0.5	1378.95	-	-	-	-	Faulty
5	2	0.95	0.5	1378.95	-	-	-	-	Faulty
6	2	0.95	0.5	1378.95	600	3	-	-	
7	2	1.2	0.5	1792.63	900	3	-	-	
8	2	1.2	0.5	1792.63	1000	2	-	-	
9	4	1.2	0.5	1792.63	700	2	-	-	
10	2	1.2	0.5	1792.63	600	2	-	-	

11	2	2.0	0.5	3102.64	2000	2	-	-	
12	3	2.0	0.5	3102.64	1600	2	-	-	Not properly burst
13	3	1.2	0.5	1792.63	800	2	-	-	
14	3	2.0	0.66	2413.16	1400	2	-	-	
15	3	2.6	0.86	3378.43	2500	2	-	-	
16	2	2.6	0.86	3275	2000	2	-	-	
17	3	3.2	1.0	4626.32	2600	2	-	-	Faulty
18	3	3.2	1.0	4136.85	2000	2			Faulty
19	3	3.2	1.0	4626.32	2100	3	-	-	
20	3	3.2	0.8	5515.8	1500	4	-	-	Faulty
21	2	3.2	1.0	5515.8	1500	3	-	-	Faulty
22	3	3.2	0.8	5515.8	3800	2	-	-	
23	3	3.2	0.6	6205.28	4000	2.5	-	-	
24	4	3.2	0.6	6205.28	4100	2.5	-	-	
25	3	6.4	0.58	15857.9	7000	2.3	-	-	

26	3	3.2	0.6	6205.28	4000	2.5	-	-	
27	3	6.35	0.58	16547.4	8000	2.5	-	-	Burst in the edge
28	3	6.35	0.92	15168.4	8000	2.5	-	-	
29	3	4.75	0.58	11031.6	7000	2.5	-	-	
30	3	4.75	0.92	10342.1	6500	2.5	-	-	
31	3	1.2	0.5	1378.95	250	15	-	-	
32	3	1.2	0.5	1378.95	350	10	-	-	
33	3	2	0.5	2757.9	900	8	-	-	
34	3	2	0.5	2757.9	1000	8	-	-	
35	3	2	0.6	2413.16	700	10	-	-	
36	3	2	0.6	2551.06	900	10	0	0	Strains faulty
37	3	2	0.6	2551.06	800	8	±500	±500	Strains faulty
38	3	2.6	0.6	4136.85	1200	8	±500	±500	Strains faulty
39	3	2.6	0.6	4826.32	1500	8	20	10	Strains noisy
40	3	2.6	0.6	4826.32	2000	5	20	10	Strains noisy

41	3	3.2	0.6	5033.17	2000	5	-	-	Strains faulty
42	3	3.2	0.6	6894.75	1800	5	-	-	Strains faulty
43	3	3.2	0.6	6894.75	2000	7	800	300	
44	3	3.2	0.5	7584.23	3000	7	1000	400	
45	3	3.2	0.4	6894.75	2300	7	1100	400	
46	3	3.2	0.4	8273.7	3000	7	1200	500	
47	3	3.2	0.3	9652.65	3500	7	1250	500	
48	3	4.5	1.0	10686.8	4800	7	700	200	Strain gauge not in middle
49	3	2.0	0.6	2068.42	600	10	-	-	No strain results
50	3	2.6	0.6	4136.85	600	10	600	200	The flat end
51	3	2.6	0.6	2136.85	2000	5			
52	3	3.2	0.6	6205.28	4800	4	1400	300	

Table 6.5. Summary of the experimental works on the shell under pressure pulse loading

It is also can be observed that the pressure as high as approximately 2.5 times of static design pressure can also be applied to the shell without failure if the pulse width is short enough compared to the fundamental period of the shell which is 6 msec.

The numerical fail-safe data were also obtained from ANSYS analysis and were also added to Fig.6.26. for comparison.

Table 6.6. shows the comparison between the experimental and numerical fail-safe date for the shell.

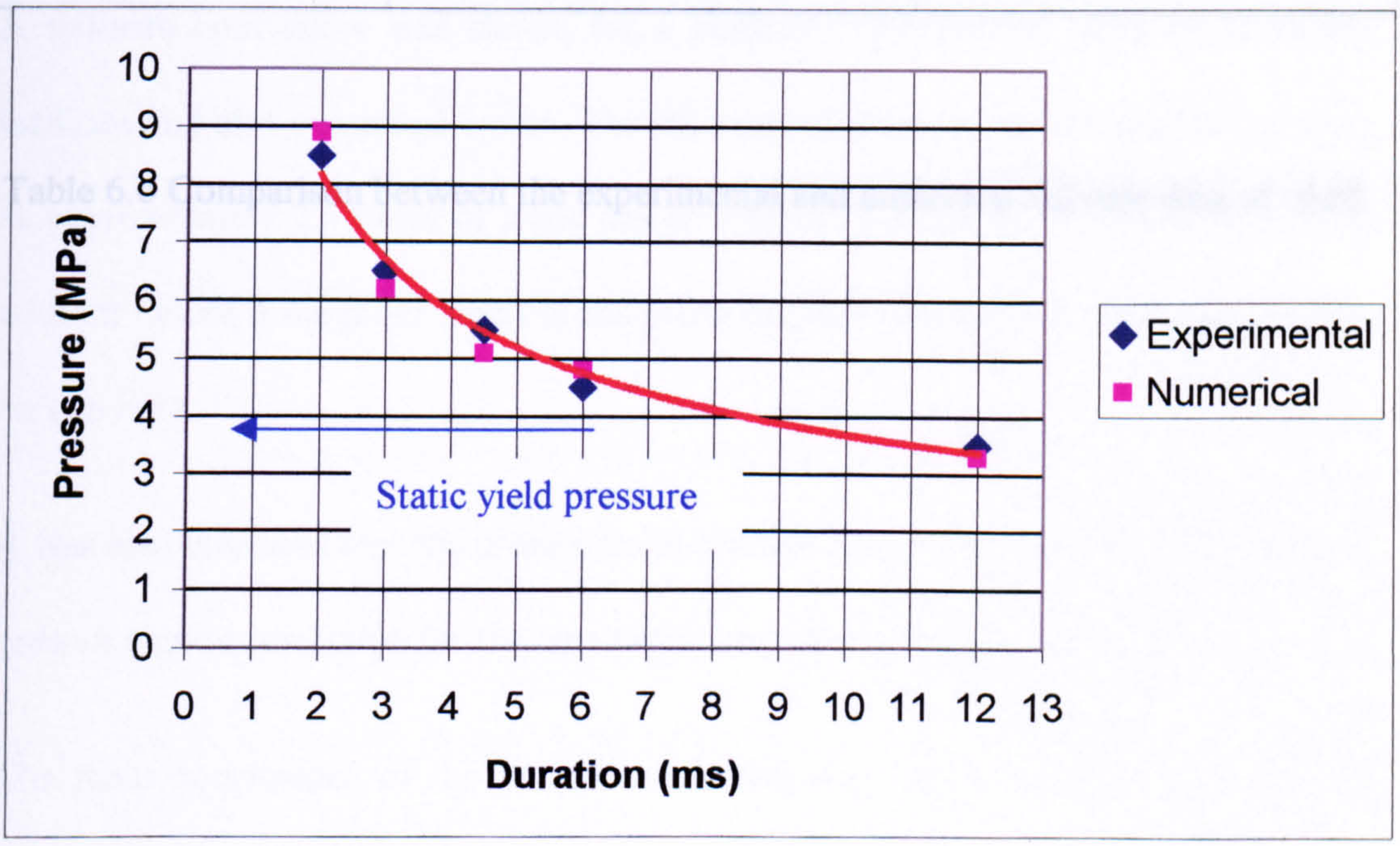

Fig. 6.26. Fail-safe limit curve for the shell

Duration (ms)	Experimental pressure (MPa)	Numerical Pressure (MPa)
2	8.5	8.9
3	6.5	6.2
4.5	5.5	5.1
6	4.5	4.8
12	3.5	3.3

Table 6.6 Comparison between the experimental and numerical fail-safe data of shell

6.4 Conclusions

The structural behaviour due to pressure pulse loading for a number of geometries have been investigated and discussed in this chapter. A logical way to predict and determine the failure modes for the complex structures has been approached by experimenting and analysing from a very simple but basic plate structure. It was to build up and fully understand the structures response to sudden loading such as pressure pulse loading in this research.

A fail-safe limit curve was shown for a number of geometries using experimental facilities and also numerical works. The limit curves showed that the pressure as high as approximately 2.5 times of static design pressure for the structure can be applied without failure if the pulse width of the pressure pulse loading is short and less than a certain limit.

It was also indicated that the present finite element numerical method could relatively present a good prediction for the structure response to pressure pulses.

The main conclusions of the present work and also the recommendations for the further work are discussed in the next chapter.

7. Conclusions and recommendations

7.1 Introduction

The overall objective of this work was to investigate the structural behaviour under pulse loading and to provide a methodology for design of process plant structures, particularly plates and shells, under impulsive loading by investigating the effect of time duration and the maximum applied pressure of impulse loads on the maximum allowable stresses of the structures.

The aim of this chapter is to present the overall conclusions to the work. Some recommendations are also presented for the further work.

7.2 Conclusions

The survey on the existing literature revealed that there is no standard failure criterion for the structures or components subjected to dynamic loading such as impact and pressure pulse loading. The reason was found to be the complexity of the case and also the involvement of nonlinearities in such problems.

As discussed and showed there are analytical solutions for elastic and plastic problems when the structure is under the pressure pulse loading however the complexity of the matter arise when the structural response to pressure pulse loading is subjected to the transition part of the material behaviour in stress-strain curve. As the material properties also play important roles of determining the material response to the pressure pulses it was found that the nonlinearities of the material should be wisely and realistically chosen.

In order to investigate the response and behaviour of the structures to pressure pulse loading an experimental set-up was made and also numerical finite element method was used to predict the strain histories of the structures. A simple geometry i.e. circular plate first was experimented under pressure pulse loading with different peak pressures and also various pulse width by means of changing a few factors in the experimental shock tube used in the present research. Then the cylindrical vessels and also a full scale heat exchanger was experimentally investigated under high pressure loading caused by bursting internal high pressure tubes.

Numerical works have also been carried out in parallel to predict the structures response to the pressure pulse loading. From the comparisons of the experimental

results with results form the numerical works, it was found that the numerical finite element method could predict the structural behaviour to pressure pulse loading. It should be mentioned that the modelling must be made properly to predict and obtain realistic results compared to the practical cases.

A fail-safe limit curve was also provided experimentally and numerically for various cases namely circular plates, small cylindrical structure and full size heat exchanger subjected to pressure pulse loading. These curves which deduced from a number of experimental works and numerical runs revealed that the pressures higher than static design pressures can be applied to the structures if the pulse width is short and remains in the safe region of the limit curve.

The above fail-safe curve should be determined for different cases as the dynamic response of the structures are different from case to case and depend on too many factors, as discussed through this research, including the nonlinearities.

The study has demonstrated the usefulness of applying the finite element method to examine and investigate any complex structures under dynamic condition. This has relevance in many applications where high pressure exist and may lead to spike in low pressure units under abnormal conditions. In some cases the transient will arise due to intervention of the protection device, whilst in others, such as external explosions, it is a feature then this can be translated to an engineering benefit in any subsequent risk analysis.

It can be concluded that the design criteria for structures under dynamic loading can be more flexible since the dynamic yield criteria are different from static ones and the introduced fail-safe curve may enhance the structural safety.

7.3 Recommendations

The investigation of structural behaviour under pressure pulse loading was carried out. However there are some factors, which play important roles in dynamic behaviour of structures.

The following recommendations can be the subject of the further research:

- Stress-strain curve of material could be different for the dynamic case compared to the static one. In other words, the strain rate of materials varies from static to dynamic. Therefore the study of stress-strain curve can be carried out.

- As structures behave differently under impact loading such as projectile, structural failure due to impact loading higher than static design load can be investigated.

- Temperature has a crucial effect on material strength and nonlinearity. The mechanical damage and failure of structures should be studied under high temperature.

- Heterogeneous materials such as composites are widely used. Their behaviour under shock loading may result economical design.

- Various failure criteria such as ones based on displacement, stress and energy can be compared to obtain the better design codes.

In terms of application area, there are few industrial applications, which can be mentioned for the future research. One of the popular applications is explosion in process plants and its effect on pressure vessels, which was covered here. The following applications may be of interest for the future research:

- High-pressure pipes in pipelines may burst and cause the high pressure loading on the adjacent pipes and components. This can be studied in detail.

- Under water explosion is another application, which can be investigated considering the submarine structures.

- Micro-channels can be used under high-pressure environment. The study of failure investigation of micro-channels can lead to determining the failure of micro size structures.

- Aerospace and aircraft structures are another application, which can be exposed to high pressure loading and explosions that may be considered for the future research.

At last, not least, the accuracy and capability of numerical methods such as finite element analysis to predict the failure and behaviour of very complex structures can be investigated.

This research area has very wide applications and it is still a novel subject area in engineering design to enhance the safe dynamic design of structures.

8. References

1. Abrahamson, G.R.; Goodier, J.N., 1962, "Dynamic plastic flow buckling of a cylindrical shell from uniform radial impulse", Proceeding of fourth US National Congress of Applied Mechanics 2, 939-950

2. Abrahamson, G.R.; Lindberg, H.E., 1971, "Peak load-impulse characterisation of critical pulse loads in structural dynamics", Dynamic response of structures, Proceeding of a Symposium held at Stanford University, California, 31-53

3. American Society of Mechanical Engineers (ASME), 1983, "Article D-3, Shells of revolution under external pressure", Section VIII, Pressures Vessels, Division 2, Alternative rules, 225-230

4. Anderson, D.L.; Lindberg, H.E., 1968, "Dynamic pulse buckling of cylindrical shells under transient lateral pressures", AIAA Journal, 6(4), 589-598

5. Baltov, A.; Minchev, O.; Ivanova, J., 1993, "Dynamic carrying capacity of elasto-visco-plastic cylindrical shells", Archive of Applied Mechanics, 63, 189-194

6. Ben-Haim, Y., 1993, "Convex models of uncertainty in radial pulse buckling of shells", Journal of Applied Mechanics, ASME, 60(3), 683-688

7. Brevart, B.J.; Fuller, C.R., 1996, "Energy exchange between the coupled media of impulsively excited, fluid-filled, elastic cylinders", Journal of Sound and Vibration, 190(5), 763-774

8. British Standard Institution, 1990, "Tensile testing of metallic materials – Part 1. method of test at ambient temperature", BS EN 10 002-1

9. Brown, D.M.; Nolan, P.F., 1985, "The effect of external blast on cylindrical structures", Institution of Chemical Engineers (IChemE) Symposium 93, England, 229-245

10. Bulson, P.S., 1986, "Explosions and structures", Applied Solid Mechanics-1, Glasgow, 26-27 March 1985, Publication by Elsevier Applied Science Publication, London, 205-222

11. Dharaneepathy, M.V.; Keshava, R.; Sathacumar, A.R., 1995, "Critical distance for blast-resistance design", Computers and Structures, 54(4), 587-595

12. Duffy, T.A.; Baker, W.E.; Lewis, B.B.; Greene, J.M., 1993, "Confinement of explosions in spherical vessels", Piping, Supports and Structural Dynamics, ASME, PVP 264, 85-91

13. Ferri, A, 1961, "Fundamental data obtained from shock-tube experiments", Pergamon Press

14. Fowler, D.W.; Herndon, R.C.; Wahrmund, R.C., 1969, "Analysis of potential overpressure of a heat exchanger shell due to a ruptured tube' ASME Petroleum Mechanical Engineering Conference

15. Galambos, T.V., 1988, "Selected topics in dynamic stability", Guide to Stability Criteria for Metal Structures, John Wiley and Sons, 627-659

16. Gaylord, E.H.; Mainstone, R.J., 1980, "Tall building criteria and loading", American Society of Civil Engineers (ASCE)

17. Geefken, P.R.; Kirkpatrick, W.; Holmes, B.S., 1988, "Response of impulsively loaded cylindrical shells", International journal of Impact Engineering, 7(2), 213-227

18. Gugan, K, 1979, "Unconfined vapour cloud explosions", The Institution of Chemical Engineers (IChemE), 60-71

19. Holmes, B.S.; Kirkpatrick, S.W., 1988, "Response of metal tanks to impulsive spot loading: Experiments and calculations", Impact: Effects of Fast Transient Loadings, Ammann et al. (eds), Rotterdam, 317-331

20. Holmes, B.S.; Kirkpatrick, S.W.; LeMond, J., 1990, "Ductile failure of shells following multiaxial dynamic strain histories", American Society of Mechanical Engineers, Applied Mechanics Division, AMD, 107, 13-19

21. Hoo Fatt, S.M.; Wierzbicki, T., 1992, "Damage of ring-stiffened cylinders under dynamic pressure loading", Proceedings of the Second International Offshore and Polar Engineering Conference, San Francisco, USA, June 1992, 587-595

22. Horoschun, G., 1992, "Design of blast resistant structures", Explosive Engineering, March 1992, 10-15

23. Jiang, J.; Oslon, M.D., 1991, "Non-linear dynamic analysis of blast loaded cylindrical shell structures", Computers and Structures, 41(1), 41-52

24. Jiang, J.; Oslon, M.D., 1993, "New design analysis techniques for blast loaded stiffened box and cylindrical shell structures", International Journal of Impact Engineering, 13(2), 189-202

25. Jones, N., 1989, "Some comments on the modelling of material properties for dynamic structural plasticity", International Conference of Mechanical Properties of Materials at High Rates of Strains, Oxford, 435-445

26. Kirkpatrick, S.W.; Holmes, B.S., 1988, "Structural response of thin cylindrical shells subjected to impulsive external loads", AIAA journal, 26(1), 96-103

27. Kirkpatrick, S.W.; Holmes, B.S., 1989, "Effect of initial imperfections on dynamic buckling of shells", American Society of Civil Engineers (ASCE), Journal of Engineering Mechanics, 115(5)

28. Kohnke, P., 1992, "ANSYS user's manual for revision 5.0", Swanson analysis systems, Inc.

29. Kormi, K.; Duddell, D.A., 1991, "Response of structures to impulse and impact loading II", Proceedings of the First International Offshore and Polar Engineering Conference, Edinburgh, UK, 156-164

30. Lewis, M.W.; Kashiwa, B.A.; Meier, R.W.; Bishop, S., 1994, "Non-linear dynamic fluid-structure interaction calculations with coupled finite element and finite volume programs", High Performance Computing in Computational Dynamics, CED-Vol. 6, 15-24

31. Li, Q.M.; Jones, N., 1995, "Blast loading of a short cylindrical shell with transverse shear effects", International Journal of Impact Engineering, 16(2), 331-353

32. Liang, C.; Lio, C.; Ma, Y., 1991, "A large deformation elastic-plastic dynamic analysis of square plate and spherical shell subjected to shock loadings", Computers and Structures, 39(6), 653-661

33. Lindberg, H.E, 1964, "Buckling of a very thin cylindrical shell due to an explosive pressure", Journal of Applied Mechanics 31, 261-272

34. Lindberg, H.E.; Florence, A.L., 1987, "Dynamic Pulse Buckling", Martinus nijhoff Publication, 67 & 97-137 &189-199

35. Lindberg, H.E.; Sliter, G.E., 1969, "Response of re-entry-vehicle-type shells to transient surface pressures", AFWL-TR-68-56, Report by SRI International to Air Force Weapons Laboratory, June

36. Mal'tsev, V.A.; Konon, Y.A.; Adishchev, V.V., 1984, "Experimental study and analysis of the vibration of an explosively loaded thin-walled spherical shell", Combustion, Explosion and Shock Waves, 20(2), 214-218

37. Manoach, E., 1994, "Dynamic large deflection analysis of elastic-plastic mindlin circular plates", International Journal of Non-linear Mechanics, 29(5), 723-735

38. Molyneaux, T.C.K.; Li, L.; Firth, N., 1993, "Impact responses of circular cylindrical shells under explosive loading", Advances in Engineering Software, 18, 7-13

39. Mustafa, B; Al-Hasani, T.S.; Reid, S.R., 1993, "Axisymmetric dynamic buckling of submerged cylindrical shells", Computers and Structures, 47(3), 339-405

40. Nicholas, R.W., 1971, "Explosive pressure", Pressure vessel engineering technology, Elsevier Publication, 465-467

41. O'regan, S.D.; DiMaggio, F., 1990, "Dynamic response of submerged shells with appendages", Journal of Engineering Mechanics, 116(10), 2293-2309

42. Oslon, M.D., 1991, "Efficient modelling of blast loaded plate and cylindrical shell structures", Computers and Structures, 40(5), 1139-1149

43. Payton, R.G.; 1961, "Dynamic membrane stress in a circular elastic shell", ASME Trans., 83, Series E, Journal of Applied Mechanics, 28(3), 411-416

44. Pedron, C.; Combescure, A., 1995, "Dynamic buckling of stiffened cylindrical shells of revolution under a transient lateral pressure shock wave", Thin-walled Structures, 23, 85-105

45. Pegg, N.G., 1991, "Dynamic pulse buckling of cylinders of various a/h ratios", Computers and Structures, 39(1/2), 173-183

46. Pegg, N.G., 1994, "A numerical study of dynamic pulse buckling of cylindrical structures", Marine Structures 7, 189-212

47. Pegg, N.G., 1994, "Effects of impulse duration and combined impulse-hydrostatic pressure on buckling stability of cylindrical structures", Journal of Ship Research, 38(2), 164-171

48. Prantil, V.C.; Kirkpatrick, S.W.; Holmes, B.S.; Hallquist, J.O., 1986, "Response of very thin shell under an impulse load", Finite Element Methods for Plate and Shell Structures 2, Edited by T.J.R. Hughes and G. Hinton, Prineridge press, UK

49. Ruiz, C.; Salvatorelli, F.; Thompson, V. K., 1989, "Elastic response of thin-wall cylindrical vessels to blast loading", Computers and Structures, 32(5), 1061-1072

50. Schwer, L.; Holmes, B.S.; Kirkpatrick, S.W., 1988, "Response and failure of metal tank from impulsive spot loading: experiments and calculations", International Journal of Solids and Structures, 24(8), 817-833

51. Shin, Y.S.; Hooker, D.T., 1994, "Shock-induced damage response patterns of submerged structures", PVP-Vol. 272, Sloshing, Fluid-Structures Interaction and Structural Response Due to Shock and Impact Loads, ASME, 167-173

52. Spence, J.; Tooth, A.S., 1994, "Pressure vessel design, concepts and principles", E & FN Spon Publication

53. Stanley, A.J.; Ganesan, N., 1995, "Impulse response of cylindrical shells with a discontinuity in the thickness subjected to an axisymmetric load", Journal of Sound and Vibration, 184(3), 369-387

54. Teeling-Smith, R.G.; Nurick, G.N., 1991, "The deformation and tearing of thin circular plates subjected to impulsive loads", International Journal of Impact Engineering, 11(1), 77-91

55. The Institute of Petroleum, 2000, "Guidelines for the design and safe operation of shell and tube heat exchangers to withstand the impact of tube failure", The Institute of Petroleum, London, ISBN: 0 85293 286 3

56. Tinawi, R.; Filrattault, A.; Dore, C., 1993, "Damage to base of LNG tanks from blast loading: case study", Journal of Performance of Constructed Facilities, 7(3), 148-163

57. To, C.W.S.; Wang, B., 1993, "Time-dependent response statistics of axisymmetrical shell structures", Journal of Sound and Vibration, 164(3), 554-564

58. Underwood, P., 1972, " Transient response of inelastic shells of revolution", Computers and Structures, 2, 975-989

59. Wierzbicki, T.; Hoo Fatt, M., 1993, "Damage assessment of cylinders due to impact and explosive loading", International Journal of Impact Engineering, 13(2), 215-241

60. Wierzbicki, T.; Nurick, G. N., 1996, "Large deformation of thin plates under localised impulsive loading", International Journal of Impact Engineering, 18(7), 899-918

61. Xu, J.; Kirkvik, R.N., 1991, "Design against explosion loads in offshore structures", Proceedings of the First International Offshore and Polar Engineering Conference, Edinburgh, UK, 183-189

62. Xu, X., 1991, "Inelastic response of stiffened cylindrical shells to underwater shock waves considering fluid-structure interaction", Computational Mechanics, Cheung, Lee & Leung (eds), Rotterdam, 535-540

63. Zhao, Y.; Yu, T.X.; Fang, J., 1995, "Saturation impulses for dynamically loaded structures with finite-deflections", Structural Engineering and Mechanics, 3(6), 583-592